A COMBINED SEDIMENTOLOGICAL-MINERALOGICAL STUDY OF SEDIMENT-HOSTED GOLD AND URANIUM MINERALIZATION AT DENNY DALTON, PONGOLA SUPERGROUP, SOUTH AFRICA

by

Nigel Hicks

Submitted in fulfilment of the academic requirements for a degree of Master of Science in the School of Geological Sciences, University of KwaZulu-Natal Durban

March 2009.

As the candidate's supervisor I have approved this thesis for submission

Signed: _____ Name: _____ Date: _____

PREFACE

The experimental work described in this thesis was carried out in the School of Geological Sciences, University of KwaZulu-Natal, Durban, form January 2006 till November 2008, under the supervision of Doctor Axel Hofmann.

These studies represent original work by the author and have not otherwise been submitted in any form for any degree or diploma to any tertiary institution. Where use has been made of the work of others it is duly acknowledged in the text.

DECLARATION 1 - PLAGIARISM

I, Nigel Hicks declare that:

1. The research reported in this thesis, except where otherwise indicated, is my original research.
2. This thesis has not been submitted for any degree or examination at any other university.
3. This thesis does not contain other persons' data, pictures, graphs or other information, unless specifically acknowledged as being sourced from other persons.
4. This thesis does not contain other persons' writing, unless specifically acknowledged as being sourced from other researchers. Where other written sources have been quoted, then:
    a. Their words have been re-written but the general information attributed to them has been referenced.
    b. Where their exact words have been used, then their writing has been placed in italics and inside quotation marks and referenced.
5. This thesis does not contain text, graphics or tables copied and pasted from the Internet, unless specifically acknowledged, and the source being detailed in the thesis and in the References sections.

Signed: ……

DECLARATION 2 - PUBLICATIONS

Details of contribution to publications that include research presented in this thesis:

PUBLISHED:

Hicks, N., 2007. The Sedimentology of the auriferous and uraniferous Mandeva Formation, Pongola Supergroup, Northern KwaZulu-Natal. *Faculty of Science and Agriculture Postgraduate Research Day Programme and Abstracts*, University of KwaZulu-Natal. pp 29.

Hicks, N. & Hofmann A., 2008. The sedimentology of the auriferous Mandeva Formation within the White Umfolozi Inlier, Pongola Supergroup, South Africa. *SEG-GSSA Student conference abstracts.* pp 42-43.

Hicks, N. & Hofmann, A., 2008. A combined sedimentological-mineralogical study of sediment-hosted gold and uranium mineralization at Denny Dalton, Pongola Supergroup, South Africa. *SEG-GSSA conference abstracts* pp 130-131.

IN PREPARATION:

Hicks, N. & Hofmann, A., 2008. Gold mineralization associated with detrital pyrite at Denny Dalton Mine, Pongola Supergroup, South Africa. *South African Journal of Geology.*

Signed: ……

ABSTRACT

The ~2.98 - 2.87 Ga Pongola Supergroup in South Africa is subdivided into the lower volcano-sedimentary Nsuze Group, and the upper sedimentary Mozaan Group, the latter comprising a several kilometres thick succession of fluvial to shallow marine sandstones and shales. Thin beds of gold and uranium-bearing conglomerates are locally present in the Mandeva Formation near the base of the Mozaan Group and have been mined at Denny Dalton in northern KwaZulu-Natal. The style of mineralization strongly resembles that of the Witwatersrand goldfields, however appears to be of low grade and limited tonnage.

The ~1 m thick basal conglomerate, the "Mozaan Contact Reef" (MCR, herein referred to as CG 1), at Denny Dalton hosts erratic gold and uranium mineralization. The conglomerate is laterally discontinuous and occupies east-northeast trending scour channels. Polymict, matrix-supported conglomerates are common, while clast-supported conglomerates are rare. Well rounded, pebble to cobble-sized clasts of vein quartz and chert are hosted in a sandy matrix of quartz, pyrite and sericite. Where mineralized, the CG 1 hosts abundant rounded pyrite grains, interpreted as detrital in origin, with subordinate U-bearing minerals, such as brannerite and uraniferous leucoxene. Rounded detrital pyrite occurs in three phases, compact, porous and radial.

Gold forms inclusions within massive pyrite grains, which are concentrated in shoots associated with the basal parts of the channel scours. SEM-EDX results, as well as the high reflectivity of the gold show a high Ag content, indicative of a primary origin for the gold within the pyrite grains. Uranium within CG 1 is hosted primarily as secondary inclusions of uranium within black chert pebbles within the basal cobble-sized regions of the conglomerate. Geochemical comparison of the chert pebbles at Denny Dalton with similar chert from the Nondweni Greenstone Belt indicates that the uranium is secondary in origin as no U anomalies occur in the Nondweni chert. Geochemical and SEM analysis of the uppermost conglomerate (CG 4) indicate the presence of uraninite and coffinite within the uppermost horizon as both fillings of voids within, and coatings on, detrital pyrite grains.

Palaeocurrent data indicate a likely source terrain for the detrital material to the west of the inlier. This orientation, as well as differing mineralogical and sedimentological aspects between the Mandeva Formation and the correlative Sinqeni Formation within the main Pongola basin, indicate a separate and more proximal provenance for the auriferous conglomerates of the White Umfolozi Inlier. The Mandeva Formation is a fluvial to shallow marine sequence that has been affected by cyclic sea-level changes. The basal conglomerates of the Denny Dalton Member were deposited in a proximal braided alluvial plain environment. The conglomerates fine upwards into trough cross-

bedded quartz arenites which appear to have been deposited as shallow marine sands in a shoreface environment. They are overlain with a sharp contact by a laterally extensive unit of polymictic conglomerate which represents a transgressive ravinement surface within the wave zone and marks the onset of a major marine transgression into the Pongola basin. The conglomerate is overlain by massive grits and coarse-grained quartz arenite. This unit is overlain with a sharp and locally sheared contact by shales and subordinate banded iron formation which can be traced into other parts of the Pongola basin and indicates continued rapid transgression onto large parts of the Kaapvaal Craton with deeper marine, sub-storm wave base sediments being deposited in quiet-water environments on a sediment-starved shelf.

The heavy mineral assemblage as well as bulk geochemical data is consistent with a granitoid-greenstone source terrain for the conglomerates and sandstones. The geochemical composition of chert pebbles from the CG 1 is similar to the composition of cherts present in the Nondweni Greenstone Belt that is situated ~30 km west of the White Umfolozi Inlier. Multiple sulphur isotope ($\delta^{34}S$, $\delta^{33}S$) values for detrital pyrite from the MCR are consistent with an origin from mantle-like rocks, such as hydrothermal sulphide-quartz veins in a granitoid-greenstone setting. Palaeocurrent, mineralogical and geochemical data all point to a likely granitoid-greenstone provenance to the west of the White Umfolozi Inlier.

CONTENTS

CHAPTER 1

INTRODUCTION

1.1 GENERAL

The ~2.98 - 2.87 Ga Pongola Supergroup crops out in a ~260 km long basin on the south-eastern edge of the Kaapvaal Craton cropping out in northern KwaZulu-Natal, Mpumalanga and Swaziland, with exposures in the south forming a number of small inliers (SACS, 1980) (Figure 1.1). It is subdivided into two groups, the lower, volcano-sedimentary Nsuze Group and upper, sedimentary Mozaan Group, which formed in two different depositional and tectonic environments. The Nsuze Group is thought to have been deposited in a rift environment indicating that continental accretion had ceased and that the Kaapvaal Craton had stabilized after emplacement of the ~3.1 Ga granitoids (Matthews, 1990). In addition, the sedimentary rocks of the Mozaan Group are predominantly shallow marine to fluvial in origin and are traceable throughout the ~260 km extent of the basin, indicating that the Kaapvaal Craton was stable by ~2.9 Ga. The Pongola Supergroup thus forms one of the earliest intra-continental sedimentary basins recorded on Earth (Matthews, 1990).

The Pongola Supergroup attains a maximum thickness of 10 650 m (SACS, 1980) in the northern domain, however, thicknesses vary greatly between the different areas and appear to thin towards the southern inliers. The structural domains within which the Pongola Supergroup rocks are hosted vary within the different outcrop areas. The study area forms a ~5 km by 15 km northwest trending rectangle through the White Umfolozi Inlier, bounded in the west by the Nsuze-Mozaan unconformity and the Pongola-Dwyka unconformity in the east (Figure 1.1).

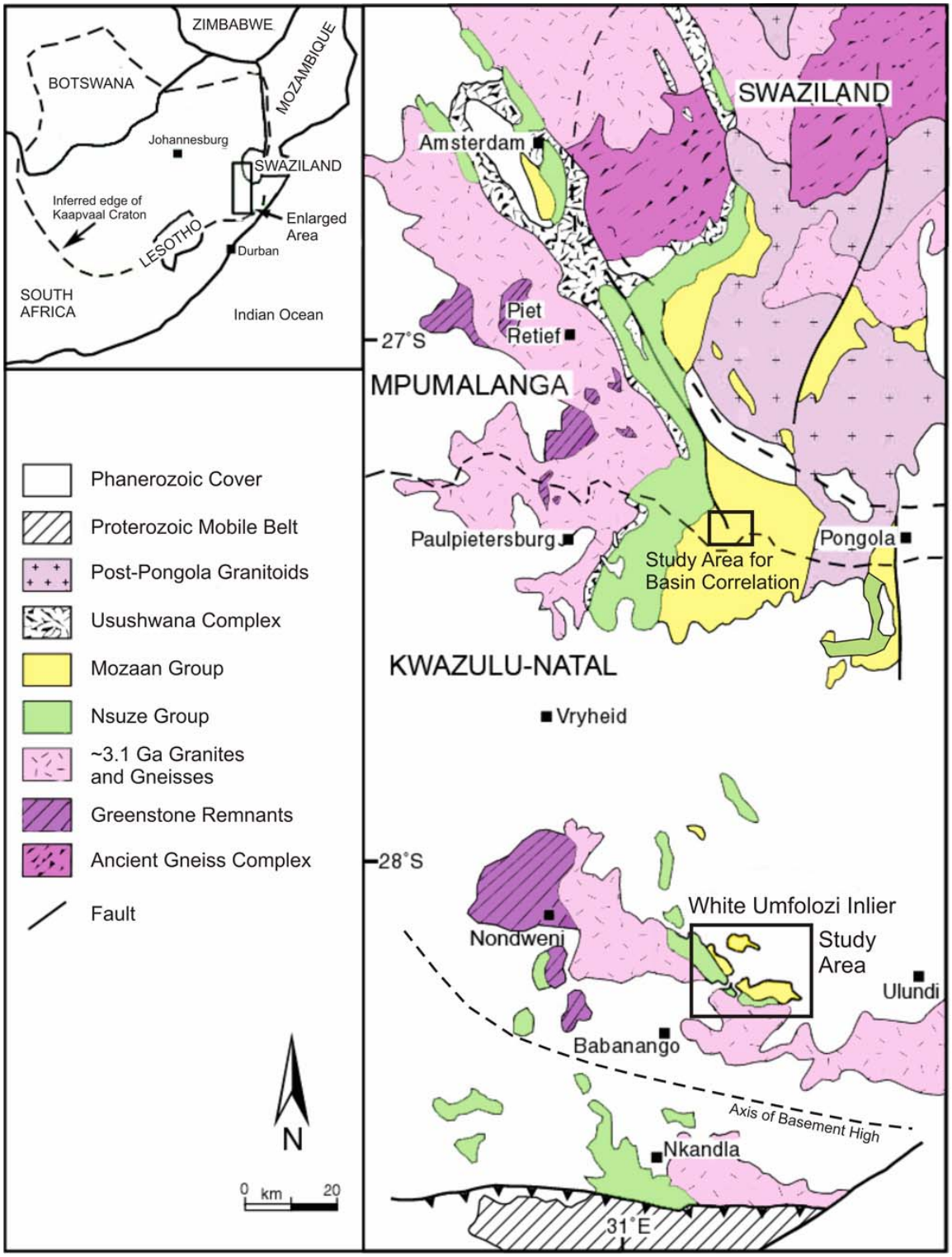

Figure 1.1: Locality map showing regional outcrop of the Pongola Supergroup and associated granites and greenstones. (modified after Gold and Von Veh, 1995).

1.2 PHYSIOGRAPHY

The White Umfolozi Inlier crops out ~30 km west of Ulundi in northern KwaZulu-Natal and covers some 300 square kilometres, forming an erosional window surrounded by Phanerozoic cover. The topography is rugged with elevations ranging from 500 m to 1 450 m above sea level. Rolling hills and river valleys predominate, with valleys formed by fluvial erosion and the surrounding hills being capped by cover sequences.

The climate of the area is temperate with vegetation dominated by thorn-scrub and grassland. Summers are warm to hot with mild, dry winters. Rainfall in the region averages 780 mm and occurs mainly during summer months (www.weathersa.co.za, 08/10/08).

Access to the White Umfolozi Inlier is by the R34 road between Melmoth and Vryheid. A number of gravel district roads and farm tracks lead off the main road into the more remote parts of the inlier near Denny Dalton. Outcrop is best exposed in the actively eroding river valleys where fluvial action has removed much of the surrounding vegetation.

1.3 AIMS AND OBJECTIVES

This study is intended to identify the mineralogy, lithostratigraphy, and the palaeo-depositional environment of the lowermost Mandeva Formation of the Mozaan Group within the White Umfolozi Inlier. The lowermost lithologies are of particular interest due to the auriferous nature of the conglomerate horizons within the Denny Dalton Member at the base of the formation. The study attempts to define the nature, extent and provenance of the mineralization within the Mandeva Formation.

1.3.1 FIELD STUDY METHODS

Geological mapping of the Mozaan Group in the White Umfolozi Inlier was carried out over a period of 7 months between November 2006 and May 2007, during which approximately 100 square kilometres were mapped. The mapped area was later digitized onto digital versions of the 1 : 50 000 topographical maps (Sheets 2831 AA, AB, AC and AD) . This was followed by detailed mapping undertaken in the economically important Denny Dalton area. Mapping within other areas of interest within the Pongola basin was undertaken on satellite images attained from Google Earth (www.earth.google.com).

Sedimentological logs and measured sections were produced using the software Strater to aid sedimentological analysis and lithological correlation along strike throughout the inlier (see Figure 1.2 for key). Sedimentary analysis enabled the identification of changes in the dominant depositional environments through the formation.

The key below is used in all detailed stratigraphic and drill core logs drawn within the Mandeva Formation in Chapters 3 and 5, and in other areas of Mozaan Group outcrop such as the Main Pongola basin and Nondweni areas in Chapter 6, unless otherwise stated.

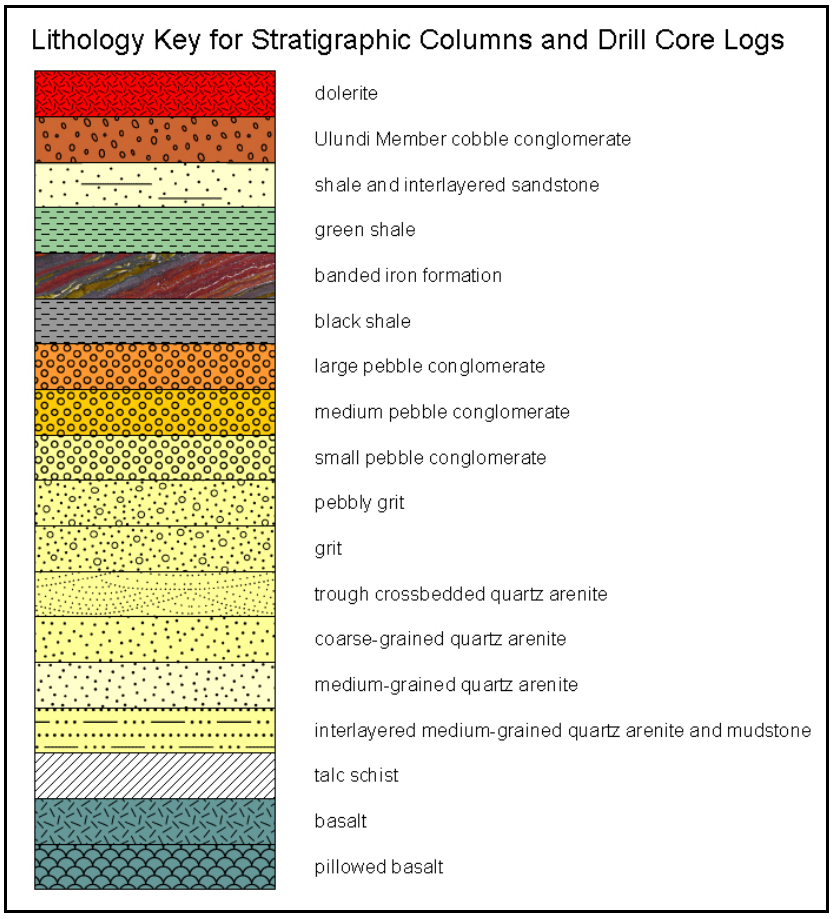

Figure 1.2: Lithology key for detailed stratigraphic columns prepared in this thesis.

1.3.2 PALAEOCURRENT ANALYSIS

Palaeocurrent data was restored to the horizontal using the software Stereostat. Bedding readings taken in the Mandeva Formation throughout the White Umfolozi Inlier indicate that the inlier is folded into a shallowly plunging syncline with a fold axis plunge and plunge direction of 10°/066°. This plunge and plunge direction was used to restore all palaeocurrent data to its original position.

1.3.3 CORE SAMPLES

A number of diamond drill holes were drilled by Caracle Creek International Consulting (CCIC) for Acclaim Exploration, in the vicinity of the Denny Dalton gold mine during an exploration programme which ran between June 2006 and May 2007. The author was contracted as a field geologist on the project to oversee the drilling programme. The author was given permission to sample two drill cores from the project. Drill core TSB 06-23 was drilled in the Denny Dalton Mine area to a depth of 57 m. The three conglomerate zones intersected constitute the Denny Dalton Member, which crops out at the base of the Mozaan Group. Quarter core sampling was done between 30 m and 55 m depth. Drill core TSB 07-26 was drilled north of the Denny Dalton Mine to a depth of 240 m. Half core sampling was done between 160 m and 185 m depth. This sampling intersected the Vlakhoek Member banded iron formation as well as the uppermost conglomerate zone of the Mandeva Formation (CG 4) (Figure 3.4). Drill core logs were produced on Strater to define the stratigraphic positions for geochemical analysis. All drill core logs use the lithological key provided in Figure 1.2.

1.3.4 MICROSCOPY, ORE MICROSCOPY, AND SEM ANALYSIS

Reflected and transmitted light microscopy was undertaken on 24 conglomerate samples as well as transmitted light microscopy on other sedimentary units throughout the Mandeva Formation. 24 polished sections and 4 polished blocks of the conglomerates were analysed for ore microscopy. An intensive Scanning Electron Microscope (SEM) study was undertaken to define the ore mineralogy of the auriferous and uraniferous conglomerates at Denny Dalton Mine. SEM analysis was undertaken at the Electron Microscope units on both the Durban-Westville and Pietermaritzburg Campuses of the University of KwaZulu-Natal using a Philips LEO electron microscope.

1.3.5 GEOCHEMISTRY

Samples for geochemical analysis were taken at different stratigraphic levels from all conglomerate horizons as well as quartz arenites and grits in two diamond drill cores, TSB 06-23 and TSB 07-26. Grab samples of all three conglomerate zones, taken within the Denny Dalton Mine area were also used. X-Ray Fluorescence (XRF) spectrometry and ICP-MS analyses were carried out on all samples as well as on selected black chert pebbles obtained from the auriferous Denny Dalton conglomerate. These data are presented in Chapter 5 and in Appendix II.

Trace elements were determined using a Perkin-Elmer Elan 6100 ICP-MS against primary standard solutions and validated against certified standard rock materials. 50 mg of sample was dissolved in $HF–HNO_3$ in an Anton-Paar Multiwave high pressure and temperature microwave digester with 40

minute digestion times and evaporated to dryness in Teflon beakers before being taken up in 5% HNO_3 for analysis. The final solution was made up to 50 ml for analysis. Internal standards (10 ppb Rh, In, Re and Bi) and calibration solutions were prepared from certified single and multi-element standard solutions. Quality of data was monitored using the international standards BCR-1, BHVO-1 and BIR-1.

X-ray Flourescence (XRF) analyses for major elements were conducted using a Philips X'Unique II. Fused discs were prepared by mixing 2 g of specraflux with 0.3 g of powdered sample in a platinum bowl crucible. X-Ray Diffraction (XRD) was used to determine the ore mineralogy of some of the friable radial sulphide pebbles evident in the Denny Dalton conglomerates. Samples for X-ray diffraction analysis were crushed using an agate mortal and pestil to a particle size of less than 25 microns and hand pressed into and aluminium holder. The sample was expose to Cobalt Kα radiation (λ = 17.889Å) and scanned from 3 to 60° 2θ using a Philips 1830 system with a graphite monochromator. The data was processed using the ADP software and ICDD data books.

1.4 PREVIOUS WORK

Early data for the White Umfolozi Inlier is fragmentary, but Du Toit (1939) assigned the strata in the White Umfolozi river valley to the "Insuzi Formation" identified by Hatch (1910) in the Nkandla area in KwaZulu-Natal. Matthews (1967) completed the first comprehensive survey of the inlier, correlating the lithologies with Du Toit's (1939) "Insuzi Formation". Matthews however, identified an angular unconformity which separated the rocks of the lower "Insuzi Formation" from rocks which he correlated with the "Mozaan Formation" (Matthews, 1967). Matthews identified six lithological zones within the volcano-sedimentary "Insuzi Formation", and three lithological zones in the overlying sedimentary "Mozaan Formation". Von Brunn & Hobday (1976) and Von Brunn & Mason (1977) identified siliciclastic tidal deposits within the Mozaan Group sedimentary rocks and defined possible depositional environments for the lithologies of the "Mozaan Formation". SACS (1980) assigned Group status to Matthews' (1967) "Insuzi" and "Mozaan Formations", and assigned Formation rank to Matthews (1967) lithological zones. The South African Committee for Stratigraphy also reclassified the name "Insuzi" as "Nsuze" at the request of the Place Names Committee (SACS, 1980). Dix (1984) identified a transition from braided stream to tidal deposition within the sedimentary rocks of the Mozaan Group whilst investigating gold mineralization at the defunct Denny Dalton gold mine. Wilson and Grant (2006) defined the Nsuze Group depositional environment as a subsiding continental margin from compositional variations of the volcanic successions.

CHAPTER 2

REGIONAL GEOLOGY OF THE PONGOLA SUPERGROUP AND SURROUNDING LITHOLOGIES

2.1 PRE-PONGOLA LITHOLOGIES

The basement rocks onto which the rocks of the Pongola Supergroup were non-conformably deposited include greenstone belts as well as tonalite-trondhjemite-granite terrains.

2.1.1 ANCIENT GNEISS COMPLEX

In the Amsterdam area and in southern Swaziland (Figure 2.1), the basement to the Pongola Supergroup rocks comprises the Ancient Gneiss Complex as well as younger granites. The Ancient Gneiss Complex in Swaziland is made up of three major units, the Dwalile Supracrustal Suite, and the Ngwane and Tsawela Gneisses, with minimum ages of 3 436±6 and 3 458±3 Ma (Kroner & Tegtmeyer, 1993; Wendt, 1993) determined from zircon ages for the intrusive Tsawela Gneiss.

2.1.2 GREENSTONE BELTS

A number of Archaean greenstone belts crop out in the southeastern portion of the Kaapvaal Craton. Even though many of them do not lie with a direct contact against the rocks of the Pongola Supergroup, they form the initial proto-crust into which the pre-Pongola granitoids were emplaced.

The Barberton Supergroup in Mpumalanga and northern Swaziland is the largest and most well preserved greenstone terrain in the Kaapvaal Craton and is in sheared contact with the Ancient Gneiss Complex. The lowermost volcano-sedimentary Onverwacht Group is on average 8-12 km thick and formed between 3 550 - 3 280 Ma (Kamo & Davis, 1994). The Onverwacht Group is overlain by argillaceous rocks of the Fig Tree Group which attains a maximum thickness of ~3 km and was deposited between 3 258±3 - 3 227±4 Ma (Kohler & Anhaeusser, 2002; Kroner et al., 1991). The 3 224±6 to 3 105±3 Ma Moodies Group (Heubeck & Lowe, 1994; Heubeck et al., 1993; Kamo & Davis, 1994; Kohler & Anhaeusser, 2002) consists of a succession of repeated cycles of arenaceous rocks which fine upwards into argillaceous units.

The Nondweni Greenstone Belt crops out on the southern margin of the Kaapvaal Craton and is dominated by extrusive mafic and ultramafic rocks, with minor felsic volcanic, and sedimentary rocks

(Riganti & Wilson, 1995). A rhyolitic flow has been dated at 3 406±3 Ma using the Sensitive High Resolution Ion Microprobe (SHRIMP) technique (Armstrong, 1989; Riganti & Wilson, 1995). Greenstone belts and their associated intrusive granitoids form a possible provenance for many of the sedimentary rocks found within the southern portions of the Pongola Supergroup (Matthews, 1990).

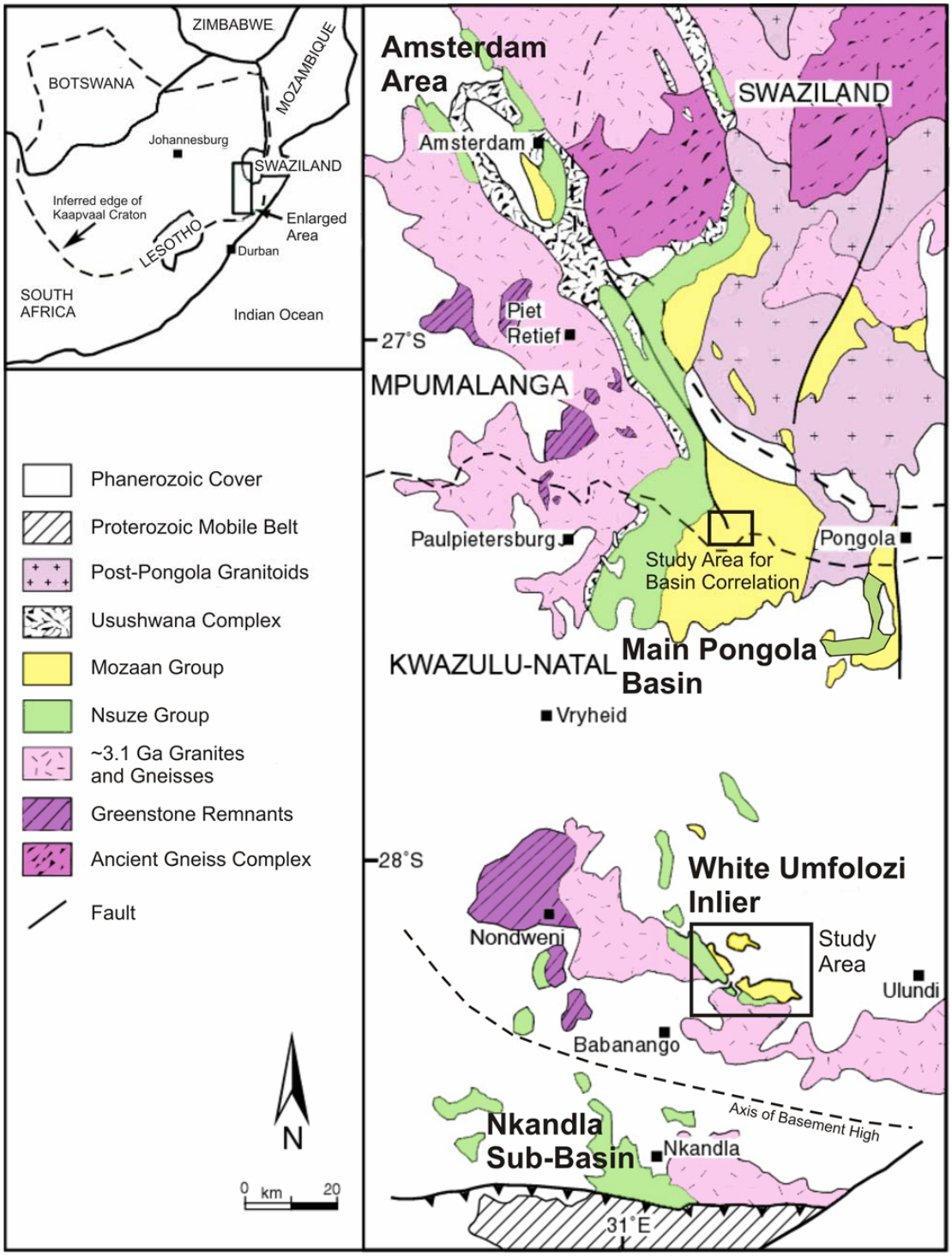

Figure 2.1: Simplified map showing distribution of the Pongola Supergroup and associated geology and the four main depositional areas (Amsterdam, Main Pongola Basin, White Umfolozi Inlier and Nkandla Sub-Basin). (modified after Gold and Von Veh, 1995). Refer to map overleaf for enlargement of study area.

2.1.3 ~3.1 Ga GRANITIC PLUTONS

After the development of the palaeo-greenstone belt succession, a number of granitoids were emplaced into it which now crop out throughout the south-eastern part of the Kaapvaal Craton. The pre-Pongola Supergroup granitoids that crop out in the Piet Retief area were dated by Griffin (2002); the Hoopwel granite yields an age of 3 267±21 Ma, whilst the gneissic granites near Piet Retief have an age of 3 147±13 Ma.

Homogeneous granites and gneisses form the basement to the Pongola Supergroup in the southern inliers. The basement granite exposed in the White Umfolozi River (Figure 2.3) east of Nondweni has a Rb-Sr isochron age of 3 162±80 Ma (Burger & Coertze, 1973; Dixon, 2003). Granitic rocks which intrude the eastern portions of the Nondweni Greenstone Belt (Figure 2.1) have a Rb-Sr isochron age of 3.29 Ga (Matthews et al., 1989) and thus give a minimum age for the Nondweni Greenstone Belt (Riganti & Wilson, 1995). These granites are associated with the same pluton that forms the basement to the White Umfolozi Inlier ~20 km to the east. The emplacement of these batholiths in the south-eastern margin of the Kaapvaal Craton contributed significantly to craton development which subsequently formed the basement onto which the Pongola Supergroup was deposited.

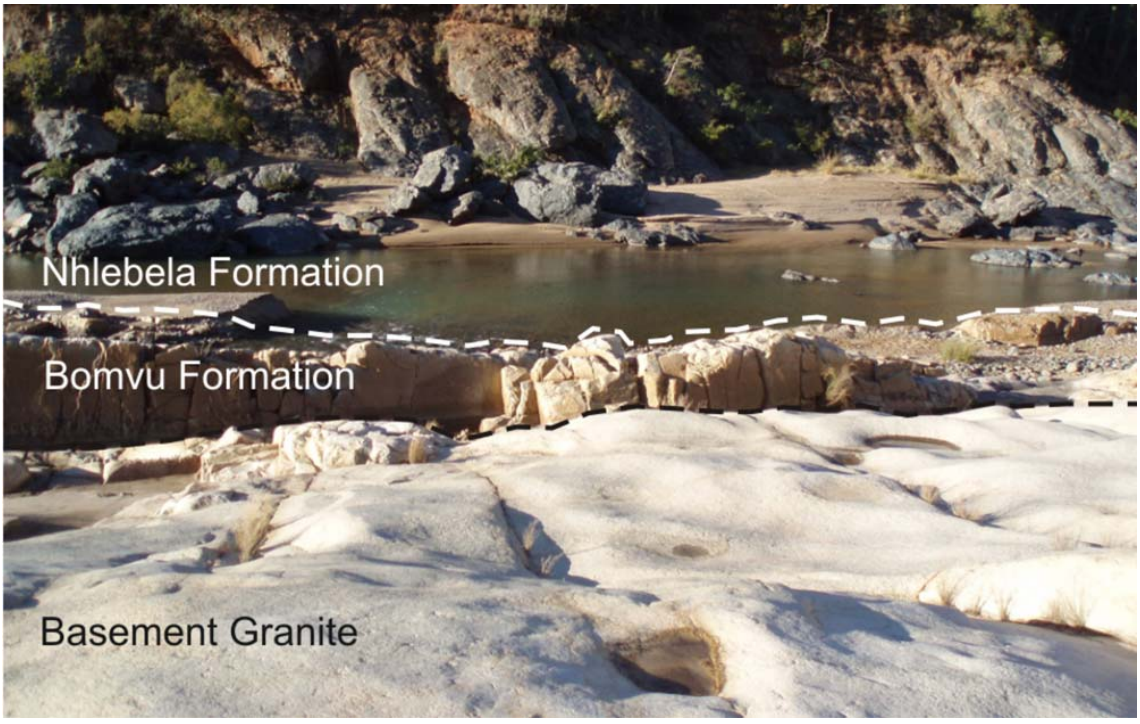

Figure 2.3: View east across the White Umfolozi River within the White Umfolozi Inlier. Basement granite cropping out in the foreground is overlain nonconformably by the ~1 m thick Bomvu Formation sandstones in the mid-ground. These are overlain by basalts and basaltic andesites of the Nhlebela Formation.

2.2 PONGOLA SUPERGROUP OUTCROP AREAS, AND LITHOLOGIES

2.2.1 AMSTERDAM AREA

Within the Amsterdam region in the Mpumalanga Province rocks of the Pongola Supergroup forms a shallow northwest trending syncline (Figure 2.1) (Matthews, 1990). Subsequent to deposition of the Pongola Supergroup the area was intruded by mafic and ultramafic sills and dykes of the ~2 820 Ma Usushwana Complex (Matthews, 1990). The Pongola Supergroup rocks of the Amsterdam area attain a maximum thickness of ~4 500 m (SACS, 1980) and are preserved in a closed synclinal trough within the Amsterdam Graben (Weilers, 1990).

2.2.1.1 NSUZE GROUP

Within the Amsterdam area, the Nsuze Group comprises the lowermost sedimentary Mantonga Formation which attains a maximum thickness of ~280 m (SACS, 1980). This is overlain conformably by the ~2 000 m thick Bivane Formation basalts and subordinate andesites (SACS, 1980). Zircons from a rhyodacite of the Bivane Formation lavas in southern Swaziland yield an age of 2 984 ± 4 Ma (Hegner et al., 1994) .

2.2.1.2 MOZAAN GROUP

The Bivane Formation is overlain conformably by two formations of the Mozaan Group, the Skurwerant and Redcliff Formations. The Skurwerant Formation forms the lowermost unit of the Mozaan Group in the type area and is dominated by two quartzite units separated by a thin ~30 m thick laterally extensive ferruginous shale unit (Weilers, 1990). A whole rock Pb-Pb date of 2 860 ± 26 Ma was attained from the ferruginous shale of the Madola Member of the Skurwerant Formation (Walraven & Pape, 1994). The Skurwerant Formation is conformably overlain by ferruginous shales and intercalated sandstones of the Redcliff Formation (SACS, 1980; Weilers, 1990).

2.2.2 MAIN PONGOLA BASIN

The main Pongola basin is folded into two synclinal folds, the Piensrand and Tobolsk synclines (Figure 2.4) (Gold & Von Veh, 1995). The Pongola Supergroup thickens southwards towards the Pongola River and attains a maximum thickness of ~8 000 m in the Piet Retief / Paulpietersburg area (Weilers, 1990).

2.2.2.1 NSUZE GROUP

According to SACS (1980), within the Pongola Supergroup type locality in the vicinity of the Pongola River, the volcano-sedimentary Nsuze Group is divided into two formations. The lower ~850 m thick Mantonga Formation (SACS, 1980) consists of immature medium to coarse-grained sandstones and intercalated conglomerate lags which were deposited in a braided stream environment (Watchorn and Armstrong, 1980). It is overlain conformably by the volcanic Bivane Formation which attains a maximum thickness of ~5 200 m (SACS, 1980). This formation consists of basalts, basaltic andesites and andesites with minor dacites and rhyolites which were extruded in a sub-aerial environment (Weilers, 1990). The Ozwana Subgroup overlies the Bivane Formation volcanics and was previously believed to represent the lowermost unit of the Mozaan Group (SACS, 1980), however more recently Joubert & Johnson (1998) placed the phyllites and mica-bearing schists of the subgroup within the Nsuze Group.

2.2.2.2 MOZAAN GROUP

Within the Piet Retief area (Gold, 2006) subdivided the Mozaan Group into ten separate formations. These are dominated by argillaceous and arenaceous sedimentary rocks which were deposited in shallow marine to shelf, and fluvial braid-plain environments (Beukes and Cairncross, 1991).

The lowermost Sinqeni Formation crops out as a thin unit of conglomerate, the Dipka Member, which is overlain conformably by ~610 m thick succession of quartzites and minor banded iron formation (SACS, 1980). The Sinqeni Formation is overlain with a sharp erosional contact by the thick ~1 000 m Ntombe Formation (Gold, 2006). Shales dominate this formation with minor interlayers of quartzite and banded iron formation.

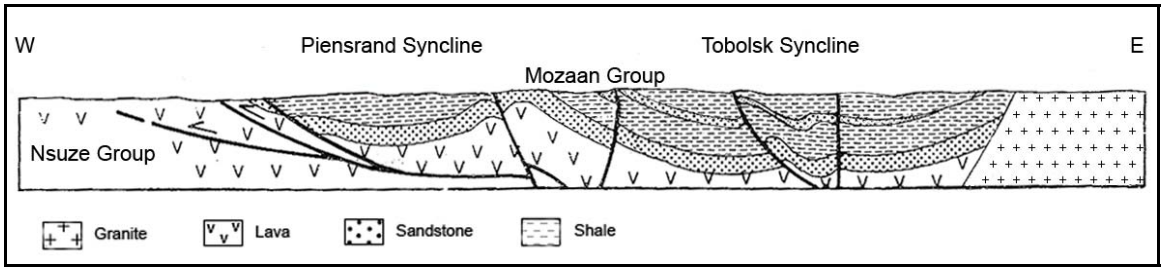

Figure 2.4: Schematic cross section of the main Pongola basin showing outcrop of the Mozaan Group in two synclinal troughs. The Mozaan Group is intruded to the east by a post-Pongola Supergroup granitoid (modified after Gold and von Veh, 1995.)

The Ntombe Formation is overlain by three predominantly quartzitic formations. These are the Thalu, Hlashana and Delfkom Formations respectively. The Thalu Formation includes a minor iron formation, the Scotts Hill Member, whilst the Hlashana and Delfkom Formations are composed of quartzite with interlayered shales (SACS, 1980). The Delfkom Formation is the most prominent and contains the Klipwal diamictite, possibly the oldest known glacial deposit on Earth (Gold & Von Veh, 1995). A thin volcanic unit, the Tobolsk Member, overlies the Delfkom Formation and occurs as a 40 - 50 m thick highly amygdaloidal basalt (Beukes and Cairncross, 1991).

The Tobolsk Member is overlain by two predominantly quartzitic formations, the Khiphunyawo and Bongaspoort Formations. These are overlain by amygdaloidal andesites and dacites of the Gabela Formation (Gold, 2006). The Mozaan Group is capped by the Ntanyana Formation which is dominated by grey sandstones (Gold, 2006).

2.2.3 WHITE UMFOLOZI INLIER

The White Umfolozi Inlier is the largest of the southern erosional inliers (Figure 2.1 and 2.2). It crops out in the Denny Dalton area in northern KwaZulu-Natal as a northwest-southeast trending inlier, surrounded by sedimentary rocks of the Karoo Supergroup. The White Umfolozi River has incised a large valley into the pre-Karoo rocks, exposing the Pongola Supergroup and basement granites and gneisses.

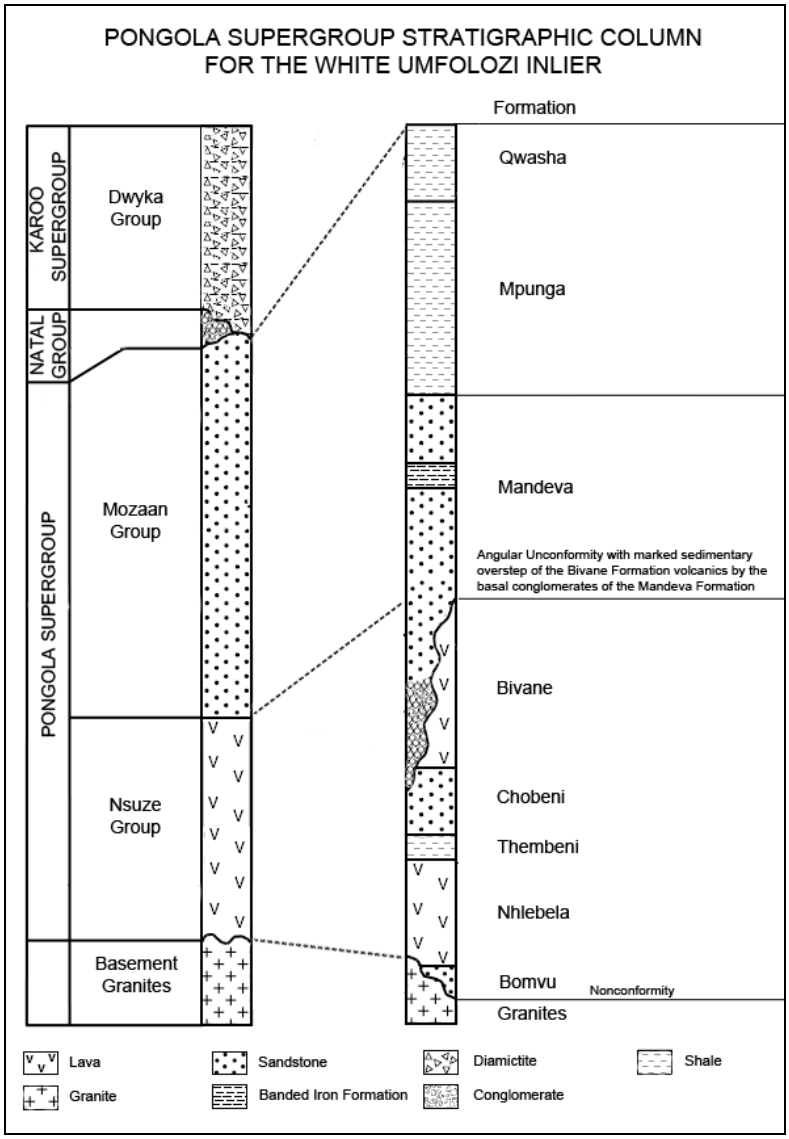

Figure 2.5: Stratigraphic column for the White Umfolozi Inlier compiled by the author, showing the Groups and Formations identified within the inlier and their respective lithologies, as well as all associated unconformities.

2.2.3.1 NSUZE GROUP

The Nsuze Group in the White Umfolozi Inlier crops out as a ~1 800 m thick succession (Matthews, 1967) of interlayered volcano-sedimentary units the lowermost of which rests nonconformably on basement granites and gneisses (Figure 2.5). It consists of a basal sedimentary unit of feldspathic sandstone, two volcanic sequences of basalts, andesites and dacites, with a thick sedimentary sequence of arenaceous, argillaceous and rudaceous rocks which split the volcanics. Minor lenses of volcaniclastic material are often evident immediately above and/or below the volcanics.

The Bomvu Formation is a <60 m thick feldspathic sandstone deposited nonconformably upon granitic basement by long-shore currents in a near-littoral, transgressive environment (Matthews, 1967). The Nhlebela Formation is a ~125 m thick unit of amygdaloidal basalt and andesite which lies conformably on the basal sandstones but also oversteps it in places, resting nonconformably on the granitic basement. Pillow structures and hyaloclastites are evident in the lower part of the unit but not in the upper, indicating partial subaqueous eruption.

The Thembeni Formation which conformably overlies the Nhlebela Formation lavas comprises mainly volcaniclastic, grey to green siltstones and shales. The Chobeni Formation is dominated by a fairly uniform sequence of quartz sandstones with numerous lenses of carbonate-rich, dolomitic sandstones, dolomite and greywacke. The evidence of stromatolites within the dolomites is of importance as there is no other recorded occurrence of stromatolites in the Nsuze Group (Mason & Von Brunn, 1977) and is indicative of a shallow marine depositional environment within the southern inliers of the Pongola basin.

The Bivane Formation which conformably overlies the Chobeni Formation is a thick succession of amygdaloidal lavas of basaltic, andesitic and dacitic composition. Pyroclastic rocks, pahoehoe, and ropy lava structures near the base of the formation indicate a predominantly sub-aerial extrusive environment.

2.2.3.2 MOZAAN GROUP

In the White Umfolozi Inlier the Mozaan and Nsuze Groups are separated by an angular unconformity marked by a ~10º difference in dip (Figure 2.6). The sedimentary rocks of the Mozaan Group dip east-northeast at an average dip of 10º whereas the underlying Nsuze Group dips at 20° to the northeast (Matthews, 1967). The Mozaan Group in this area is known for its conglomeratic units which are similar to conglomeratic units of the Witwatersrand Supergroup and are also auriferous in nature (Hatch, 1910., Matthews 1967., Weilers 1990.).

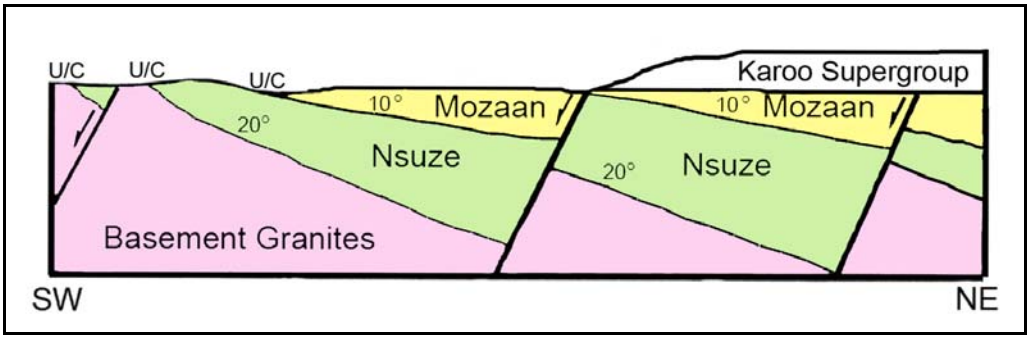

Figure 2.6: Cross section of the White Umfolozi Inlier showing listric normal faulting which causes repetition of strata. The differences in dip between the Nsuze and Mozaan Groups is also shown. (modified after Matthews, 1990)

The Mandeva Formation is composed of coarse-grained quartz arenite with subordinate conglomerate and banded iron formation. Sub-rounded to rounded quartz and chert pebbles predominate in the conglomerates which fine upwards to quartz arenite. The lower conglomerate is auriferous in nature and the "reef" which was mined at Denny Dalton (Figure 2.2) is ~1 m in thickness. Matthews (1967) indicated that the lower part of the Mandeva Formation wedges out and represents the first member in a transgressive sequence. Due to the chemical maturity of the quartz arenites within the Mandeva Formation the depositional environment could have been a near-littoral, open-sea environment (Matthews, 1967).

The lower sandstones and conglomerates of the Mandeva Formation are overlain with a sharp contact by an 8 - 12 m thick green to black shale with interlayered banded iron formation. The sharp contact between the shale and underlying coarse sandstones indicates a marine transgression from lower shoreface to deep-marine.

At the base of the sandstones which overlie the banded iron formation a thin conglomerate of vein quartz pebbles indicates a hiatus and marine regression from shallow marine to near shore

environments. The sandstones above the banded iron formation feature minor argillaceous lenses at the end of each cycle. Symmetrical ripple laminations, bifurcating ripples, and interference ripples indicate that this formation was deposited in a near-littoral, shallow marine environment (Matthews, 1967).

The upper sandstones are overlain by a dark-grey shale unit which indicates an change in depositional environment to a tranquil deeper marine setting. This marks a marine transgression as the ~590 m thick Mpunga Formation consists of mainly dark-grey shale with minor wedge shaped quartzite intercalations (SACS, 1980).

The Qwasha Formation makes up the youngest unit in the Pongola Supergroup in the White Umfolozi inlier (SACS, 1980). It consists predominantly of ferruginous shale, with abundant thin lenses of quartzitic sandstones up to 3 m in thickness. This formation varies in thickness but is greater than 150 m (SACS, 1980) and is overlain with an angular unconformity by the Karoo Supergroup.

2.2.4 NONDWENI AREA

Pongola Supergroup rocks crop out as small isolated remnants within the Nondweni area, ~30 km west of the White Umfolozi Inlier (Figure 1.1). Versfeld (1988) correlated these outliers with units cropping out ~40 km to the southeast in the Nkandla region (Figure 2.1) which had been described by du Toit (1931). The succession in the area is fragmentary and therefore, Versfeld (1988) roughly correlated these units with the Nsuze Group identified by du Toit (1931) in the Nkandla area due to evidence of an angular unconformity between the underlying greenstone lithologies and the Pongola Supergroup rocks. Dixon (2003) however, correlated the conglomerates and quartz arenites with the basal Mozaan Group strata seen in the White Umfolozi Inlier to the east (see Chapter 6).

The basal unconformity exposed in the outlier at Mystery Hill (Figure 6.11) (Versfeld, 1988) is overlain by a ~20 m thick poorly sorted upward-fining succession of conglomerate and quartz arenite. This lowermost unit is overlain by a ~70 m thick cross-bedded quartz arenite (Versfeld, 1988). At Patsoana Mission (Figure 6.11) the basal unconformity is considered as occurring in a zone of no outcrop between pillowed basalt of the Witkop Formation (part of the Nondweni Greenstone Belt), and altered andesites of the Nsuze Group. The andesites are overlain by a thin talc schist which is subsequently overlain by conglomerates and quartz arenites identical to the succession at Mystery Hill.

2.2.5 NKANDLA AREA

In the southernmost part of the Kaapvaal Craton the Pongola Supergroup crops out as an elongate east-west inlier in the Nkandla area in northern KwaZulu-Natal. SACS (1980) stated that, unlike the northern inliers, only the Nsuze Group is evident in this region. However, regional mapping by Matthews (1990) indicated a folded unconformity within the Mhlatuze synclinal wedge, which was regarded as the contact between the Nsuze and Mozaan Groups, although this is not universally accepted (Weilers, 1990). Rocks correlative to the Mozaan Group have also been identified within the Buffalo River gorge area to the west of the main Nkandla Inlier (Dixon, 2003).

2.2.5.1 NSUZE GROUP

The Nsuze Group is preserved as the Nsuze Nappe, a steep imbricate set of northward-verging allochthonous sheets along the southern margin of the Kaapvaal Craton (Matthews, 1990). Groenewald (1984)working in the Nkandla area subdivided the Nsuze Group into five Formations: The Ndikwe, Mdlelanga, Qudeni, Vutshini and Ekombe Formations. The Ndikwe Formation is a ~1000 m thick sequence of volcaniclastic and epiclastic sedimentary rocks. The Mdlelanga Formation comprises a 1200 m thick succession of quartz wackes and quartz arenites and forms the base of the Nsuze Group, interfingering with the Ndikwe Formation. The 50 to 750 m thick Qudeni Formation overlies the Ndikwe and Mdlelanga Formations and comprises basaltic andesite, andesite and dacite volcanics. The Vutshini Formation is a ~1 000 m thick sedimentary succession of argillaceous and arenaceous rocks. The highest stratigraphic unit of the Nsuze Group is the Ekombe Formation which consists of a ~60 m thick succession of andesitic volcanics (Groenewald, 1984; Weilers, 1990).

2.2.5.2 MOZAAN GROUP

The Mhlatuze synclinal wedge forms the northern extent of the main Nkandla Inlier. The highly faulted and folded basal units to the south rest on granitoid basement and are defined by a well developed basal conglomerate, overlain by quartz arenites and subordinate banded iron formation (Matthews, 1990). Immediately north of the Mhlatuze wedge undeformed basal units of Pongola Supergroup are exposed and can be correlated to the lower units of the Mozaan Group within the White Umfolozi area due to the lack of volcanics, as well as stratigraphic correlation between the basal conglomerates and overlying banded iron formations (Matthews, 1990).

2.3 POST-PONGOLA SUPERGROUP INTRUSIVE ROCKS

2.3.1 USUSHWANA COMPLEX

The Usushwana Complex crops out in the Amsterdam area and southern Swaziland (Figure 2.1). The initial stage of the intrusion consisted of ultramafic to mafic sills within the Mozaan Group (Walraven & Pape, 1994). These intrusions were followed by an extrusive phase of dacitic and later rhyolitic volcanism (Hammerbeck, 1982). The final plutonic phase occurred in separate mafic and a felsic units which were subdivided into the Piet Retief Gabbro Suite and the Hlelo Granite Suite respectively (Hammerbeck, 1982). Hunter and Reid (1987) suggested a "best-estimate" age of ~ 2860 Ma for the Usushwana Complex as dating has yielded poorly constrained ages (Anhaeusser, 2006). However Davies *et al*. (1970) reported a Rb-Sr isochron age of 2874 ± 30 Ma for granophyres, whilst Hegner *et al*. (1984) obtained a Sm-Nd whole-rock/mineral age of 2873 ± 31 Ma for pyroxenites (Anhaeusser, 2006).

2.3.2 HLAGOTHI IGNEOUS COMPLEX

A number of post-Pongola Supergroup intrusive rocks intrude the Pongola Supergroup in the White Umfolozi Inlier. Petzer (2007) identified two separate post-Pongola Supergroup dyke swarms of basaltic to basaltic andesitic composition that trend northeast through the White Umfolozi Inlier. Groenewald (1984) identified dykes of similar composition and trend in the Nkandla area. These dykes are intrusive into the Hlagothi Igneous Complex which "yielded a poorly constrained Pb-Pb age of between 2980 and 3050 Ma" (Anhaeusser, 2006). Groenewald (1984) showed that the dykes have undergone low-grade metamorphism indicating that their intrusion pre-dates the main tectonic events that have affected the Pongola Supergroup.

2.3.3 POST-PONGOLA SUPERGROUP GRANITOIDS

Matthews (1985) identified three post-Pongola Supergroup granitoid intrusives in the areas around Piet Retief and southern Swaziland (Figure 2.1). The Spekboom Granite emplaced as a large elongate pluton to the southeast of the main Pongola basin in the Piet Retief area and crops out as a foliated medium- to coarse-grained biotite granite (Matthews, 1985). The Kwetta Granite crops out as a megacrystic, biotite hornblende granite (Matthews, 1985) in southern Swaziland, whilst the Godlwayo Granite forms a small, rectangular pluton composed of medium to fine-grained unfoliated adamellite (Matthews, 1985). Meyer *et al*. (1993) provided a zircon age for the Kwetta Pluton of 2671 ± 3Ma thereby constraining the minimum age for the deposition of the Mozaan Group.

Maphalala and Kröner (1993) however, obtained an age of 2824 ± 6 Ma (Pb/Pb single-zircon evaporation) for the post tectonic Mooihoek pluton, which crops out in southern Swaziland and crosscuts the folded Mozaan Group strata (Gutzmer et al., 1999). Gutzmer *et al*., (1999) obtained an age of 2837 ± 5 Ma (SHRIMP U-Pb zircon) for a quartz porphyry sill that intruded the Mozaan Group in southern Swaziland prior to folding. These age relationships imply that Pongola Supergroup deposition must have occurred prior to 2837 ± 5 Ma with deformation of the Pongola Supergroup occurring sometime between then and the intrusion of the Mooihoek pluton at 2824 ± 6 Ma (Gutzmer et al., 1999).

2.4 PHANEROZOIC LITHOLOGIES

2.4.1 NATAL GROUP

The Palaeozoic Natal Group which crops out extensively south of the White Umfolozi Inlier, is a monotonous succession of reddish grey arkosic sandstones with minor interbeds of siltstone, shale and conglomerates (Marshall, 2006). The Natal Group represents a sedimentary succession that was predominantly deposited in a fluvial, braided river environment (Marshall, 2006), in an elongate NE-SW trending basin, subparallel to the modern shoreline during the Ordovician (Liu & Cooper, 1998).

Three small outliers of Natal Group crop out within the Denny Dalton Mine area (Figure 2.2). The outliers are dominated by red-brown, monomict large-cobble to boulder conglomerate (Figure 2.7). The conglomerate is clast-supported with clasts of well rounded quartzite which show high sphericity. This unit is correlated with the Ulundi Member of the Durban Formation which crops out as lenticular bodies in the northern parts of the Natal basin (Marshall, 2006). The conglomerates overlie the Mozaan Group lithologies unconformably and are in turn unconformably overlain by Karoo Supergroup lithologies.

Figure 2.7: Ulundi Member monomict, cobble conglomerate within the Denny Dalton Mine area. Note pressure solution pit evident on the elongate cobble to the left of the hammer.

Figure 2.8: Dwyka tillite overlying glaciated pavement within the Denny Dalton Mine area. Striated basement rocks are Mozaan Group quartz arenites. Photo facing west - Arrow indicates glacial movement from right to left.

2.4.2 KAROO SUPERGROUP

The majority of the cover rocks which unconformably overlie the Pongola Supergroup belong to the Carboniferious to early-Jurassic Karoo Supergroup. The Dwyka Group forms the lowermost sequence in the Karoo Supergroup and was deposited during the Carboniferous-Permian glaciation (Johnson et al., 2006). The Dwyka Group sedimentary rocks are characterised by generally massive tillite with minor conglomerate, sandstones and argillaceous rocks (Johnson et al., 2006). The glacial origin for the Dwyka Group is clearly evident due to the highly undulatory pre-Karoo palaeotopography and numerous striated pavements on the underlying lithologies (Figure 2.8).

Within the White Umfolozi area Dwyka Group lithologies are dominated by massive and stratified diamictite facies. Massive diamictite consists of blue/grey mud matrix with random clasts of various size and composition. Both clast-rich and clast-poor diamictites are evident within the White Umfolozi area. Granitic clasts dominate and reflect the composition of the basement rocks in the area. Intercalated with the massive diamictite are stratified diamictite deposits, well defined bedding planes are evident with clasts occurring predominantly as dropstones. Glacial outwash conglomerates are rare, but are evident within the Denny Dalton Mine area.

The Permian Ecca Group overlies the Dwyka Group with a sharp contact (Johnson et al., 2006). At its base, the Pietermaritzburg Formation is characterised by argillaceous sedimentary rocks which were deposited in an extensive landlocked anoxic basin (Tankard et al., 1982). Within the mapping area the Pietermaritzburg Formation is absent but attains a maximum thickness of ~100 m on some of the scarps bordering the area.

Within the mapping area the Vryheid Formation rests directly on the Dwyka Group and caps a number of small buttes within the northern reaches of the area. The Vryheid Formation consists predominantly of deltaic coarsening upward cycles of muds, siltstones and immature sandstones (Johnson et al., 2006).

2.4.3 KAROO VOLCANISM

Early Jurassic eruptions of continental flood basalts halted Karoo sedimentation (Visser, 1998). A number of Karoo age dolerite dykes and sills intrude the White Umfolozi Inlier and form part of the feeder system to the Karoo flood basalts (Duncan & Marsh, 2006). Sills range in thickness from 5 to 50 m, with dykes ranging in thickness from centimetre to several metres in scale.

CHAPTER 3

STRATIGRAPHY AND SEDIMENTOLOGY OF THE MANDEVA FORMATION

3.1 INTRODUCTION

The Mandeva Formation forms the basal unit of the Mozaan Group within the White Umfolozi Inlier in northern KwaZulu-Natal. The formation comprises four siliciclastic lithofacies; three arenaceous, and one argillaceous, which attain a total thickness of ~200 m. The units comprise a basal conglomerate zone, the Denny Dalton Member, which is overlain by compositionally mature quartz arenites. A ~10 m thick unit of shale and banded iron formation, the Vlakhoek Member, separates the Klipkloof quartz arenite from the Upper quartz arenite. The Denny Dalton Member overlies the Bivane and Chobeni Formations of the Nsuze Group with an angular unconformity; the former having an average dip of 12° compared to 20° for the latter. Matthews (1967) indicated that this unit formed during the initial part of a marine transgression as it overlaps the underlying Bivane Formation volcanics. The Bivane Formation volcanics wedge out on the farm Vlakhoek 548 (Figure 3.1) and are only exposed at small erosional inliers in the extreme southern sectors of the inlier.

3.2 THE DENNY DALTON MEMBER

The Denny Dalton Member is a succession of conglomerates and grits which form the base of the Mozaan Group. This unit is laterally persistent and increases in thickness from ~12 m in the White Umfolozi sector in the northwest of the inlier to ~45 m in the Nobamba sector in the east (Figure 3.1). The Denny Dalton Member is characterised by its auriferous and uraniferous conglomerate zones which have been intermittently mined at Denny Dalton over the past century.

3.2.1 THE WHITE UMFOLOZI SECTOR

For ~3 km along strike from the White Umfolozi River in the White Umfolozi sector, no conglomerate is developed in the Denny Dalton Member (Figure, 3.1 and 3.2). It is defined by an 8 m thick succession of grits and trough cross-bedded quartz arenites which show restored palaeocurrent directions towards the east (Figure 3.2). Beds range in thickness from 20 to 50 cm and often show normal grading from grit at the base to coarse-grained quartz arenite at the top. Rock pavements covered with asymmetrical ripple marks are evident in the White Umfolozi River gorge (Figure 3.3) with restored palaeocurrent directions towards the east.

The northernmost outcrop of the Denny Dalton Member in the study area is within the Mvutshini stream (of which the Nsileni is a tributary) in the northwest extremities of the White Umfolozi sector (Figure 3.1). Outcrop is poor, with much of the member covered by Dwyka Group tillite. Coarse-grained quartz arenites dominate with minor grits developed at the base of a number of beds. Within the White Umfolozi sector the Denny Dalton Member is overlain with a sharp erosive contact by ~20 m of mineralogically mature coarse-grained quartz arenites.

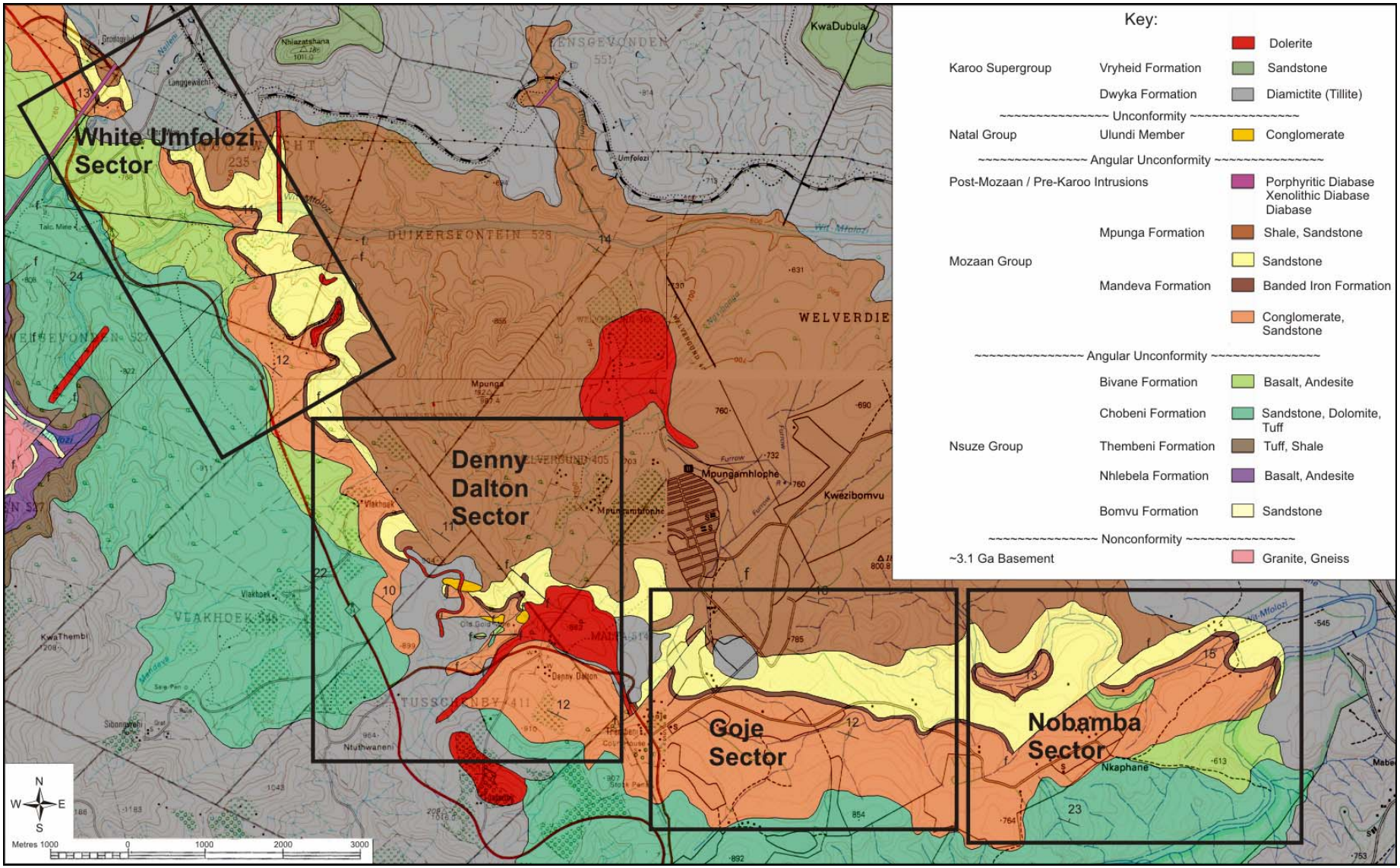

Figure 3.1: Geological map of the study areas in the White Umfolozi Inlier. See Appendix I for large version of map.

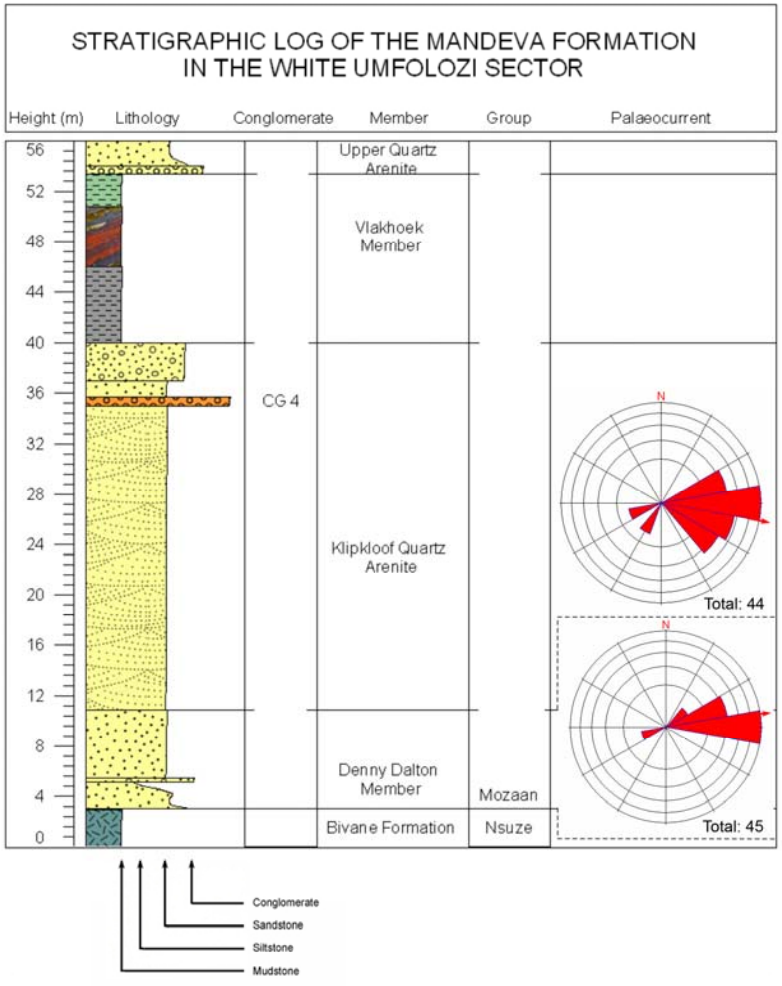

Figure 3.2: Stratigraphic log of the Mandeva Formation within the White Umfolozi sector. The palaeocurrent diagrams indicate restored palaeocurrent directions from crossbedding for the Denny Dalton Member (lower diagram) and the Klipkloof quartz arenite (upper diagram).

Figure 3.3: Assymetrical ripple pavement in coarse-grained quartz arenites of the Denny Dalton Member within the White Umfolozi sector. Pencil points to easterly flow direction.

3.2.2 THE DENNY DALTON SECTOR

The type area for the Denny Dalton Member crops out in the Nxobongo stream 1 km west of Denny Dalton in the Denny Dalton sector (Figure 3.1). Three overall fining-upwards cycles can be identified in the Denny Dalton sector (Figure 3.4).

Conglomerate 1 (CG 1) is a laterally discontinuous unit which form lenticular horizons that occupy east-northeast trending scour channels (Figure 4.3). Polymictic, matrix-supported pebble conglomerates are common, while clast-supported conglomerates, dominated by cobble-sized clasts are rare. Clast-supported, cobble-sized black chert conglomerates are dominant within the Denny Dalton Mine adit area (Figure 3.5 and 3.6). This conglomerate is laterally discontinuous, and is often absent from the stratigraphic record. The facies varies sharply over ~100 m as CG 1 crops out as a, matrix-supported, medium to large vein quartz pebble conglomerate within the lower reaches of the Nxobongo stream (Figure 3.7 and 4.5). At this locality the matrix is dominated by sand-sized quartz grains surrounded by sericite with virtually no pyrite. Pebbles are subrounded to rounded and comprise vein quartz and chert with a quartz-sericite-pyrite matrix. Pebble conglomerates are generally moderately-sorted with clasts size ranging from small to large-pebble. The conglomerates appear internally massive but the succession of beds show an overall fining-up pattern. The matrix is predominantly coarse-grained, well-rounded quartz with elongate sericite crystals and variable amounts of rounded to subrounded fine to coarse sand-sized detrital pyrite.

CG 1 fines upward over ~2 m to a laterally discontinuous pebbly grit or matrix-supported medium-pebble conglomerate. The clasts are predominantly subangular black chert and vein quartz. This unit was termed the "Hanging Wall Reef" during numerous exploration projects in the area, but forms part of the lowermost fining-upward cycle in the Denny Dalton Member and is therefore classified as part of CG 1. The pebbly grits of the upper CG 1 give way to ~5 to 7 m thick, compositionally mature, trough cross-bedded quartz grits with no sulphide mineralization.

The compositionally mature upper grits of the first cycle are overlain with a sharp, locally erosive contact by the second fining-upward cycle. The base of this cycle comprises a matrix-supported polymictic medium to large-pebble conglomerate (CG 2) which fines upward to a pebbly quartz arenite. Pebbles comprise subangular vein quartz and subangular to angular chert with a medium to coarse-grained quartz-sericite and localized pyrite matrix (Figure 3.8). A number of thin, normally graded beds (~20 cm thick) can be identified within this cycle, each consisting of a basal pebble lag and overlying pebbly quartz arenite.

This cycle is overlain with a sharp contact by the third fining-upward cycle. The base of this cycle comprises a polymictic medium-pebble conglomerate (CG 3) which fines to a pebbly grit (Figure 3.9). Pebbles are mainly subangular vein quartz with a medium to coarse-grained quartz-sericite matrix. The CG 3 is the uppermost unit in the Denny Dalton Member and is overlain with an erosive contact by a 20 m thick succession of mineralogically mature, trough cross-bedded quartz arenites, the Klipkloof quartz arenite.

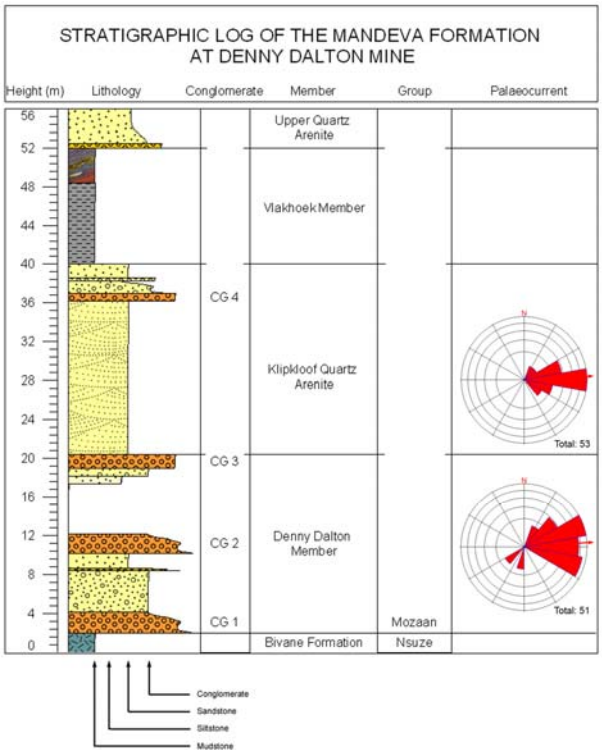

Figure 3.4: Stratigraphic log of the Mandeva Formation within the Denny Dalton Mine area. The palaeocurrent diagrams indicate restored palaeocurrent directions from crossbedding for the Denny Dalton Member (lower diagram) and the Klipkloof quartz arenite (upper diagram).

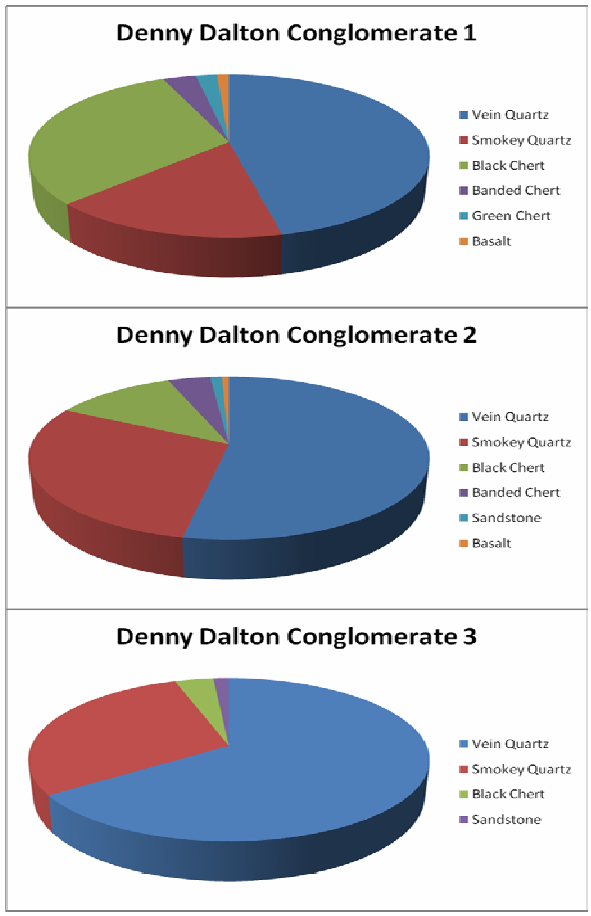

Figure 3.5: Pie charts calculating percentage compositions of clasts within conglomerates of the Denny Dalton Member in the Nxobongo stream downstream from the Denny Dalton Mine. Charts show an increase in vein quartz clasts in the upper conglomerates at the expense of black chert clasts.

Figure 3.6: Clast-supported cobble conglomerate (CG 1) within the mine area at Denny Dalton.

Figure 3.7: Matrix supported medium to large-pebble conglomerate (CG 1) overlying sheared Bivane Formation volcanics along basal unconformity within the Nxobongo stream.

Figure 3.8: Matrix-supported medium to large-pebble conglomerate (CG 2) within the Nxobongo stream. Note the iron-oxide staining within the conglomerate due to the oxidation of pyrite.

Figure 3.9: Matrix-supported medium-pebble conglomerate (CG 3) below the main crusher house in the Nxobongo stream.

3.2.3 THE GOJE SECTOR

Outcrop of the Denny Dalton Member in Goje township, 2 km east of Denny Dalton, (Figure 3.1) is obscured by post-Pongola cover lithologies, and recent housing and agriculture. However a narrow sliver remains exposed within the Goje stream and allows for stratigraphic correlation between the Denny Dalton and Nobamba sectors.

Within the sector, the Denny Dalton Member attains a maximum thickness of 25 m. The basal CG 1 thickens towards the east, attaining a maximum thickness of 5 m. Conglomerate distribution is discontinuous along strike; where present, the CG 1 is exposed as a polymictic large-pebble conglomerate. Overall clast size decreases from cobble to pebble between the Denny Dalton and Goje sectors, which may indicate a slight change in facies. Clasts are mainly subangular vein quartz with minor chert. The matrix is composed of coarse-grained subrounded quartz grains surrounded by sericite with minor pyrite. Where present, the CG 1 fines upward into trough cross-bedded gritty sandstones, which have an average thickness of 10 m. The grits comprise 90% quartz with thin (~3 cm) lenticular beds of fine-grained sericitic quartz sandstone. The grits form the top of the first fining-upward cycle and are overlain by conglomerates of the second cycle along a sharp contact.

The base of the second fining-upward cycle is dominated by a polymictic, medium-pebble conglomerate (CG 2). Clasts comprise subrounded vein quartz and chert within a medium sand-sized

quartz-sericite matrix. Locally, small detrital pyrite grains form bedding-parallel stringers within the matrix. The conglomerate fines upward to coarse-grained quartz arenite. The (CG 2) conglomerate succession thickens towards the east from the Denny Dalton sector as several single pebble lags are evident within the quartz arenite in the Goje sector.

The contact between the second and third fining-upward cycles is not well exposed in the Goje sector and the two zones appear to grade into each other. The overall ~10 m thick conglomerate zone - both CG 2 and CG 3 - consists of a number of normally graded beds ~20 cm thick which grade from a basal medium to coarse-pebble lag, to gritty or pebbly quartzite at the top of the bed (Figure 3.10). This conglomerate zone forms the uppermost unit of the auriferous Denny Dalton Member and is overlain with an erosive contact by a ~20 m thick package of mineralogically mature trough cross-bedded quartz arenites.

Figure 3.10: Medium-pebble conglomerate (CG 3) within the Goje stream.

3.2.4 THE NOBAMBA SECTOR

The Denny Dalton Member crops out within the Nobamba Tribal District ~6 km east of Goje in the White Umfolozi River valley. The White Umfolozi River has incised a large gorge through the Mozaan Group sedimentary rocks exposing the underlying Nsuze Group volcanics as a narrow inlier within the gorge. (Figure 3.1) The Denny Dalton Member attains a maximum thickness of 46 m with all three conglomerates present (Figure 3.11).

The basal unit above the unconformity is characterised by a ~1 m thick polymictic large-pebble to cobble conglomerate (CG 1). The conglomerate crops out extensively on the southern bank of the river (Figure 3.12), although sudden lateral variation along strike causes the conglomerate to pinch out over a strike of ~100 m and is not evident on the northern bank (Figure 3.13). This laterally discontinuous conglomerate can be correlated to the lowermost cobble conglomerates seen in the Denny Dalton sector. Where present, the conglomerate is matrix-supported and consists of subrounded clasts of vein quartz and chert with minor subordinate volcanic clasts. The matrix is dominated by coarse-grained quartz and sericite with no pyrite evident.

The CG 1 conglomerate is overlain with a sharp contact by unmineralized gritty sandstone. The grit attains a thickness of ~9 m in the section and is separated into two ~4.5 m thick beds with a minor ~50 cm pebble conglomerate evident at the base of the second bed. The base of the CG 2 fining-upward cycle crops out ~10 m above the basal unconformity and is defined by a polymictic small to medium-pebble conglomerate. Clast composition is predominantly subangular vein quartz with subordinate chert. The matrix is predominately quartz with minor sericite; no major sulphide mineralization is evident. The CG 2 cycle consists of three normally graded beds which consist of a basal small to medium-pebble conglomerate which fines upward to a grit, each bed attains an approximate thickness of 5 m.

The CG 2 cycle is overlain with a gradational contact by ~10 m of coarse-grained sandstones and grits with subordinate pebble conglomerates (Figure 3.11). The conglomerates attain thicknesses of ~50 cm to 1 m and crop out as basal units within separate beds of coarse-grained sandstone. The conglomerates are predominately small-pebble conglomerates with clasts of vein quartz and chert. Sulphide stringers are associated with the conglomerates as well as basal contacts of foresets in the sandstones.

The coarse-grained sandstones are overlain with a sharp contact by the CG 3 fining upward cycle. The base of this cycle is defined by a matrix-supported polymictic medium to large-pebble conglomerate which fines upwards to a small to medium-pebble conglomerate. Clasts are

predominately subangular vein quartz with only minor chert with a matrix composition of coarse-grained well-sorted quartz-pyrite-sericite. The CG 3 fining-upward cycle forms the uppermost unit of the Denny Dalton Member in the Nobamba sector and is overlain with a sharp erosive contact by a ~30 m thick unit of unmineralized trough cross-bedded quartz arenite, the Klipkloof quartz arenite.

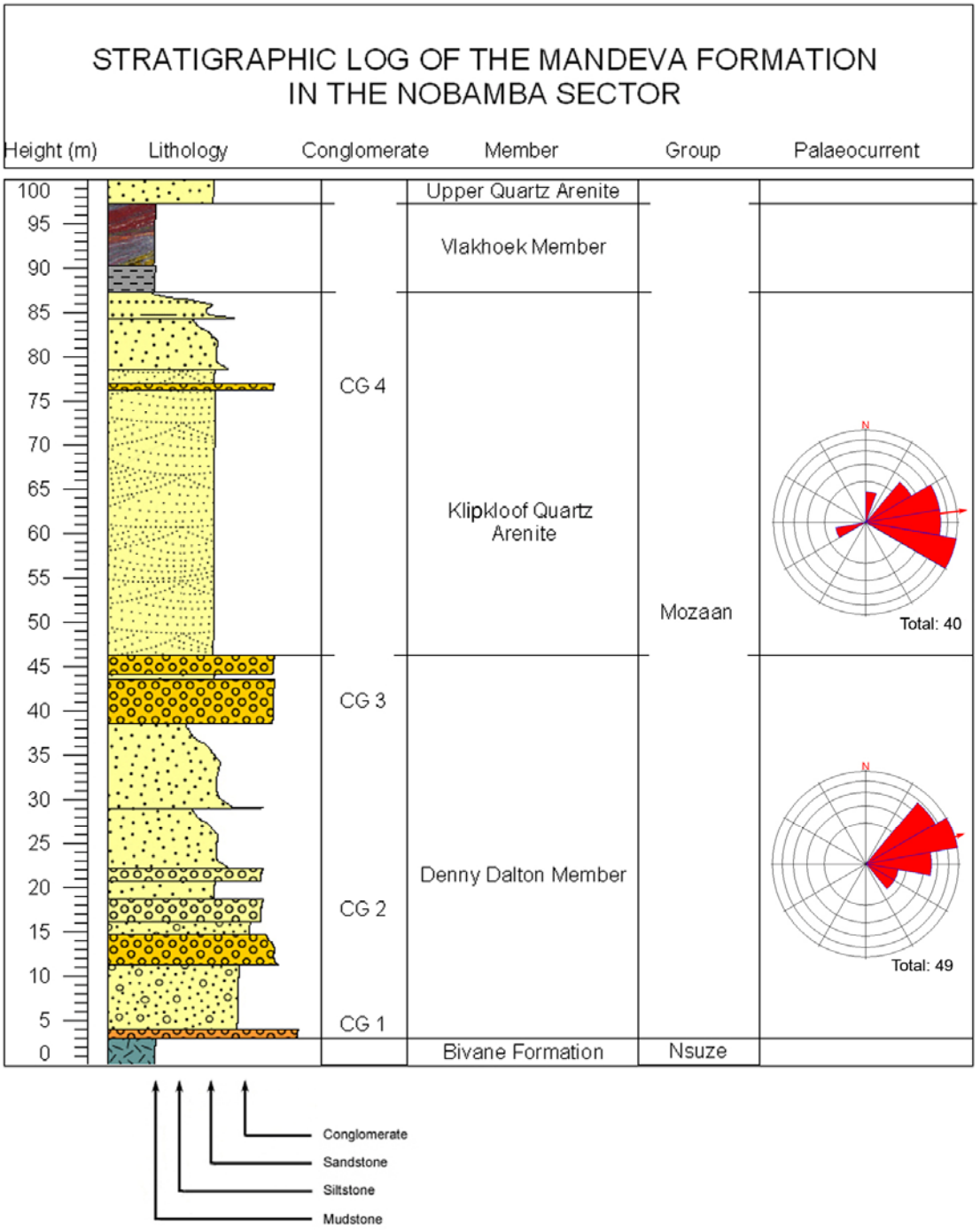

Figure 3.11: Stratigraphic log of the Mandeva Formation within the White Umfolozi River gorge in the Nobamba sector. The palaeocurrent diagrams indicate restored palaeocurrent directions from crossbedding for the Denny Dalton Member and the Klipkloof quartz arenite.

Figure 3.12: Matrix-supported large pebble to cobble conglomerate overlying sheared Bivane Formation volcanics along basal unconformity (dashed) on southern bank of the White Umfolozi River in the Nobamba sector.

Figure 3.13: Basal unconformity (dashed) with no conglomerate evident, northern bank of the White Umfolozi River, Nobamba sector. Coarse-grained sandstones overlie sheared Bivane Formation volcanics.

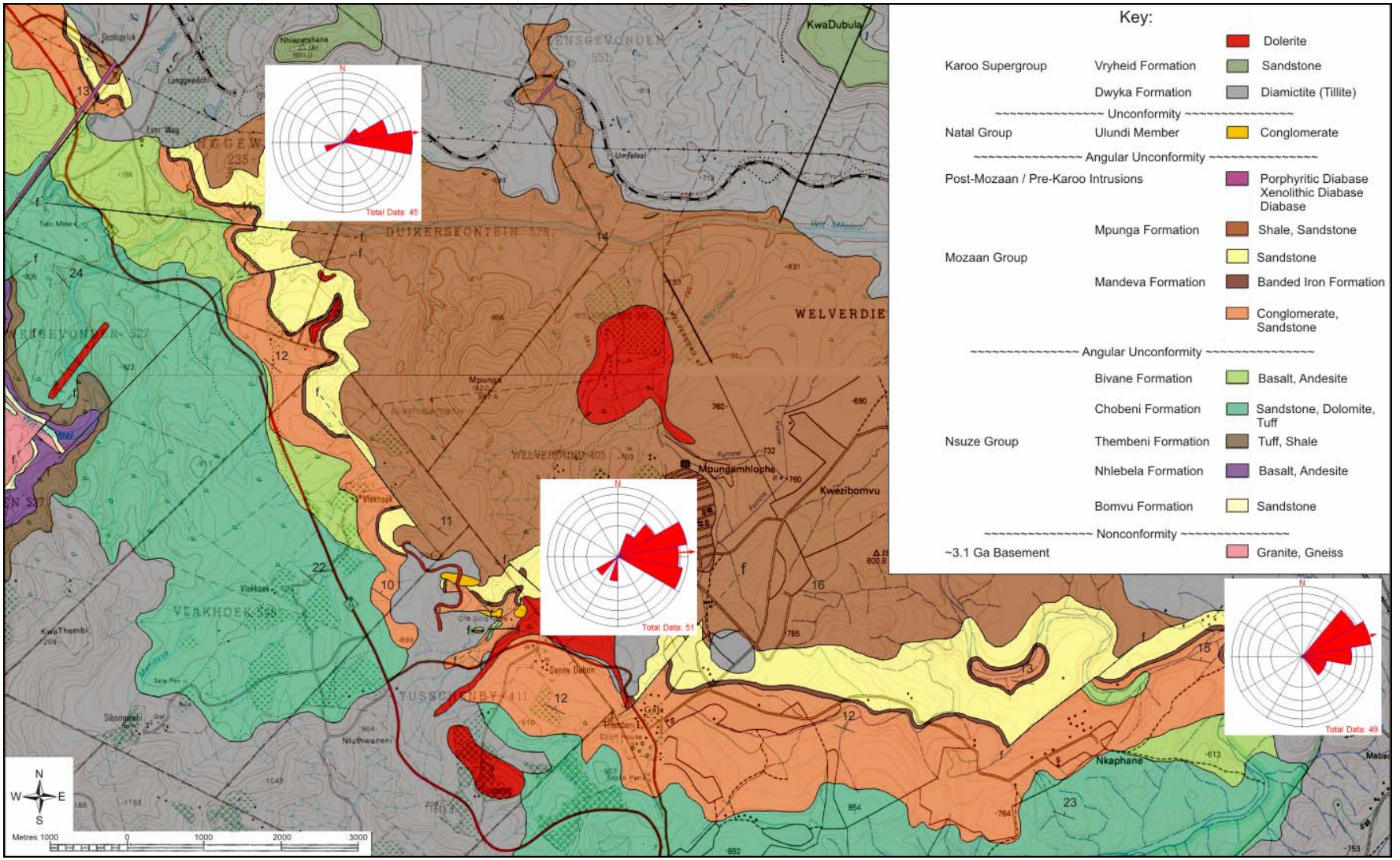

Figure 3.14: Rose diagrams showing palaeocurrent orientations of the Denny Dalton Member within the main mapping sectors of the inlier. Note the overall east north-easterly trend in all three sectors.

3.3 KLIPKLOOF QUARTZ ARENITE

The Denny Dalton Member is overlain throughout the White Umfolozi Inlier by mineralogically mature, medium to coarse-grained quartz arenites. The type area for the unit is within the White Umfolozi gorge on the farm Langgewacht 235 (Figure 3.1), now renamed Klipkloof. The quartz arenites attain a minimum thickness of 20 m in the White Umfolozi sector, with a maximum of 30 m in the Nobamba sector. Beds range in thickness from 0.5 to 2 m with a mean of ~1 m (Figure 3.15 and 3.16). Small-scale (~20 cm) trough cross-bedding is dominant within the individual beds. Mineralogically the quartz arenites are mature with a modal composition of > 95% quartz. Grains are well-rounded and very well-sorted. Restored palaeocurrent orientations for this unit show a consistent easterly trend with the vector mean of 84 readings being 086° (Figure 3.17). Herringbone cross-bedding and hummocky cross-stratification are both identified within the top ~5 m of the quartz arenite unit.

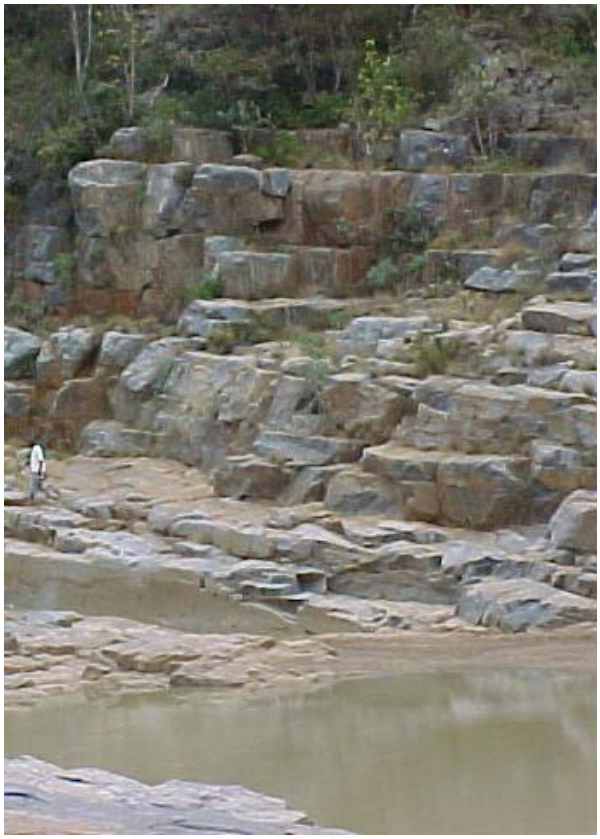

Figure 3.15: Thickly bedded Klipkloof quartz arenite within the White Umfolozi River gorge.

Figure 3.16: Possible large-scale hummocky cross-stratification in the Klipkloof quartz arenite, in the Nxobongo stream. Arrow points to hammer for scale.

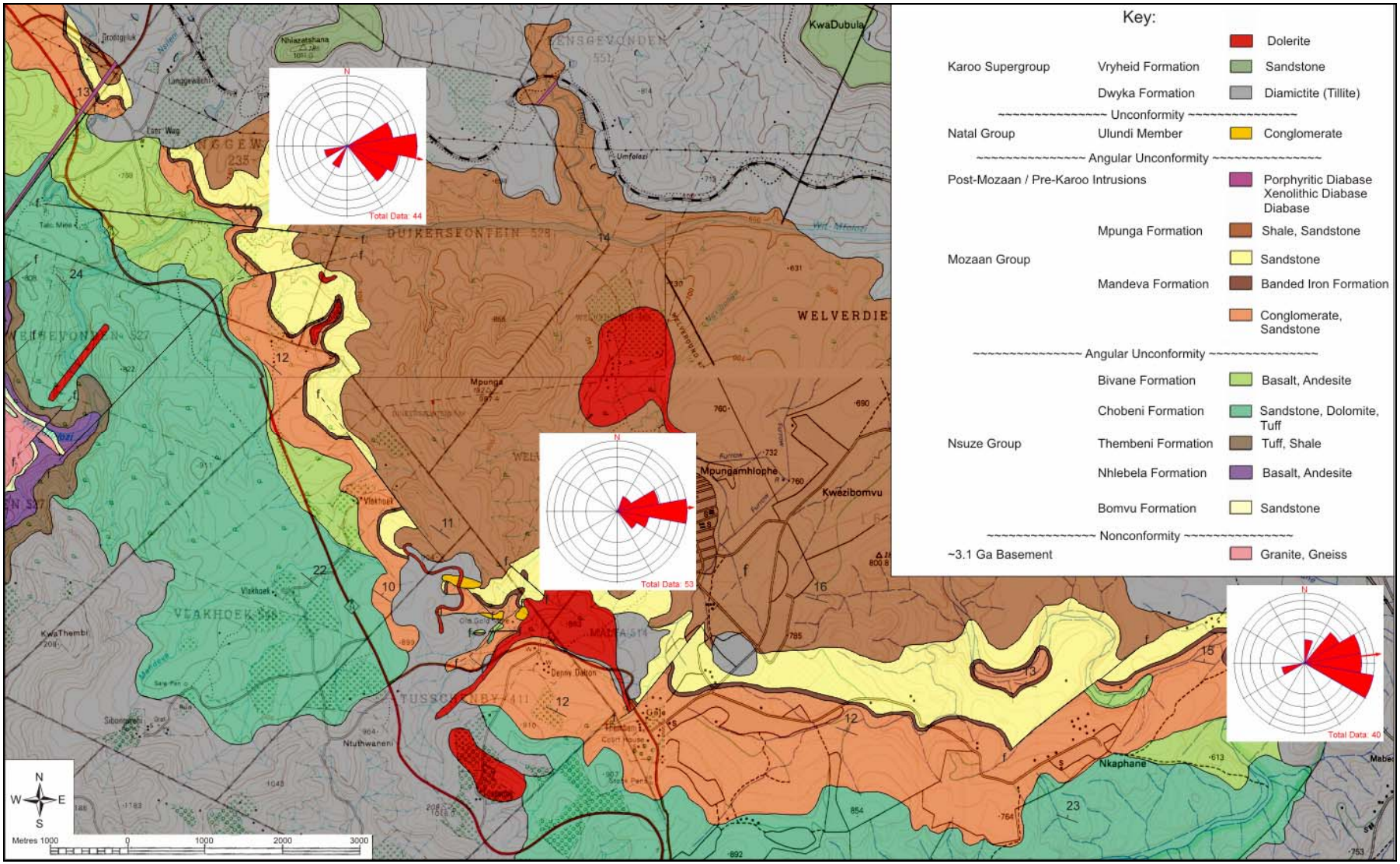

Figure 3.17: Rose diagrams showing palaeocurrent orientations of the Klipkloof quartz arenite unit within the main mapping sectors of the inlier. Note the overall easterly trend in all three sectors.

Overlying the quartz arenite with a sharp erosive contact is a medium to large-pebble conglomerate (CG 4) ~0.5 to 1 m thick. Clasts are mainly vein quartz with only minor massive and banded chert, and range in roundness from subangular to rounded (Figure 3.18). The interstitial matrix is predominantly quartz with localized pyrite evident within the White Umfolozi sector. This unit is laterally extensive and can be identified throughout the ~15 km strike of the inlier. The conglomerate is sharply overlain by gritty quartz arenite with graded beds having an average thickness of ~1.5 m (Figure 3.19). Two normally graded beds are identified within the White Umfolozi sector and form the uppermost unit within the Klipkloof Member. Within the upper of the two beds mud clasts and thin siltstone drapes are identified within the gritty sandstones.

Figure 3.18: Subrounded vein quartz conglomerate (CG 4), White Umfolozi sector.

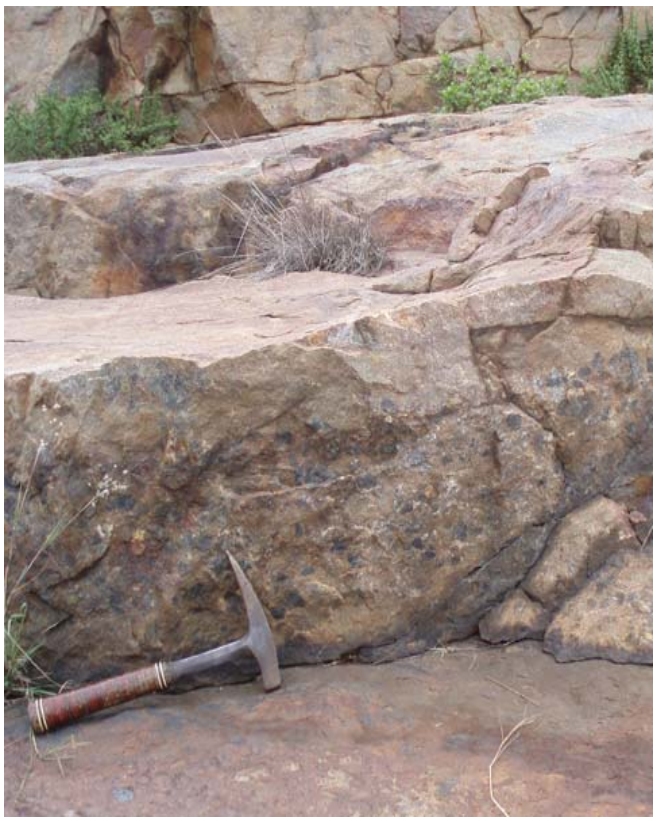

Figure 3.19: Conglomerate (CG 4) overlain by upward fining grits ~ 4 m below the contact with the overlying Vlakhoek Member shales, White Umfolozi sector.

The Klipkloof unit is capped by small dune bedforms with amplitudes of ~10 cm and wavelengths of ~1 m (Figure 3.20). The dunes are symmetrical with dune crest orientations of ~40°/220° and crop out in several river-washed pavements throughout the inlier (Figure 3.21 and 3.22; Appendix I). Dune crests are undulatory and bifurcating dunes are common. Dunes crests are often truncated by later washout structures. The dune pavements are overlain with a sharp and locally sheared contact by interbedded ferruginous shales and siltstones of the Vlakhoek Member.

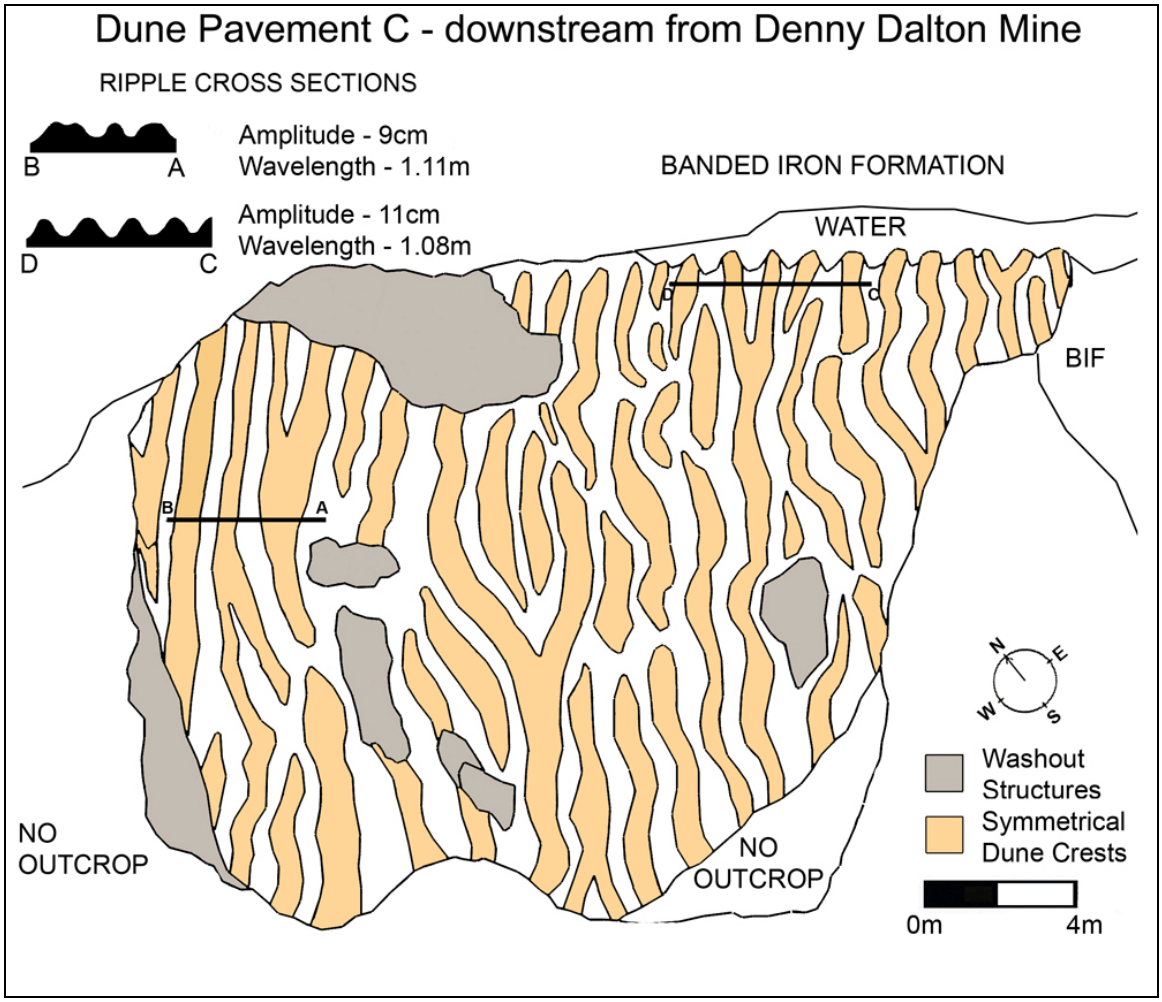

Figure 3.20: Plan of the dune pavement C exposed in the Nxobongo stream downstream from the Denny Dalton Mine.

Figure 3.21: Dune pavement capping the Klipkloof quartz arenite in the Nxobongo stream, Denny Dalton sector. Dune crests orientated northeast-southwest.

Figure 3.22: Dune pavement capping the Klipkloof quartz arenite in the White Umfolozi sector. Dune crests orientationated east northeast-west southwest.

3.4 VLAKHOEK MEMBER

The Klipkloof quartz arenite is overlain with a sharp and locally sheared contact by shales and siltstones of the Vlakhoek Member. This sharp contact is identified within the White Umfolozi, Denny Dalton and Goje sectors (Figure 3.23). In the Nobamba sector however, alternating beds of shale and coarse siltstone form a fining-up sequence from the underlying gritty quartz arenites (Figure 3.24). The Vlakhoek Member attains an average thickness of 11 m and is laterally persistent throughout the White Umfolozi Inlier. The lowermost 5 m of the member comprises dark grey to black laminated mudrock with interlayered fine siltstone at its base. The siltstone interlayers attain a maximum thickness of 5 cm with a mean of 2 cm and are only present within the lower 2 m of the unit. Ferruginous mudstone interlayers are evident in the upper 2 m of the unit and exhibit a characteristic faint red colouration.

Figure 3.23: Sharp, locally sheared contact between Klipkloof quartz arenite and Vlakhoek Member shales, Nxobongo stream, Denny Dalton sector. Photo facing northeast.

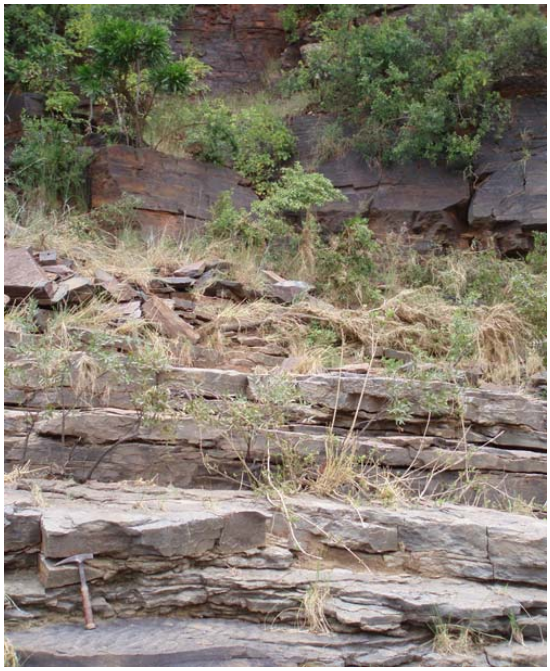

Figure 3.24: Upward fining sequence below Vlakhoek Member shales, White Umfolozi River gorge, Nobamba sector. Photo facing west.

The lower mudstone unit is overlain by 3 m of well banded, Superior-type banded iron formation (Figure 3.25). Macrobands of iron oxides are interlayered with bands of jaspilite, the former being predominantly magnetite. Macrobands are separated by sharp contacts, with bands ranging in thickness from 1 to 5 cm in thickness (Figure 3.26). Microbands 1 to 3 mm thick are often present within jaspilitic macrobands. The banded iron formation is overlain with a gradational contact by ~3 m of foliated green shale.

Figure 3.25: Vlakhoek Member banded iron formation and green shale overlain with sharp erosive contact by Upper quartz arenites of the Mandeva Formation, White Umfolozi River gorge on farm Langgewacht 235, White Umfolozi sector (photo courtesy Dr. A. Hofmann). Photo facing east.

Figure 3.26: Magnetite and jaspilite macro-banding, Vlakhoek Member, White Umfolozi River northeast of Nkaphane, Nobamba sector.

3.5 UPPER QUARTZ ARENITE

The foliated green shale of the Vlakhoek Member is overlain with a sharp erosive contact by a thin pebble conglomerate layer which consists mainly of vein quartz. This conglomerate layer is continuous throughout the White Umfolozi Inlier, but thickens from a single pebble lag in the White Umfolozi sector (Figure 3.27) to a 5 to 10 cm thick small pebble conglomerate in the Goje and Nobamba sectors. Conglomerate is followed by a succession of normally and inversely graded quartz-rich sandstone beds. Normally graded beds comprise coarse grit at the base which fines up to medium to coarse-grained sandstone which hosts symmetrical and interference ripple bedforms, and is capped by thin mud drapes which are affected by polygonal desiccation cracks, (Figure 3.28). Rip-up mud clasts are evident within the coarser fraction. Inversely graded shale/siltstone/sandstone beds are identified towards the top of the succession. This pattern is dominant for ~9 m above the contact with the Vlakhoek Member. Above this, the thin mud intercalations are not evident with a coarse-sand to grit fraction dominant. These beds show planar and trough cross-bedding with no major coarsening or fining upward patterns; however multidirectional and symmetrical ripple laminations (Figure 3.29) are evident on the bedding surfaces. Noffke et al. (2008) identified microbially induced sedimentary structures such as gas domes (Figure 3.30) along the bedding surfaces of the upper quartz arenite unit. The upper quartz arenites of the Mandeva Formation are overlain with a sharp contact by ferruginous shales of the Mpunga Formation.

Figure 3.27: Sharp erosive contact between Vlakhoek Member green shales and upper Mandeva quartz arenites. Note single pebble lag along contact and fining upward sequence to top of the bed. (photo courtesy Dr. A. Hofmann).

Figure 3.29: Multidirectional ripple marks in upper Mandeva quartz arenites in the White Umfolozi sector.

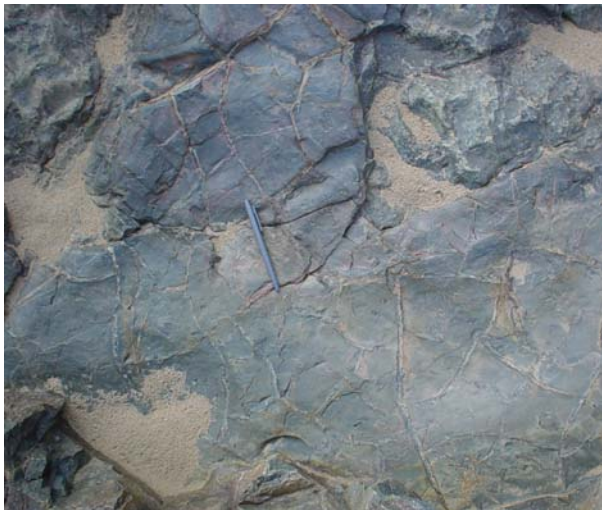

Figure 3.28: Polygonal desiccation cracks in mud drape, upper Mandeva quartz arenites within the White Umfolozi sector (photo courtesy Dr. A. Hofmann)

Figure 3.30: "Gas dome" structures within upper Mandeva quartz arenites in the White Umfolozi sector.

3.6 MINERALOGY

Standard petrographic thin sections were made from conglomerates, grits and quartz arenites from the Mandeva Formation. All sections were taken from samples recovered from drill holes TSB 06-23 drilled within the mine area, and TSB 07-26 which was drilled ~1 km north of the mine. Exact drill hole co-ordinates are however confidential, samples were taken with consent from Acclaim Exploration.

Table 3.1: Relative abundance and genetic classification of clasts and minerals in the Mandeva Formation conglomerates.

Type	Clasts (> 2mm)	Matrix minerals (< 2mm)	
		Allogenic	Authigenic
Quartz	X	X	X
Chert	X	X	
Sericite			X
Rutile		X	
Monazite		X	
Muscovite			X
Zircon		X	
Sandstone	X		
Mafic volcanic	X		

3.6.1 CONGLOMERATES

Conglomerates within the Mandeva Formation are predominantly matrix-supported with clast-supported conglomerates only evident in CG 1. Clasts in all conglomerate zones comprise varying amounts of black chert, banded chert and vein quartz clasts in a sandy matrix of predominantly quartz and sericite with minor muscovite.

Vein quartz pebbles predominate in all but the CG 1 conglomerate where black chert pebbles form the most abundant variety. Vein quartz pebbles are glassy white to mottled blue-grey in colour. A variety of chert pebbles occur within the conglomerates, with black chert being most abundant. Green and banded cherts occur as rare well-rounded small-pebbles within the CG 1 conglomerate. Pebbles of sandstone and basalt rarely occur but have been identified within the CG 1.

The matrix of the conglomerates consists of sand-sized quartz and sericite, with varying amounts of pyrite. Rutile, leucoxene, monazite, chromite and zircon constitute the heavy minerals in the matrix and are discussed in detail in the ore mineralogy section in Chapter 4 (page 69). Rutile, monazite and zircon all occur as rare grains ~0.5 mm in diameter.

Quartz grains are well-rounded to sub-rounded and form the predominant matrix mineral within the Mandeva Formation conglomerates. Quartz cementation is identifiable by relict grain boundaries of quartz grains (Figure 3.32). Secondary quartz fills fractures in many minerals and often partially replaces pyrite grains. Pyrite constitutes the second most abundant mineral within the matrix of all the conglomerates. A number of pyrite types are present in the matrix and are discussed in further detail in the ore mineralogy section (page 69)

Fine, clay-sized sericite occurs throughout all the Mandeva Formation conglomerates and is concentrated in fractures and pore spaces between sand-sized quartz grains in closely packed areas. In zones of larger pore space sericite is evenly distributed throughout the matrix and constitutes a large portion of minerals present. Sericite often replaces weathered pyrite grains and also forms on corroded grain boundaries (Figure 3.33) and would have formed under low temperature diagenetic or metamorphic conditions.

3.6.2 GRITTY QUARTZ ARENITE

Gritty quartz arenites are interlayered with the lower conglomerates within the Denny Dalton Member and are composed of predominantly granule-sized vein quartz with a sericite matrix. Grains are generally sub-rounded to rounded and range in size from small pebble-sized vein quartz and chert to coarse sand-sized quartz grains. Pyrite grains occur as rounded sand-sized grains. Overgrowths of quartz and sericite are also common on detrital pyrite grains (Figure 3.33).

Large pebble-sized clasts are rare within the gritty quartz arenites, but where present, well-rounded vein quartz clasts are dominant with black chert being a minor constituent. Vein quartz clasts are smoky to mottled blue-grey in colour. Fine-grained sericite matrix is uniformly distributed throughout the gritty quartz arenites and occurs as fine-grained elongate crystals which surround larger quartz grains. Sericite often occurs as distorted flakes between clastic grains.

3.6.3 KLIPKLOOF QUARTZ ARENITE

The quartz arenites within the Mandeva Formation are compositionally mature and contain more than 95% quartz. The arenites are medium to coarse-grained with well-rounded quartz grains dominant. Within the Klipkloof quartz arenites, coarse-grained monocrystalline quartz exhibits undulose extinction with stylolites at grain boundaries. No matrix is evident with grain-grain boundaries dominant (Figure 3.34). Based on the QtFL diagram all samples plot within the quartz arenite field (Figure 3.31).

3.6.4 UPPER QUARTZ ARENITE

The upper sandstone unit which crops out above the Vlakhoek Member has a high, (~95%) quartz content. Quartz grains are subrounded and well-sorted, with most boundaries being sutured grain-grain contacts. The unit consists of normally and inversely graded beds (Figure 3.35). The high overall quartz content of the upper sandstones also places this unit in the quartz arenite field on the QFL diagram (Figure 3.31).

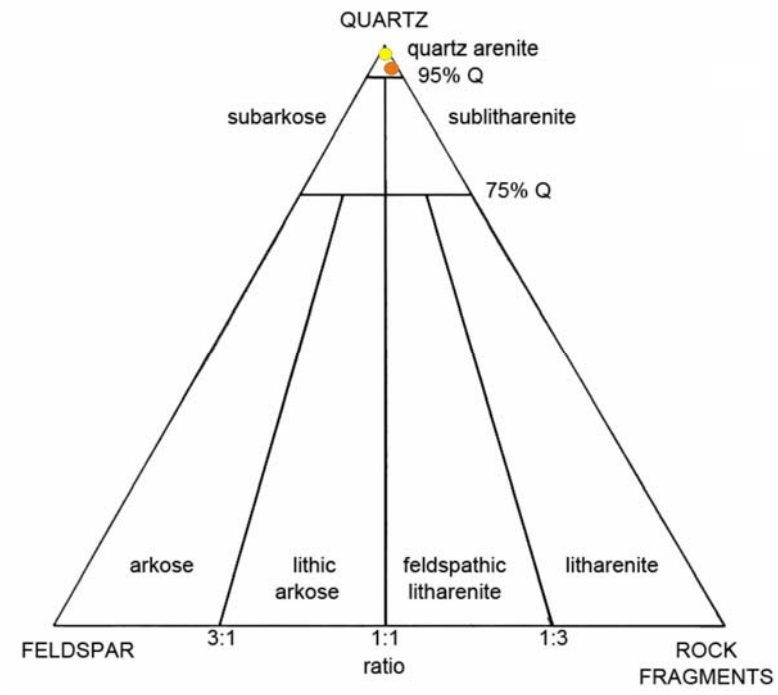

Figure 3.31: Sandstone classification diagram, indicating classifications of thin section samples. (Yellow - quartz arenite; Orange - conglomerate). (modified after Folk, 1974).

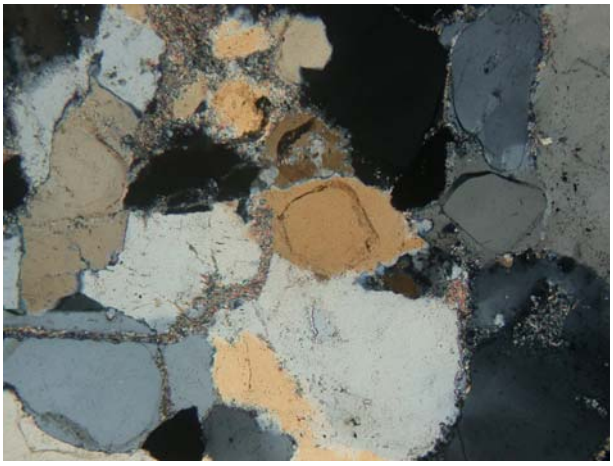

Figure 3.32: Photomicrograph of quartz cement overgrowths around quartz grains within the basal conglomerate zone. Note quartz cement surrounding quartz grain in centre of photo. Field of view: 4 mm

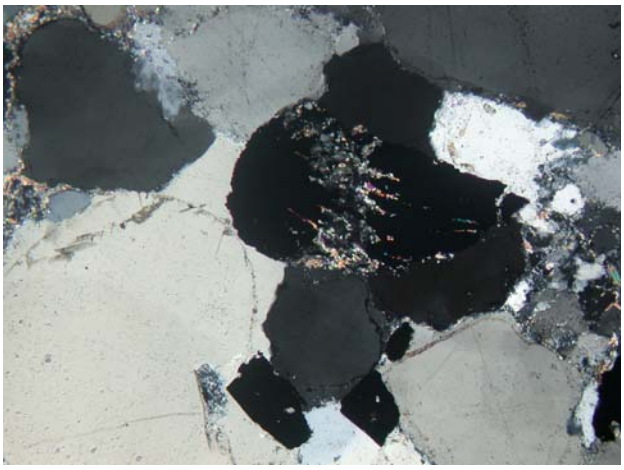

Figure 3.33: Photomicrograph of quartz and sericite overgrowth on rounded pyrite within gritty quartz arenite. Field of view: 4 mm

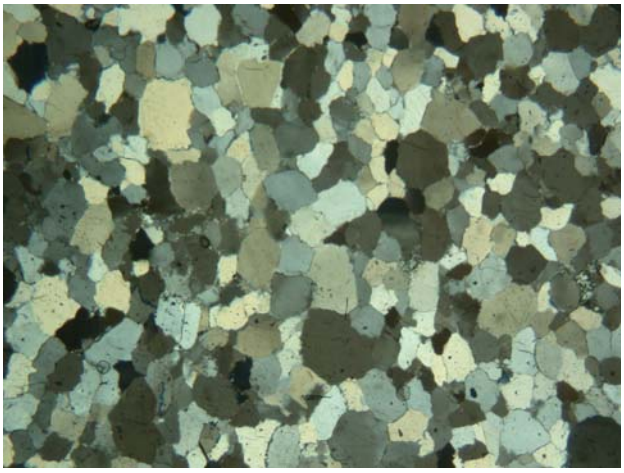

Figure 3.34: Photomicrograph of Klipkloof quartz arenite. Note sutured grain-grain boundary contacts within the quartz arenite. Field of view: 4 mm

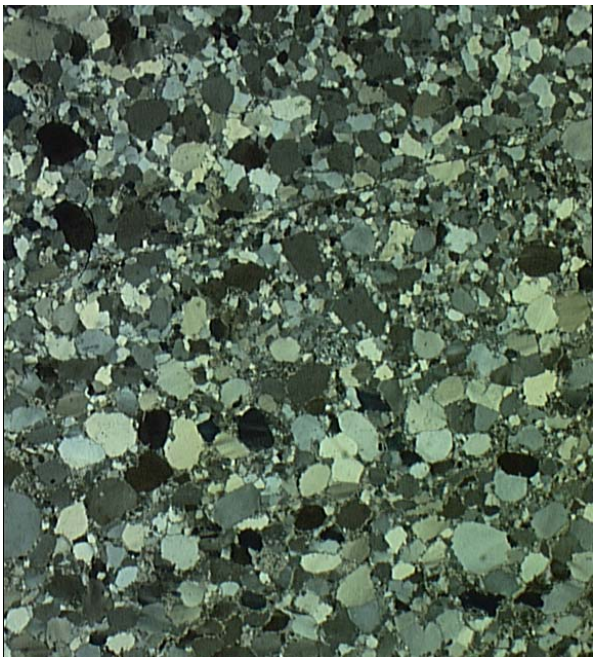

Figure 3.35: Photomicrograph of upper quartz arenite overlying the Vlakhoek Member. Note the graded bedding in the quartz arenite. Field of view: 4 mm.

3.7 STRUCTURAL GEOLOGY

3.7.1 NSUZE GROUP

Within the White Umfolozi Inlier, D_1 listric normal faulting orientated ~320º caused pre-Mozaan Group tilting of the Nsuze Group strata to ~10º NE within the White Umfolozi Inlier. Subsequent to the listric faulting, pre-Mozaan D_2 extension resulted in further normal faulting with a ~060°/240° trend. This generated a number of horst and graben structures within the Nsuze Group in the White Umfolozi Inlier. The vertical offset of the tilted strata, combined with current topographic features, create apparent sinistral and dextral offsets along these faults in the order of 100's of metres dependent on their hanging wall slip orientations.

3.7.2 MOZAAN GROUP

Within the White Umfolozi Inlier, post-Mozaan Group NW-directed D_3 thrusting set up numerous 1 - 10 cm thick bedding-parallel shears within the more argillaceous rocks of the Mandeva Formation. The dune pavement which caps the Klipkloof quartz arenite and the overlying Vlakhoek Member are separated by a ~100 cm thick bedding-parallel shear (Figure 3.37). Shearing is difficult to determine, but is probably on a cm-scale and could have taken place along contacts during the folding of the inlier. Shearing is also found along the Nsuze-Mozaan unconformity. This produced a distinct fabric in the underlying Bivane Formation volcanics along the unconformity. This fabric seems to be present throughout the White Umfolozi Inlier. Within the Nxobongo stream the fabric has a dip and strike of 16°/089° (Figure 3.7 and 3.13). Folding within the White Umfolozi Inlier probably occurred during the post-Mozaan Group D_3 compressional event. The inlier is folded in a shallow NE trending syncline (Figure 3.1). Minor folding is restricted to argillaceous units within the Mozaan Group with fold axes orientated 060° (Figure 3.36, 3.38 and 3.39).

Normal, post-Mozaan Group reactivation along some of the older ~320º orientated Nsuze-age faults has been identified within the Denny Dalton Mine area on farm Vlakhoek. This normal faulting represents the D_4 post-Mozaan Group deformation event, causing repetition of strata, and could account for the ~10º NE dip of the Mozaan Group lithologies in the White Umfolozi Inlier.

D_5 deformation set up a number of ~100º trending normal faults throughout the inlier. Faulting during this period resulted in a number of horst and graben structures with offset on this fault system in the 1 - 100 m scale. These faults are truncated by, and thus predate, the Karoo unconformity (Figure 3.40).

D_6 deformation within the inlier is identified by a number of ~020º trending normal faults. This fault system shows offset in the 20 - 100 m scale and offsets all lithologies within the study area. Conjugate ductile fracture sets trending ~020/246 indicate a (σ_1) orientation of ~040°/220º with maximum extension (σ3) orientated at ~130º/310º during this deformation event.

Figure 3.36: Folding within Vlakhoek Member banded iron formation in the Nobamba sector. Fold axes are shallow plunging and orientated ~060°.

Figure 3.37: Bedding parallel shearing along contact between the Klipkloof dune pavement and the overlying Vlakhoek Member shales in the Nxobongo stream north of the Denny Dalton Mine. Displacement however is difficult to determine. Photo facing northeast.

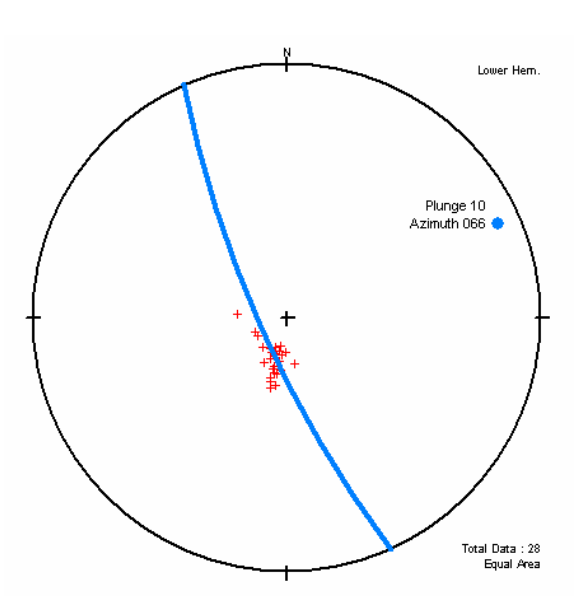

Figure 3.39: Stereonet plot of average bedding from 28 localities from Mandeva Formation throughout the White Umfolozi Inlier. Average bedding readings indicate that the inlier is folded into a shallow NE plunging synform.

Figure 3.38: NW imbrication within the Klipkloof - Vlakhoek shear zone, within the Nxobongo stream north of the Denny Dalton Mine, Denny Dalton sector. Imbrication shows top-to-the-right movement.

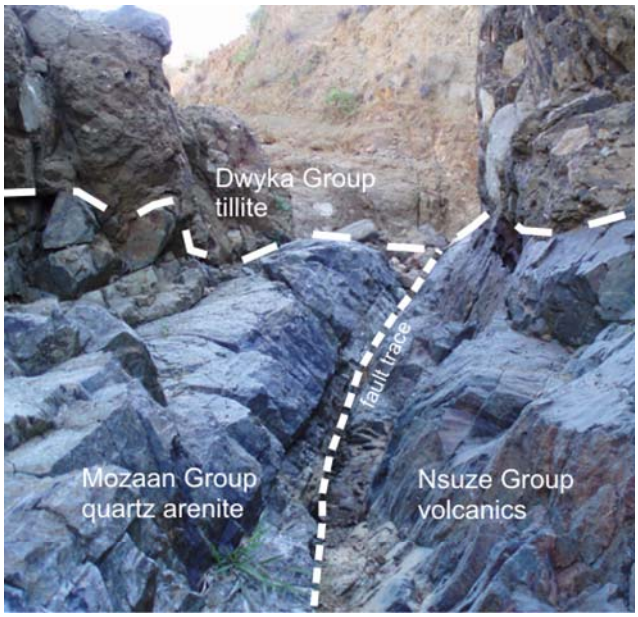

Figure 3.40: D_5 Pre-Karoo 100° normal fault within the Denny Dalton Mine area. Nsuze Group volcanics crop out in the footwall on the right with Mozaan Group quartz arenites in the hanging wall on the left. Dwyka tillite lies unconformably above both lithologies and truncates the fault. Photo facing west.

3.8 DISCUSSION

3.8.1 THE DENNY DALTON MEMBER

The onlapping nature of the Denny Dalton Member with respect to the underlying Nsuze volcanics is indicative of uplift, tilting and erosion of the Nsuze Group, prior to deposition of the Mozaan Group rocks. The creation of accommodation space for Mozaan Group deposition could have been due to basin subsidence or base level rise.

The Mozaan Group sedimentary rocks are predominantly shallow marine in origin. However some units in the lower Mozaan Group can be attributed to near coastal, braidplain environments. The Denny Dalton Member is correlated with the Dipka Member of the Sinqeni Formation within the main Pongola basin (see Chapter 5). The Dipka Member represents a braidplain depositional environment due to the unimodal southerly palaeocurrent directions in the trough and planar cross-bedded sandstones (Beukes & Cairncross, 1991).

The auriferous conglomerates at Denny Dalton are similar to fluvial bar-and-channel deposits of the Central Rand Group of the Witwatersrand Supergroup as described by Frimmel and Minter (2002). Large clast size and unimodal east-north-easterly palaeocurrent orientation suggests a relatively proximal palaeo-source area to the west of the inlier (Figure 3.14). The palaeocurrent orientations differ however from those of the main basin and reflect an alternate, more southerly provenance area for the Denny Dalton Member. The relative close proximity of the north-west trending basement high axis to the White Umfolozi Inlier (Figure 2.1) could account for the palaeocurrent differences. The inlier crops out on the south-western edge of the Pongola basin and onlaps onto the underlying basement, accounting for relatively thinner units compared to the main basin.

Fine-grained, high-density (Specific gravity > 3.0) ore minerals, such as gold, pyrite and uraninite undergo entrainment sorting and are often deposited within pore spaces between larger, less dense particles (cobbles and pebbles) thereby being sheltered and permanently deposited before having been transported far from the sediment source (Carling & Breakspear, 2006). The lateral discontinuity and thin nature of the cobble conglomerates within the Denny Dalton Member is indicative of lag deposits formed in channel scours during short-term degrading river flow conditions within a braided alluvial plain (Carling & Breakspear, 2006).

3.8.2 KLIPKLOOF QUARTZ ARENITE

The trough cross-bedded Klipkloof quartz arenites are representative of a shallow marine environment within the fair weather wave base (Figure 3.41). Trough cross-bedding is the dominant sedimentary structure whilst planar cross-bedding is a minor constituent; a uniform easterly palaeocurrent orientation is seen throughout the inlier. The herringbone crossbedding and large scale hummocky cross-stratification suggest deposition in a storm-dominated, high-energy shoreface environment (Hofmann et al., 2004). Von Brunn and Hobday (1976) identified ENE-trending linear channels with distinct pebble lags at their base within the Klipkloof quartz arenite. The mineralogical maturity of the quartz arenites as well as cross cutting scour channels which contain trough cross-bedding is evidence for intense reworking by shallow marine processes. This mineralogical and textural maturity reflects multiple reworking within tidal sands (Von Brunn & Mason, 1977).

3.8.3 UPPER CONGLOMERATE (CG 4)

The upper-most conglomerate which overlies the Klipkloof quartz arenites with a sharp contact is laterally extensive throughout the White Umfolozi Inlier. This conglomerate likely represents a high energy erosional lag deposit which forms on the transgressive ravinement surface and marks the onset of a major marine transgression into the Pongola basin (Figure 3.41). The overlying grit and coarse-grained quartz arenite unit shows no internal structure except for upward fining, graded bedding. Towards the top of the unit, thin mud drapes cap grit beds which contain rip-up mud clasts. This zone can be interpreted as a gradually deepening mid-to-lower shoreface environment. The laterally extensive dune pavement (Figure 3.21) which caps the grits would have formed in a lower shoreface environment possibly as a result of rip current activity (Reineck & Singh, 1975).

3.8.4 VLAKHOEK MEMBER

The laterally extensive banded iron formation unit which crops out throughout the White Umfolozi Inlier and into the northern regions was most likely deposited in a large epicontinental sea. This setting would allow for very calm water environments where clastic input would be minimal. Due to its lateral continuity throughout the Pongola basin, the Vlakhoek Member is defined as Superior-type iron formation and thus represents the oldest documented iron formation of this type in the world (Alexander et al., 2008). This extensive unit defines a large basinward transgression and was deposited in a shelf environment in calm waters below the storm wave base.

The nature of the underlying dune pavement and sharp contact with the overlying shales points to a sudden transgression from lower shoreface to transition zone below the fair weather wave base.

Interlayered beds of fine-grained ripple-marked sandstone and shale within the lowermost 3 m of the Vlakhoek Member could signify tidal or storm fluctuations above the storm wave base.

Continuous deepening is indicated by the lack of sandstone layers and occurrence of thin jaspilitic beds interlayered with shales below the banded iron formation. This ~2 m thick zone represents the initial onset of chemical precipitation in relatively deeper water below the storm wave base on a sediment starved shelf, where clastic sediment input was considerably reduced. Although the exact water depth is difficult to determine Alexander et al. (2008) propose that the Vlakhoek Member was deposited in very shallow water shelf environments. This hypothesis would indicate a very wide, gradually subsiding shelf with a prograding coastline that could advance 10's of kilometres into the basin with only a small sea level rise. Alexander et al. (2008) suggested that due to the low abundance of elements such as Al, Ti, Zr, Hf, Y, and Th, the banded iron formation formed as very pure chemical sediments with little clastic input.

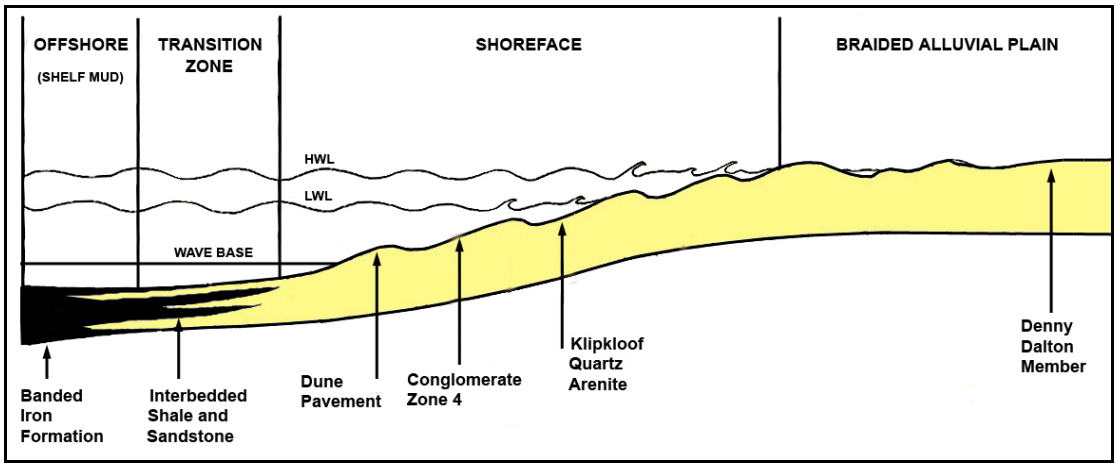

Figure 3.41: Schematic beach profile after Reineck & Singh (1975) showing depositional environments of the major units of the Mandeva Formation during initial marine transgression.

3.8.5 UPPER QUARTZ ARENITE

The quartz arenites which overlie the Vlakhoek Member with a sharp erosive contact are indicative of a marine regression within the Pongola basin. Intertidal to upper shoreface environments are identified in the coarsening upward shale/siltstone/quartz arenite successions. Bipolar palaeocurrent directions as well as mud lenses, desiccation cracks, and multidirectional ripples within the lowermost zone indicate wave-driven longshore and rip currents in an intertidal environment (Beukes & Cairncross, 1991). The lowermost intertidal zone is overlain by upper shoreface, rippled sandstones with no mud drapes. The upper quartz arenites are sharply overlain by iron-rich shales of the Mpunga Formation which marks the transition between upper shoreface and offshore mud and marks the onset of a second marine transgression into the Pongola basin.

3.8.6 SEQUENCE STRATIGRAPHY OF THE MANDEVA FORMATION

The Mandeva Formation hosts two depositional sequences. The lowermost sequence is indicative of marine transgression into the Pongola basin and hosts a lowstand systems tract (LST) and a transgressive systems tract (TST) with a condensed section (CS). The lowermost sequence boundary (SB) occurs at the Nsuze-Mozaan unconformity.

The aggradational, fluvial Denny Dalton Member would have been deposited in a LST to TST (Figure 3.42) when relative sea level was stable and accommodation space was neither being created or destroyed (Coe et al., 2003). The overlying Klipkloof quartz arenites would also have been deposited in this LST-to-TST. The contact between the Denny Dalton Member and the Klipkloof quartz arenites indicates a marine transgression, and a retrogradation of facies from fluvial conglomerate and quartz arenite to shallow marine quartz arenite, as accommodation space was slowly being created (Figure 3.42). The relative thickness of the Klipkloof quartz arenites in comparison to the Denny Dalton Member indicates that sea level rise was slow and that aggradation was more prominent than retrogradation.

The base of CG 4 marks the transgressive ravinement surface (TS) where relative sea level rise accelerated (Coe et al., 2003; Figure 3.42). The sharp erosive contact between the Klipkloof quartz arenites and CG 4 suggests a TS as these surfaces are marked by a sharp erosion surface in the shoreface zone with a winnowed lag of clasts (Coe et al., 2003). This surface marks the base of the true TST as the succession shows pronounced retrogradation due to continued deepening during relative sea-level rise (Coe et al., 2003).

The boundary between CG 4 and the overlying Vlakhoek shales marks a flooding surface within the TST (Figure 3.42). This flooding surface does not however form the base of the condensed section as the lower black shales are interbedded with fine-grained sandstone and merely indicate the shift from lower shoreface to transition zone facies.

The boundary between the lower black shales and the banded iron formation mark the maximum flooding surface (Coe et al., 2003; Figure 3.42). This surface forms at maximum relative sea-level rise and represents a period of sediment starvation in distal areas (Coe, et al., 2003). The banded iron formation and overlying green shales represent a condensed section (CS) as they formed by chemical precipitation on a sediment-starved shelf.

The contact between the green shales and overlying upper quartz arenites forms the sequence boundary between the lower and upper depositional sequences. It represents marked marine

regression and an erosional hiatus as neither the high stand systems tract, nor the falling stage systems tract are preserved (Coe et al., 2003). The overlying quartz arenites were deposited in an intertidal to upper shoreface environment and would have formed in a LST-to-TST within the upper depositional sequence.

A conglomerate lag with associated grits and pebbly sandstones crops out ~5 m below the contact between the upper quartz arenites and the overlying Mpunga Formation. This surface marks the base of the true TST and represents the TS of the upper depositional sequence (Coe et al., 2003).

The contact between the upper quartz arenites and the overlying Mpunga Formation shales marks a flooding surface and transition from shoreface to deeper marine facies (Coe et al., 2003). The overlying Mpunga Formation shales indicate pronounced relative sea-level rise and would form the TST within the upper depositional sequence.

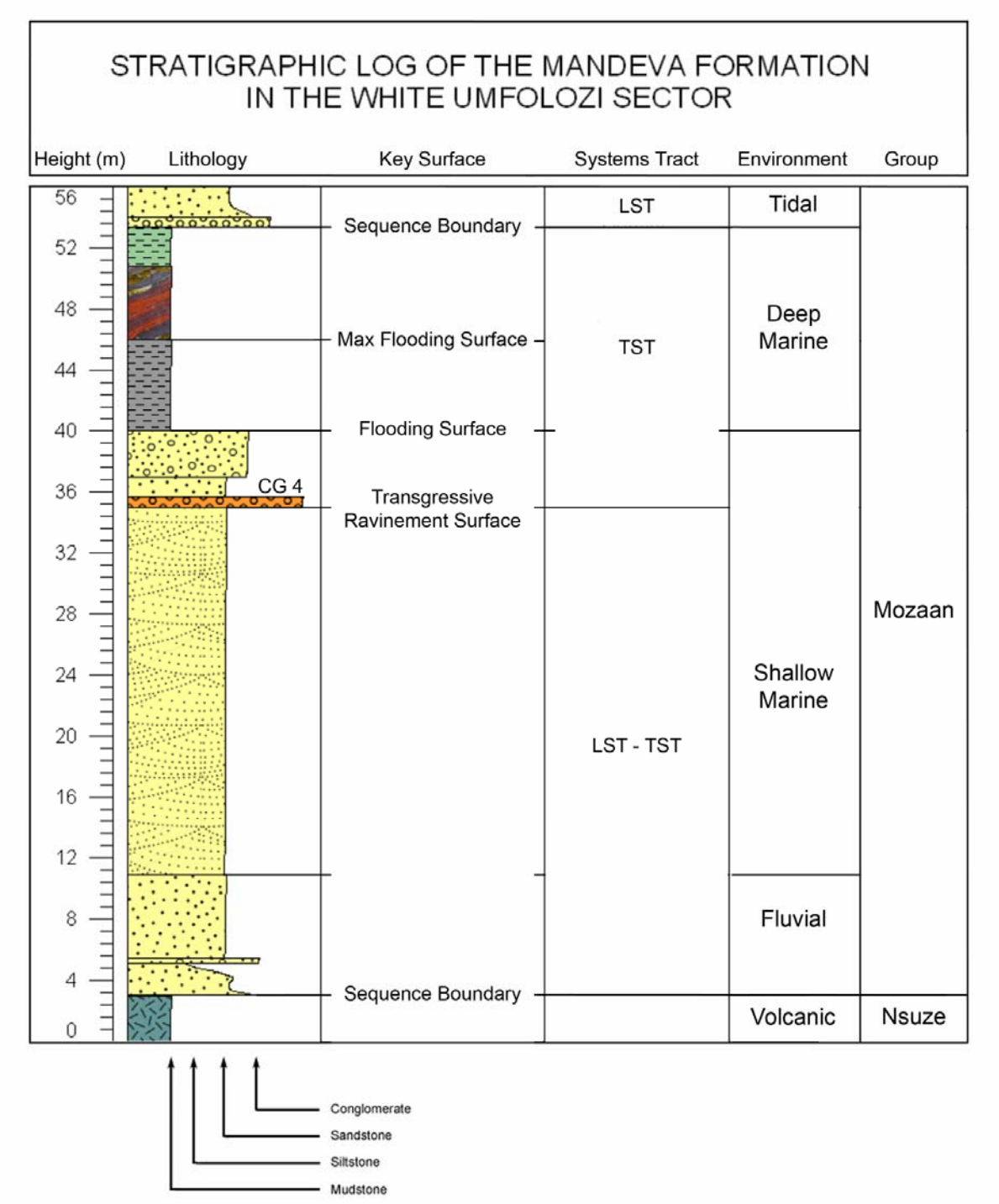

Figure 3.42: Sequence stratigraphy of the Mandeva Formation in the White Umfolozi sector showing key surfaces, systems tracts and depositional environments.

3.8.7 BASIN DEVELOPMENT

The Nsuze Group was deposited between 2.98 and 2.97 Ga ago (Hegner et al., 1994; Nhleko, 2003) in a north-south trending continental rift on the south-eastern margin of the Kaapvaal Craton, which broadened onto a subsiding continental margin to the south (Matthews, 1990). Burke et al. (1985) proposed that due to geochemical and stratigraphical characteristics similar to that of modern-day rift systems, the Pongola basin could be representative of an ancient rift. They proposed the following characteristics for ancient rift systems (Burke et al., 1985; Weilers, 1990):

(a) Lateral thickness variation over restricted distances.
(b) Volcanic rocks with a distinct bimodal silica content.
(c) Linear rift basin trends and faulted margins.
(d) A predominantly volcanic succession with intercalated sedimentary rocks, overlain by a sedimentary section poor in volcanics.

The basin geometry and stratigraphy of the northern Pongola basin can be classified as a syn-rift basin (Weilers, 1990). Matthews (1990) suggested that the main Pongola basin was defined by a faulted margin along the Mahamba fault-system where the basin deepens south-westward across the fault from ~2.5 km to 8 km. Matthews (1990) proposed that the White Umfolozi Inlier lies close to the western edge of the Pongola basin, between the Mahamba fault-system and the structural arch in the pre-Pongola basement between the White Umfolozi inlier and the Nkandla sub-basin (Figure 2.1). This could account for the only ~2.5 km thick succession within the White Umfolozi Inlier compared to the ~8 km thick main basin (Matthews, 1990). One must take into account however, the fact that much of the Mozaan Group stratigraphy within the White Umfolozi Inlier has been removed by later erosion; and that the upper units of the Nsuze Group have also been removed by erosion allowing for the overstepping nature of the Mozaan Group along the Nsuze-Mozaan unconformity.

It has been postulated that the Mozaan basin formed as a thermal sag basin brought on by thermal cooling after formation of the Nsuze rift basin (Weilers, 1990). After the termination of Nsuze-age rifting, the rocks underwent slow regional subsidence across the margins of the older structure (Matthews, 1990).

Matthews (1990) suggested that after Mozaan Group deposition, compressional tectonics associated with the Nsuze Nappe in the Nkandla area caused northward thrusting along the Nsuze-Mozaan unconformity. Gold and Von Veh (1995) suggested that the Mozaan Group within the main Pongola basin was subjected to one extensional and two regional compressional events during the late Archaean. Post-Mozaan Group D_1 deformation within the main Pongola basin occured as NNW-directed thrust and reverse faults and shear zones (Gold and Von Veh, 1995). The shearing predates

the major folding event within the main basin (Gold and Von Veh, 1995). This thrusting is evident within the White Umfolozi Inlier as D_3 deformation in the form of bedding-parallel shear zones which indicate early NW-verging thrusting. The folding within the White Umfolozi Inlier is likely associated with this compressional event as open ENE-trending folds are also developed within the main Pongola basin and are suggested to have formed contemporaneously with the NNW-directed thrusting (Gold and Von Veh, 1995).

Extensional tectonics within the main Pongola basin is manifested by normal listric faulting such as the Gunsteling fault, with downthrow to the south-southeast (Gold, 1993). Extensional tectonics evident within the White Umfolozi Inlier occur as D_4 and D_5 normal faulting which set up a number of horst and graben structures. The timing of this faulting event in relation to D_3 is difficult to determine, however it appears to postdate the D_3 folding event within the Umfolozi Inlier as the D_4 and D_5 faults are not folded.

Late stage brittle tectonics identified within the main Pongola basin occur as NW to NE trending faults and fractures which cut the post-Mozaan granitoids and some of which postdate the deposition of the Karoo Supergroup (Gold and Von Veh, 1995). NNE trending faults within the White Umfolozi Inlier offset the Karoo Supergroup lithologies and therefore form as late stage brittle tectonics and could be associated with Gondwana rifting at ~180 Ma (Visser, 1998).

CHAPTER 4

THE DENNY DALTON Au - U DEPOSIT

4.1 INTRODUCTION

Gold deposits within the basal units of the Mozaan Group have supported a number of small-scale mines throughout the Pongola basin. The most productive was the Denny Dalton Mine ~20 km west of Ulundi in northern KwaZulu-Natal which operated sporadically between 1893 and 1926 (Delpierre, 1969). Thin beds of gold and uranium-bearing conglomerate are locally present and the style of mineralization strongly resembles that of the Witwatersrand goldfields, however ore is of lower grade (avg 4 g/t) and limited tonnage (Saager et al., 1986). Mine workings are found on the farm Tusschenby 411 where the Nxobongo stream has scoured a narrow gully through the Denny Dalton Member of the Mandeva Formation into the underlying Nsuze Group strata (Figure 3.5). Twelve adits, 7 on the southeast side and 5 on the northwest side of the stream have been driven into the conglomerate zones to a distance of around 30m (Figure 4.1). The remains of the old crushing mill and a number of ruined buildings are all that remain of the mine infrastructure (Figure 4.2).

Figure 4.1: Denny Dalton Mine area showing position of three adits driven into gently dipping Denny Dalton Member of the Mandeva Formation on south eastern side of the Nxobongo stream. View towards southeast.

Figure 4.2: Remains of crushing mill from 1893 at Denny Dalton Mine.

4.2 MINING HISTORY

Gold occurrences in KwaZulu-Natal were first discovered by European settlers in 1836 but it was not until the late 1860's that gold was identified within the White Umfolozi Inlier (de Klerk, 2006). Mining at Denny Dalton occurred sporadically between 1893 and 1926. Reports of this work are fragmentary and not well documented. The farm Tusschenby 411 was acquired by Thomas Denny, John Dalton and Scott Paulson in 1893 for the purpose of gold mining. A gold processing plant was commissioned in 1893, however, gold was not produced until June 1895 when the Denny Dalton Gold Mining Co. crushed 682 t of ore which yielded 4.5 kg of gold (Hatch, 1910). Between 1905 and 1906 the Denny Dalton Tribute Syndicate crushed 1 772 t of ore which yielded 5.6 kg of gold (Hatch, 1910). Hatch mapped the adits of the defunct mine (Figure 4.3) and collected a number of reef samples which indicated a grade of 4.7 g/t over a 1 m stoping width in adits 5 and 6 (Hatch, 1910). Hatch (1910) indicated that adits 1S, 2S, 3S, 5S and 6S and 2N were extensively stoped (Figure 4.3). These adits host the highest ore grade and correlate to 2 separate ENE trending palaeochannels in which the ore is concentrated. Adits 4S and 3N (Figure 4.3) show no workings and are driven into a barren zone between the reef shoots. Campbell (1982) indicated that of 128 boreholes drilled in the mine area, only 11 payable intersections of CG 1 were found. The last record of production at Denny Dalton was that of tailings dump re-treating in 1926 (Delpierre, 1969). Since 1926 numerous exploration projects have been undertaken around the mine area to test for continuity and extensions of the reef zone. Renewed interest in the deposit is generally sparked by inflated market prices of gold and uranium that could make the prospect economical.

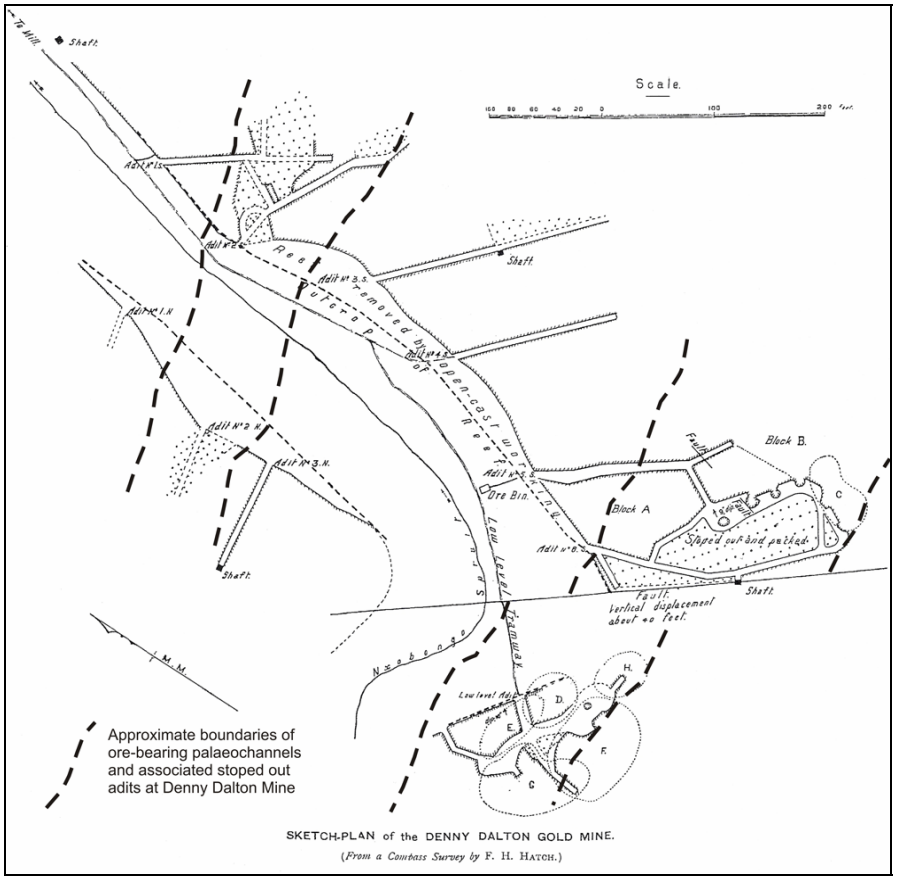

Figure 4.3: Sketch plan of the main adits at Denny Dalton Mine (modified after Hatch, 1910).

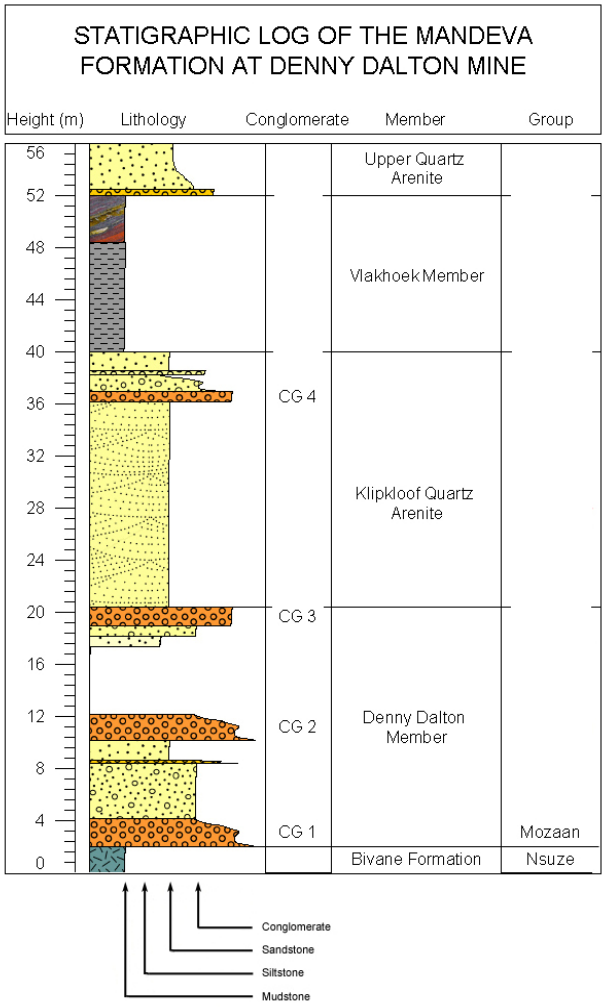

Figure 4.4: Stratigraphic log at Denny Dalton showing Members and conglomerates within the Mandeva Formation.

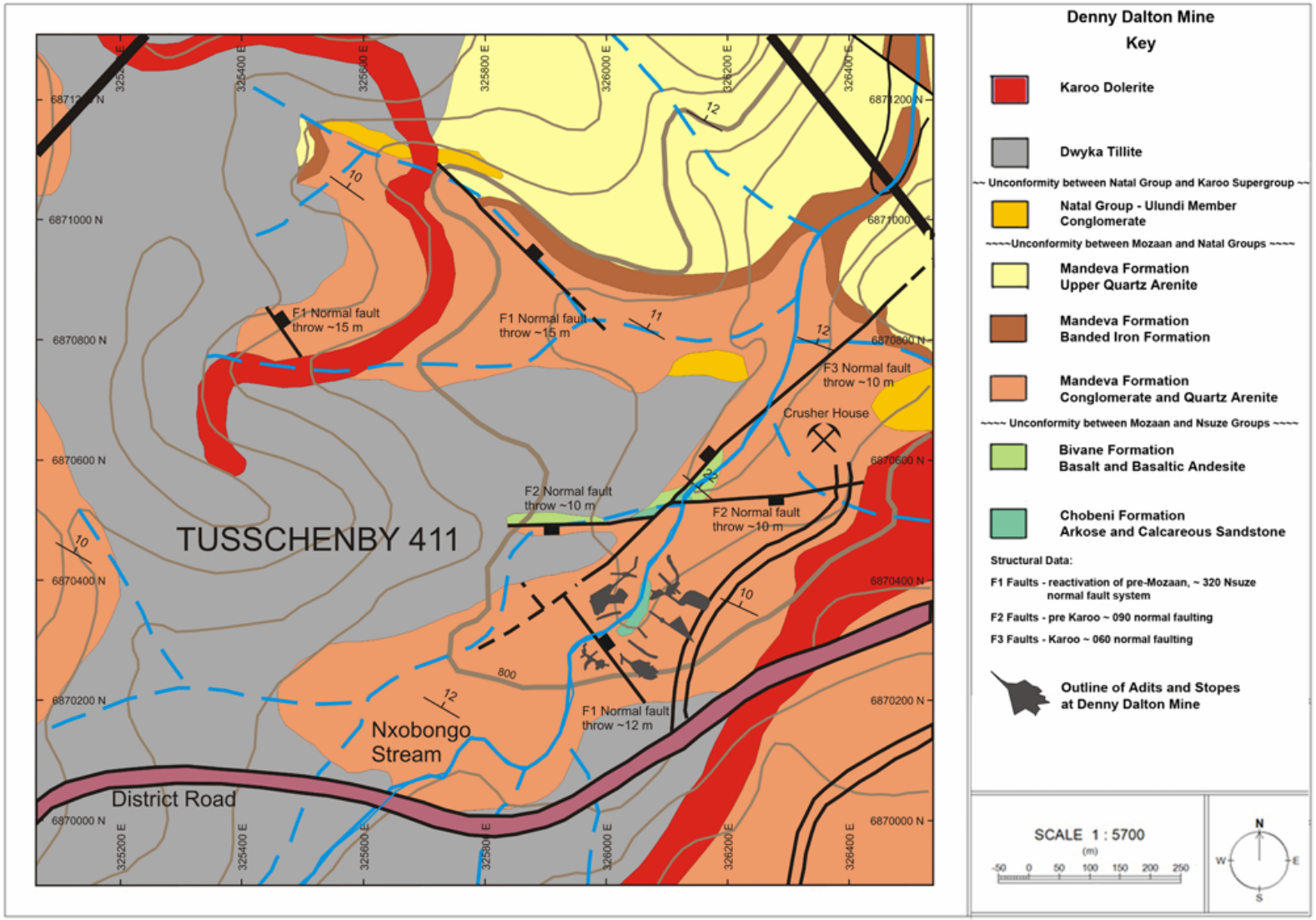

Figure 4.5: Detailed geological map of the Denny Dalton Mine area

4.3 GEOLOGICAL SETTING

At Denny Dalton Mine the main mineralized reef crops out as a ~1 m thick pebble conglomerate directly overlying the basal unconformity between the Chobeni or Bivane Formation of the Nsuze Group and the Mozaan Group (Figure 4.4 and 4.5). The conglomerate thus acquired the name "Mozaan Contact Reef" (MCR). This forms the lowermost of three fining upward conglomerate-sandstone successions which together constitute the Denny Dalton Member. The lowermost succession is here referred to as CG 1 (Figure 4.4).

Within the adit area the CG 1 conglomerate is a cobble-sized, clast-supported rock that hosts abundant rounded compact pyrite, up to 10 mm in diameter (Figure 4.6). The pyrite-bearing conglomerate often exhibits a honeycomb texture due to the weathered pyrite grains (Figure 4.7). Cobble conglomerates are concentrated within the lowermost parts of the CG 1 cycle directly above the footwall contact. The main auriferous reef zone however, is formed towards the top of the conglomerate within scour channels ~50 cm above the footwall unconformity and is associated with large pebble sized clasts (Figure 4.8).

The CG 1 conglomerate attains a thickness of ~1 m at Adit 2S (Figure 3.6 and 4.1). It is characterised by an erosive contact with the underlying Nsuze Group arkoses. The lower 25 cm is characterised by internally massive, predominantly cobble-sized, clast-supported, black chert dominated, conglomerate. The matrix comprises well rounded coarse sand-sized quartz and pyrite grains. No pebble imbrication is evident and the large clast size points towards proximal deposition. Overlying the lower conglomerate with a sharp contact is a 10 cm thick, trough cross-bedded, coarse-grained sandstone layer which hosts random cobble clasts. The sandstone comprises 98% quartz with rounded pyrite grains concentrated on the foresets. Overlying the sandstone with a sharp contact is a second ~20 cm thick, normally-graded, matrix-supported, large pebble conglomerate. No imbrication is evident and clasts are 60% well-rounded black chert. The coarse-grained matrix comprises 70% quartz and 30% pyrite grains. A ~5 cm thick layer of matrix-supported, medium- to large-pebble conglomerate overlies the large pebble conglomerate with an erosive contact. The matrix comprises 90% large rounded pyrite granules with 10% coarse-grained quartz. This layer is overlain by a ~10 cm thick matrix-supported medium-pebble vein quartz conglomerate.

Figure 4.6: Rounded pyrite bed in cobble conglomerate (CG 1) next to Adit 2, Denny Dalton Mine. Hammerhead for scale.

Figure 4.7: Honeycomb texture formed by weathering of rounded pyrites within the Denny Dalton Mine area.

Figure 4.8: Polished sample of the Denny Dalton reef zone. Rounded pyrite grains hosted in the matrix between the chert and vein quartz cobbles.

Pebbly grits overlie the CG 1 conglomerate succession and host trace amounts of both gold and uranium (Martens, 2005). Sulphides occur as ~0.5 to 1 mm subhedral grains, disseminated in the quartz-sericite matrix, or concentrated on the basal parts of foresets within trough-crossbeds.

The upper conglomerate zones, CG 2 and CG 3, consist predominantly of vein quartz clasts with sulphides occurring as ~0.5 to 1 mm detrital grains and euhedral crystals within the matrix. Sulphide content varies laterally and appears to be higher in zones of larger clast size. No gold or uranium has been identified within either of these cycles (Campbell, 1982).

A fourth, laterally persistent conglomerate, (CG 4) crops out above the Klipkloof quartz arenites which overlie the Denny Dalton Member and hosts ore grade U_3O_8 (Campbell, 1982).

4.4 ORE MINERALOGY

Ten polished sections of mineralized conglomerates within the Denny Dalton Member were taken from quarter core of drill hole TSB 06-23. Two sections were also made of the upper conglomerate CG 4, above the Denny Dalton Member from drill hole TSB 07-26. Ten polished sections and blocks were made from samples taken from the CG 1 reef package exposed at Adit 2 in the mine area (Figure 4.1). Seven polished sections were also made from grab samples taken from mine dumps outside the adits; it is presumed that these samples are from mined out sections of CG 1 as there is no record of any mining from the hanging wall. Ore and heavy minerals identified from each reef by Scanning Electron Microscopy (SEM) are shown in Table 4.1. Exact drill hole co-ordinates and ore grades are however confidential; samples from drill core was taken with consent from Acclaim Exploration.

Table 4.1: Genetic classification of ore and heavy minerals within the Mandeva Formation conglomerates. Minerals are shown in order of decreasing abundance. Grains are defined as allogenic while crystals and crystal aggregates are authigenic.

Conglomerate Unit	Minerals Present	Allogenic	Authigenic	Inclusion in mineral
Conglomerate 1 (CG 1)	Pyrite	X	X	
	Rutile	X		
	Leucoxene	X		
	Monazite	X		
	Chromite	X		
	Zircon	X		
	Galena			X - Pyrite / Rutile
	Gold			X - Pyrite / Scorodite
	Arsenopyrite	X		X - Pyrite
	Pyrrhotite			X - Pyrite
	Scorodite	X		
	Brannerite		X	
Conglomerate 2 (CG 2)	Pyrite	X	X	
	Rutile	X		
	Leucoxene	X		
	Monazite	X		
	Chromite	X		
	Zircon	X		
	Arsenopyrite	X		
	Galena			X - Pyrite / Rutile
	Thorite			X - Pyrite
Conglomerate 3 (CG 3)	Pyrite	X	X	
	Rutile	X		
	Leucoxene	X		
	Monazite	X		
	Chromite	X		
	Zircon	X		
	Galena			X - Rutile

Conglomerate Unit	Minerals Present	Allogenic	Authigenic	Inclusion in mineral
Conglomerate 4 (CG 4)	Pyrite	X	X	X - Rutile
	Rutile	X		
	Leucoxene	X		
	Chromite	X		
	Sphalerite		X	
	Uraninite		X	X - Pyrite
	Coffinite		X	
	Gersdorffite		X	
	Arsenopyrite		X	
	Galena		X	X - Rutile
	Apatite	X		

4.4.1 PYRITE

Pyrite is the most abundant ore mineral in all the sections and commonly makes up 70 to 80% of the ore minerals present in the conglomerates. Pyrite occurs as sand to pebble-sized grains, as well as anhedral to euhedral crystals within the matrix. Three generations of pyrite can be identified.

4.4.1.1 ROUNDED PYRITE

Subrounded to rounded pyrite occurs as 0.2 to 10 mm grains with abraded edges. This is the most abundant form within CG 1, comprising ~60% of the pyrite in the samples, and is concentrated as grains in the matrix between large-pebble and cobble clasts (Figure 4.6 and 4.9), and as pyrite beds along scour channels within the upper part of the conglomerate (Figure 4.8). Cataclastic shattering of large rounded pyrite grains is common with smaller rounded pyrite grains showing only minor cataclasis.

Many of the rounded pyrites show secondary pyrite overgrowths which form euhedral edges on parts of the grains and conceal the original rounded nature of the pyrite (Figure 4.10). The pyrite often exhibits replacement by quartz, indicating post-diagenetic silicification of the sediments (Figure 4.11). Gold, galena, arsenopyrite and minor pyrrhotite occur as minute inclusions within these pyrites (Figures 4.22 and 4.34A).

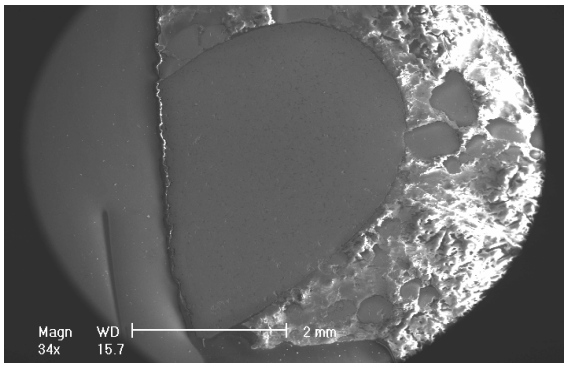

Figure 4.9: Secondary electron image of small rounded pyrite grains surrounding large rounded detrital pyrite (CG 1, Adit 2S, Denny Dalton Mine).

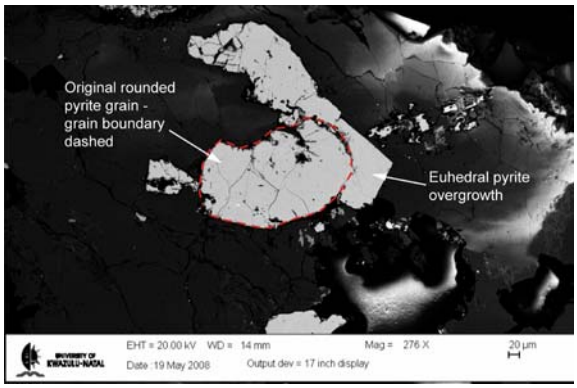

Figure 4.10: Backscattered electron image of pyritic overgrowth on rounded pyrite grain (sample CG 1 E, Adit 2S, Denny Dalton Mine).

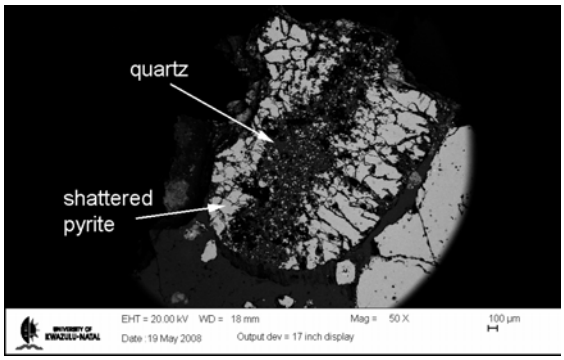

Figure 4.11: Backscattered electron image of cataclastically shattered, rounded pyrite being replaced from the centre by secondary quartz. (Sample CG 1-B, Adit 2S, Denny Dalton).

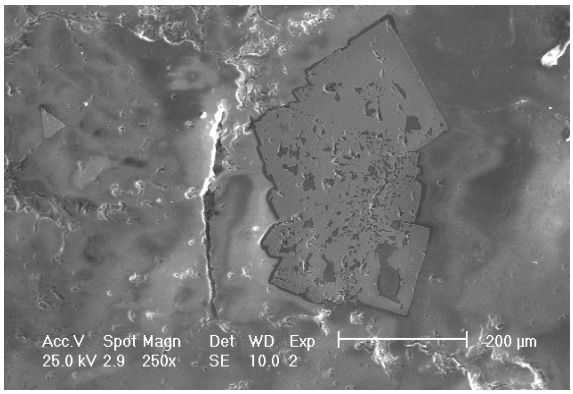

Figure 4.12: Secondary electron image of euhedral pyrite cluster with internal quartz replacement within CG 1. (Sample TSB 06-23-CG 1).

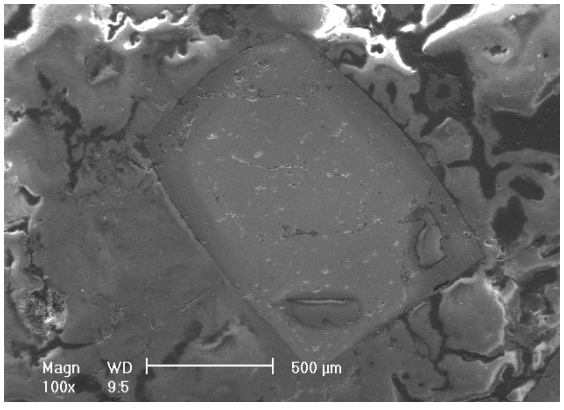

Figure 4.13: Secondary electron image of euhedral pyrite crystal. Note quartz overgrowth at bottom of the crystal. (Sample TSB 06-23-CG 3).

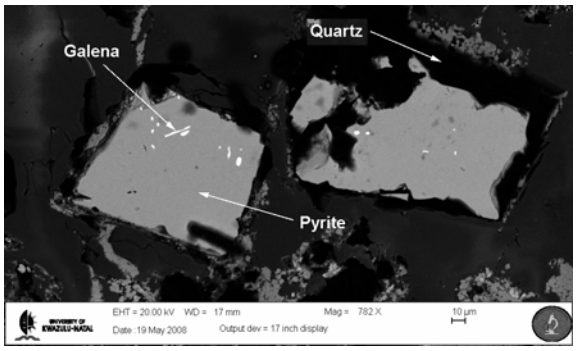

Figure 4.14: Backscattered electron image of euhedral pyrite crystals with inclusions of galena. Note quartz replacement on pyrite edges. (Sample CG 1-E, Adit 2S, Denny Dalton).

4.4.1.2 EUHEDRAL PYRITE

Euhedral pyrite is present throughout all conglomerate zones and forms single cubic crystals and clusters of euhedral to subhedral crystals occupying fracture and bedding planes (Figure 4.12 and 4.13). The same pyrite type also occurs as anhedral overgrowths on the edges of rounded pyrite grains (Figure 4.10). Euhedral pyrites are generally massive and do not show inclusions except for one sample (slide CG 1 E) where two cubic pyrites host elongate primary inclusions of galena (Figure 4.14). Cubic pyrite is often present as fracture fillings associated with quartz veins where internal replacement by quartz is often visible (Figure 4.13). It is important to note the lack of abraded or etched surfaces on the crystal edges as compared to the rounded pyrite grains.

4.4.1.3 POROUS AND RADIAL PYRITE

Well rounded, porous pyrites with diameters up to 8 mm are associated with the smaller compact pyrite within the main reef zone of CG 1 (Figure 4.15). These pyrites generally occur as rounded grains within the upper portions of the main reef zone. They do not exhibit any cataclastic shattering as identified in the massive rounded pyrite grains, possibly due to the increased pore space reducing the amount of shattering within the mineral. Pore spaces within the grains are commonly filled with quartz and sericite and no inclusions of ore minerals are evident.

Radial pyrites up to 2 cm in diameter have been observed in hand specimen and often appear as friable rounded pebbles with needle-like radial growth from a central point (Figure 4.16). This texture resembles that of marcasite ($2[FeS_2]$) however X-ray diffraction analysis of radial clasts only identified pyrite with minor pyrrhotite, probably as inclusions within the pyrite (Figure 4.17).

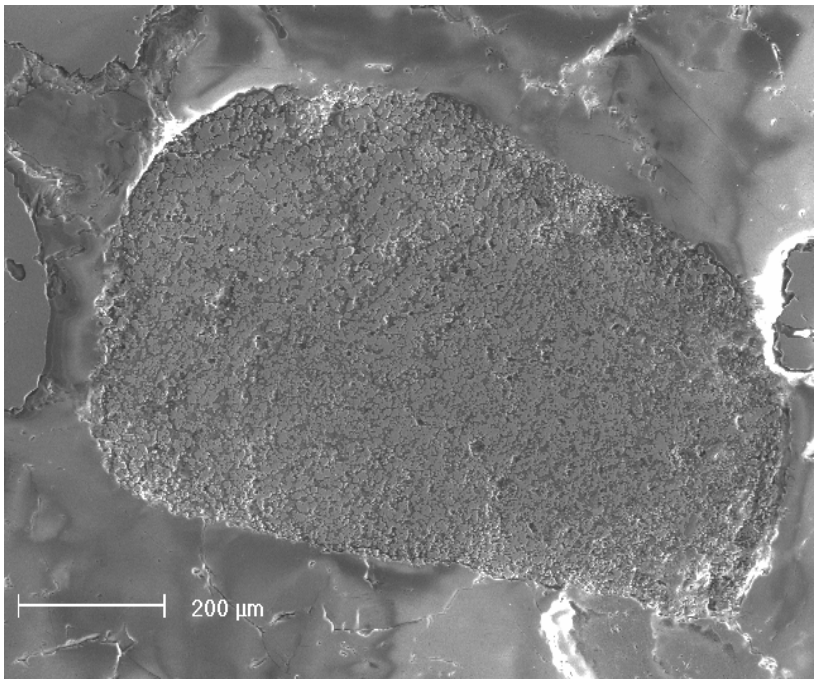

Figure 4.15: Secondary electron image of porous rounded pyrite grain in CG 1. Pore spaces are filled by sericite and quartz.

Figure 4.16: Radial pyrite in main reef zone of CG 1. Note radiating needles from central point in the grain. Long axis of grain is 2cm. Compare to rounded compact pyrite grains on either side of radial pyrite.

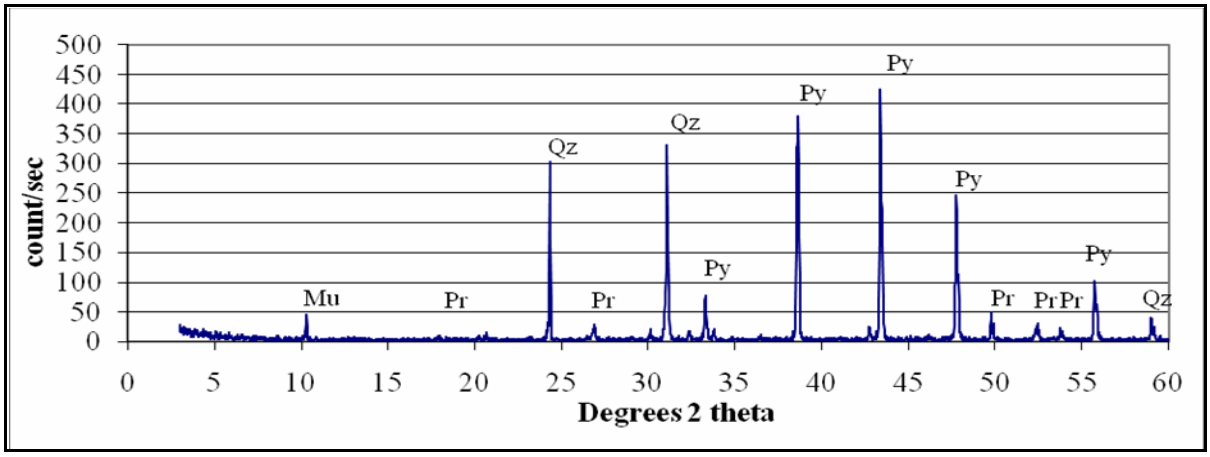

Figure 4.17: XRD spectrum of mineral peaks from radial pyrite within conglomerate zone 1 - Denny Dalton Mine. Mu - Muscovite, Pr - Pyrrhotite, Qz - Quartz, Py - Pyrite.

4.4.2 RUTILE AND LEUCOXENE

Rutile occurs as rare subrounded detrital grains within all conglomerate zones. Rutile rarely exhibits internal porosity or contains inclusions of ore minerals when compared to its microcrystalline form, leucoxene (Figure 4.18). Massive rutile grains have average grain sizes of 0.15 mm and often exhibit cataclastic shattering.

Leucoxene, a microcrystalline form of rutile, forms by the alteration of ilmenite to rutile (Battey & Pring, 1997) and is abundant throughout the conglomerates. It occurs as anhedral porous grains within the matrix. Needle-like crystals of uraniferous leucoxene are evident along grain boundaries of anhedral leucoxene grains. Atoll-textured grains often exhibit corroded centres replaced by quartz and muscovite (Figure 4.19). Leucoxene grains frequently contain inclusions of pyrite, galena and chalcopyrite (Figure 4.20).

Brannerite ($(U,Ca,Ce)(Ti,Fe)_2O_6$), a refractory uranium titanite mineral, forms as rare needle-like crystal clusters within the Denny Dalton Member, associated with fine crystalline leucoxene grains. SEM-EDX data show only minor brannerite within CG 1 or CG 2 (the Mozaan Contact Reef (MCR) and Hanging Wall Reef (HWR)).

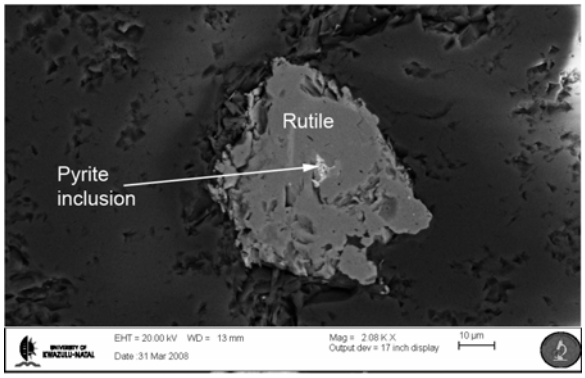

Figure 4.18: Backscattered electron image of subrounded rutile grain with minor pyrite inclusion. Note overall massive texture compared to porous leucoxene grain in Figure 4.23. (Sample CG 4.1)

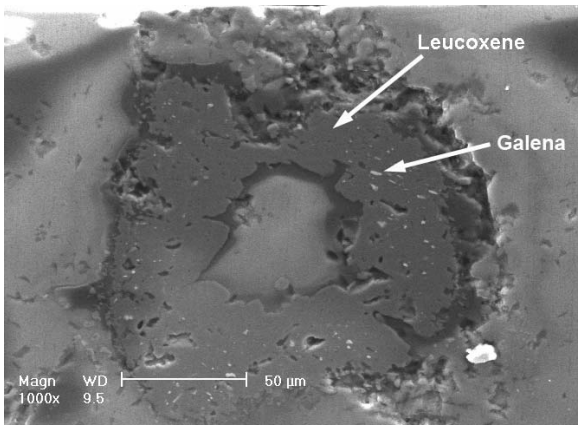

Figure 4.19: Secondary electron image of atoll textured leucoxene grain (dark grey) with elongate inclusions of galena (light silver). Central section of grain replaced by quartz. (Sample CG 1-A2a).

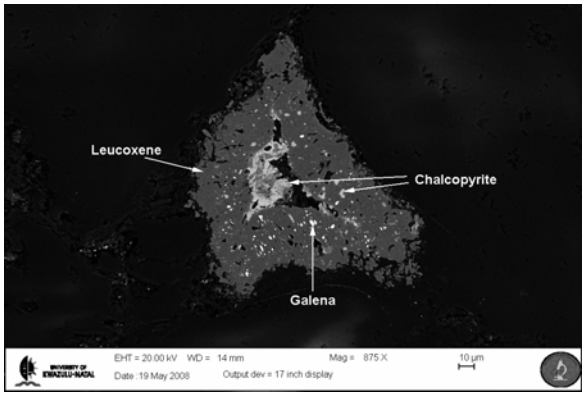

Figure 4.20: Backscattered electron image of porous anhedral leucoxene grain (dark grey) with inclusions of chalcopyrite (light grey) and galena (white).

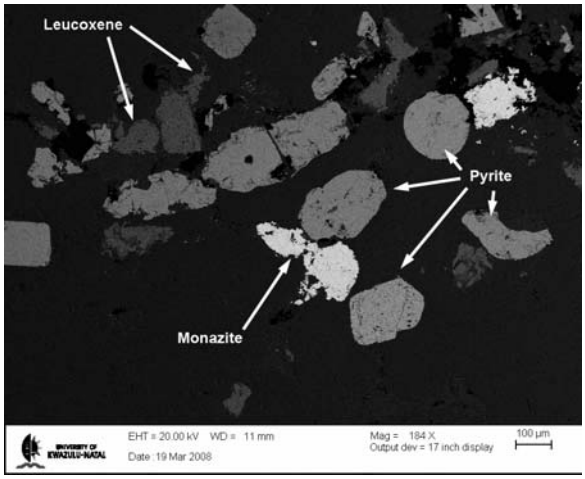

Figure 4.21: Backscattered electron image of CG 2 reef package. Note the rounded and corroded pyrite (light grey) with associated subhedral monazite (white). Dark grey subhedral and corroded grains are rutile and leucoxene.

4.4.3 MONAZITE

Monazite is an abundant detrital heavy mineral within all but Conglomerate 4. Grains are often well rounded but also occur as corroded subhedral masses with grain edges often having been replaced by silica (Figure 4.21). Original rounded grain shapes are still evident on some edges (Figure 4.21). Monazite grains often contain inclusions of galena.

4.4.4 GOLD

Gold occurs as rare pale yellow inclusions within rounded massive pyrite grains. Inclusions are generally minute ~20 μm, irregular or rod-like infillings (Figure 4.22 and 4.23). Some cavities evident in rounded pyrite occur where gold has been removed during slide preparation (Figure 4.23). The shape of the gold inclusions mimics primary euhedral pyrite crystal edges preserved within the grains (Figure 4.23). EDX analysis of gold inclusions indicates a high Ag content (Table 4.3 and 4.4).

Gold is also associated with scorodite ($FeAsO_4 . 2H_2O$) aggregates in sample CG 1-B (Figure 4.24 and 4.25). The gold occurs as inclusions in altered grains and along replaced grain boundaries.

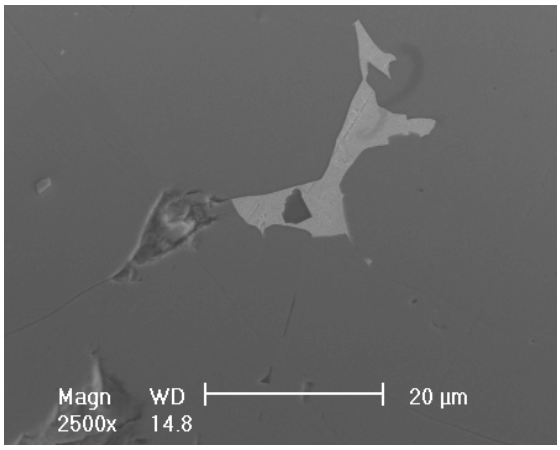

Figure 4.22: Secondary electron image of irregular gold inclusion within massive pyrite grain. Sample DD CG1 HS2, taken from CG 1 reef at Adit 2S, Denny Dalton Mine.

Table 4.2: Avg. EDX weight percentages for inclusion in figure 4.22.

EDAX ZAF Quantification	
Element	Wt %
C K	14.55
AgL	5.51
FeK	1.68
AuL	78.25
Total	100

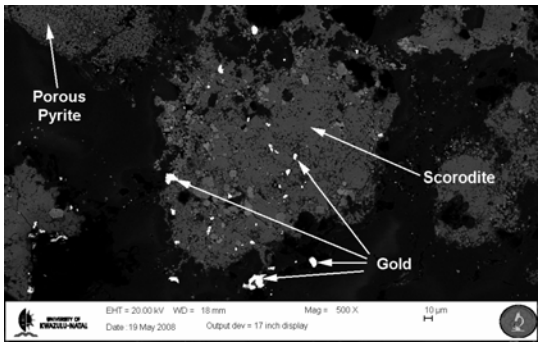

Figure 4.24: Backscattered electron image of gold inclusions associated with altered scorodite ($FeAsO_4$. $2H_2O$) aggregate. Gold crystals at the base of the image are gold crystals surrounded b secondary quartz that has overgrown the crystal aggregate edges. (Sample CG 1-B).

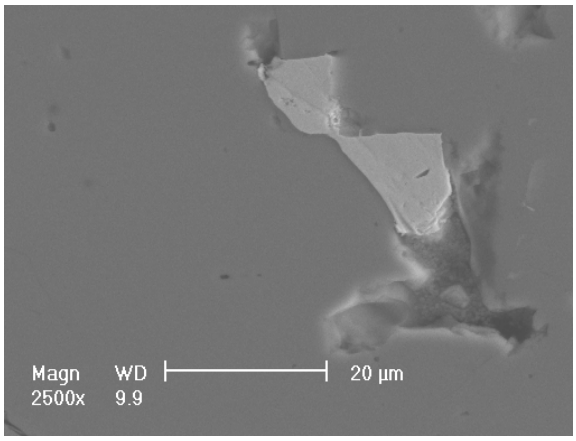

Figure 4.23: Secondary electron image of gold inclusion in massive pyrite. Note cubic edge of gold inclusion mimicking original cubic pyrite crystals. Sample DD CG1 HS1, taken from CG 1 reef at Adit 2S, Denny Dalton Mine.

Table 4.3: Avg. EDX weight percentages for inclusion in figure 4.23.

EDAX ZAF Quantification	
Element	Wt %
C K	13.69
AgL	13.06
FeK	16.19
AuL	57.06
Total	100

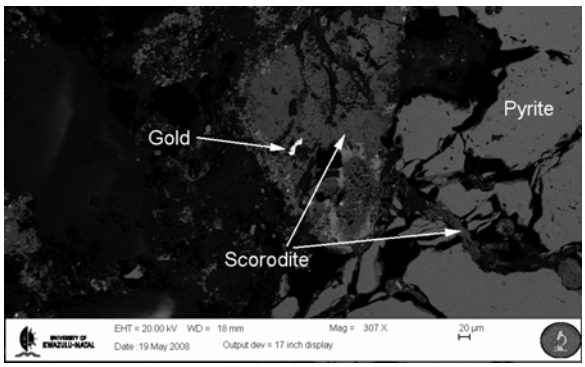

Figure 4.25: Backscattered electron image of gold inclusion in altered grain, host has been replaced with scorodite aggregate, also identified in the fractures of the surrounding cataclastic shattered pyrite. (Sample CG 1-B).

4.4.5 URANIUM MINERALS

Brannerite or uraniferous leucoxene are the only uranium bearing minerals present within CG 1 and CG 2, see section 4.4.2 (page 75). As previously mentioned SEM-EDX analysis showed a very low percentage of brannerite within the conglomerates.

Geochemical data (see Appendix II) places much of the uranium identified within the lower conglomerates within black chert pebbles, which are dominant clasts within these zones. SEM analysis of black chert pebbles from the CG 1 conglomerate at adit 2, show a high concentration of *uraninite* crystals. The UO_2 forms anhedral aggregates ~10 to 20 µm in diameter, disseminated within pore spaces in the chert pebbles (Figure 4.26). Coatings of UO_2 are also identified around singular cubic pyrite crystals and euhedral aggregates within the cherts (Figure 4.27, 4.28 and 4.29).

Within conglomerate 4, two uranium-bearing phases are present, the most abundant, *uraninite* (UO_2), forms as overgrowths and encrustations on other heavy minerals (Figures 4.30, 4.31, and 4.32). The second uranium phase evident is that of *coffinite* ($USiO_4 \cdot nH_2O$), which occurs as subhedral crystals attached to the edges of detrital pyrite grains (Figure 4.33).

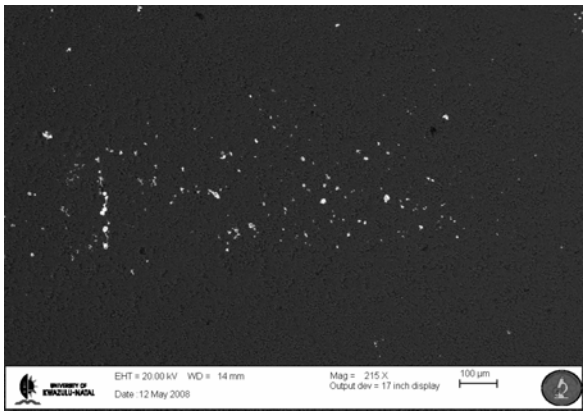

Figure 4.26: Backscattered electron image of disseminated uraninite within chert. (Sample PO6-11-C).

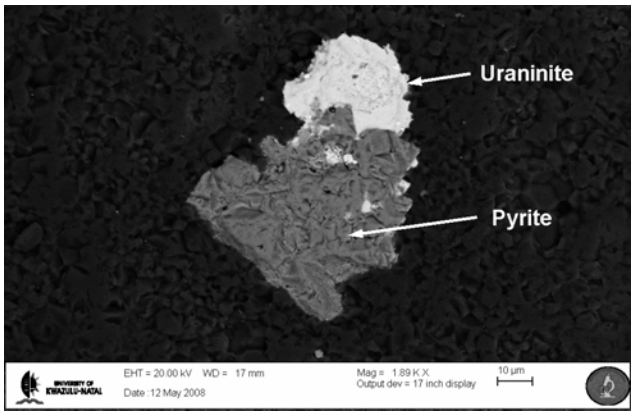

Figure 4.27: Backscattered electron image of anhedral uraninite aggregate (white) associated with cluster of euhedral pyrite in chert pebble. (Sample PO6-11-C).

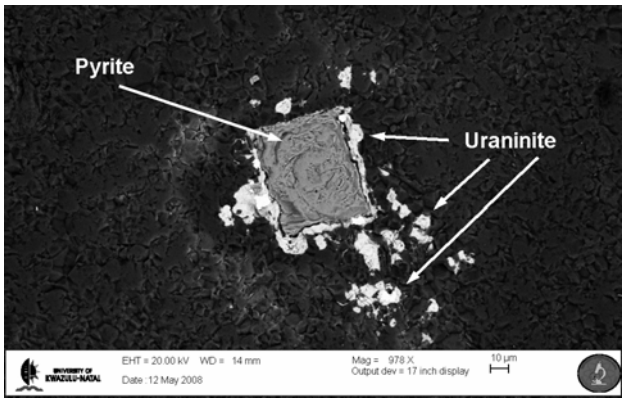

Figure 4.28: Backscattered electron image of uraninite coating and individual anhedral uraninite crystals surrounding cubic pyrite in chert. (Sample PO6-11-C1).

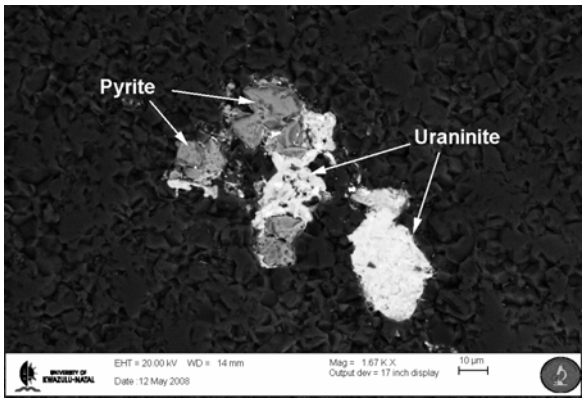

Figure 4.29: Backscattered electron image of uraninite intergrown with pyrite in chert. (Sample PO6-11-B).

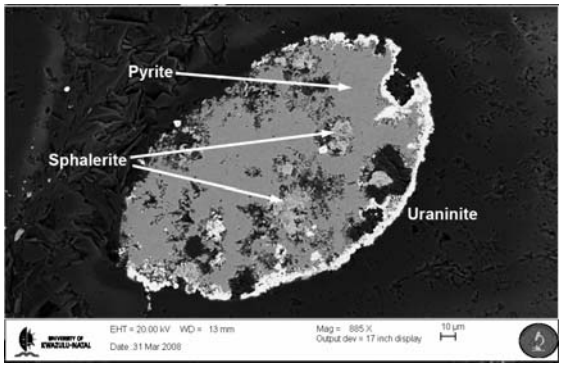

Figure 4.30: Backscattered electron image of uraninite coating (white) around rounded pyrite grain (dark grey) inclusions are sphalerite (light grey).

Table 4.4: SEM data for uraninite coating around pyrite in Figure 4.30

Elmt	Element	Sigma	Atomic
	%	%	%
O K	30.08	0.41	76.38
Si K	6.14	0.12	8.89
P K	2.47	0.11	3.23
Fe K	1.85	0.20	1.35
U M	59.46	0.45	10.15
Total	100.00		100.00

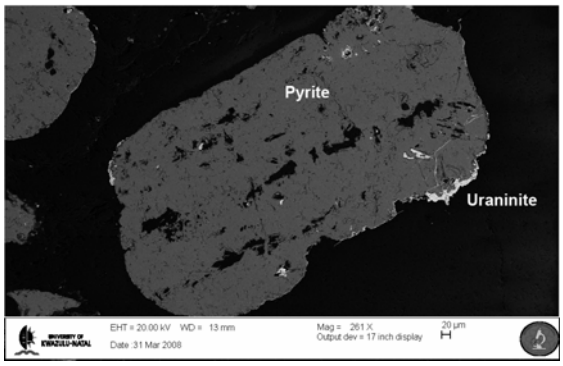

Figure 4.31: Backscattered electron image of pyrite (grey) with secondary coatings, and pore space inclusions of uraninite (white).

Table 4.5: SEM data for uraninite coating on pyrite, Figure 4.31

Elmt	Element	Sigma	Atomic
	%	%	%
C K	8.34	0.19	20.86
O K	35.80	0.44	67.21
P K	2.11	0.09	2.05
Ti K	1.26	0.12	0.79
Fe K	5.86	0.22	3.15
Pb M	2.68	0.25	0.39
U M	43.95	0.49	5.55
Total	100.00		100.00

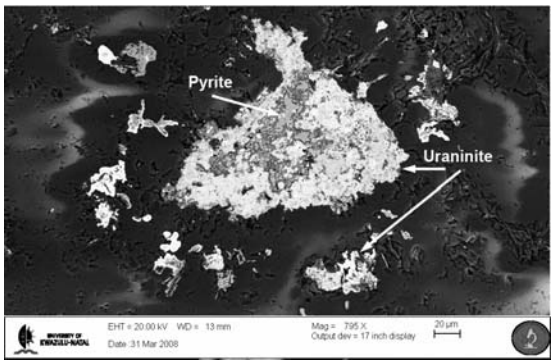

Figure 4.32: Backscattered electron image of uraninite (white) replacing corroded pyrite grain (grey).

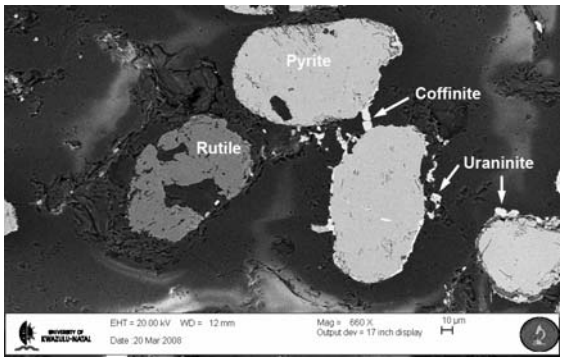

Figure 4.33: Backscattered electron image of rounded pyrite grains (light grey) with coatings of uraninite and crystals of coffinite (white) between the two grains.

4.4.6 OTHER MINERALS

Chromite forms a minor constituent in all conglomerate zones. Rounded to sub-rounded grains occur within the reef package. Diameters rarely exceed 0.3 mm and the grains show cataclastic shattering (Figure 4.34 A).

Zircon is common within the Denny Dalton conglomerates and forms well rounded grains (Figure 4.34 B). It often exhibits cataclastic shattering. Under reflected light microscopy many of the grains display a well defined zoning. A small percentage of the zircon grains are partly replaced by quartz and contain inclusions of galena.

Galena is the most abundant mineral occurring as inclusions within detrital grains. Most galena inclusions are hosted within partially corroded detrital leucoxene and monazite grains (Figure 4.20). Within CG 4, galena is predominantly hosted as inclusions within rounded pyrite grains but is also evident as rare free crystals within the matrix (Figure 4.34 C).

Arsenopyrite is present as subhedral grains, inclusions and irregular aggregates within the lower conglomerate zones. Subrounded arsenopyrite grains exhibit strong corrosion in comparison to rounded pyrite (Figure 4.34 D); grains are internally massive with corroded edges replaced by silica. One minute rhombohedral inclusion of arsenopyrite has been identified by EDX in compact rounded pyrite. Arsenopyrite in CG 4 occurs as subhedral aggregates replacing gangue around the edges of rounded pyrite grains.

Scorodite ($FeAsO_4 . 2H_2O$) is a secondary hydrated iron arsenate which completely replaces original small, fractured anhedral pyrite clusters. Scorodite forms as an alteration product of arsenopyrite and

pyrite (Griffith, 2005). Veinlets of scorodite are evident within fractures in cataclastically fractured massive pyrite grains with encrustations and coatings visible around many of the massive rounded pyrite grains. It occurs only in CG 1 where anhedral aggregates host inclusions of primary gold (Figure 4.24 and 4.25).

Gersdorffite (NiAsS) is associated with arsenopyrite in CG 4 (Figure 4.34 D) and occurs as rare irregular aggregates intergrown with arsenopyrite.

Sphalerite is an abundant ore mineral in CG 4 occurring as anhedral to subhedral masses overgrowing or replacing detrital grains such as pyrite, apatite or gangue minerals (Figure 4.34 D and E).

A single crystal of *Thorite* was identified in CG 2 associated with euhedral authigenic pyrite (Figure 4.34 F).

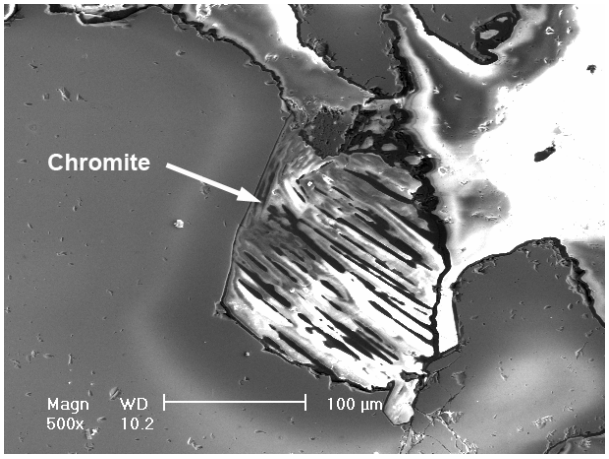
Chromite
Magn
500x
WD
10.2
100 µm

(A)

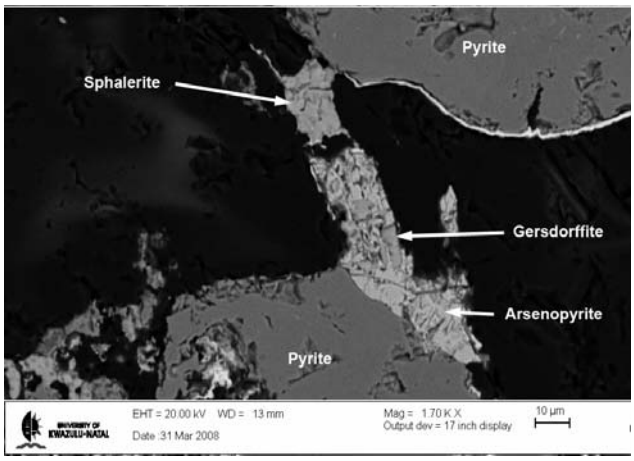
Pyrite
Sphalerite
Gersdorffite
Arsenopyrite
Pyrite
EHT = 20.00 kV WD = 13 mm
Date :31 Mar 2008
Mag = 1.70 K X
Output dev = 17 inch display
10 µm

(D)

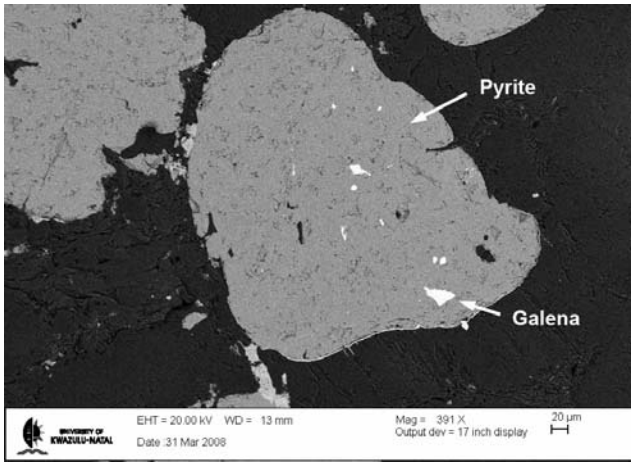
Pyrite
Galena
EHT = 20.00 kV WD = 13 mm
Date :31 Mar 2008
Mag = 391 X
Output dev = 17 inch display
20 µm

(C)

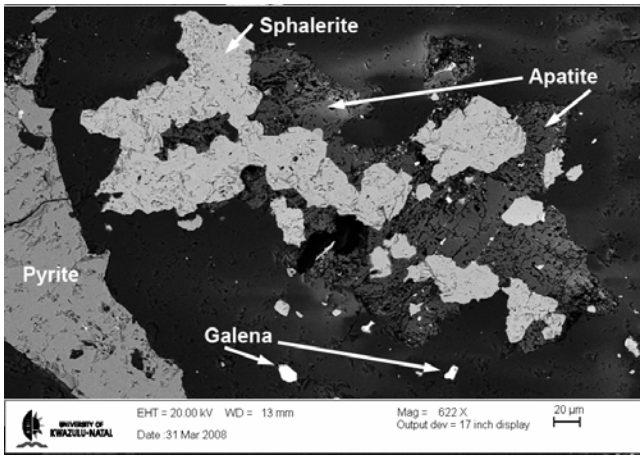
Sphalerite
Apatite
Pyrite
Galena
EHT = 20.00 kV WD = 13 mm
Date :31 Mar 2008
Mag = 622 X
Output dev = 17 inch display
20 µm

(E)

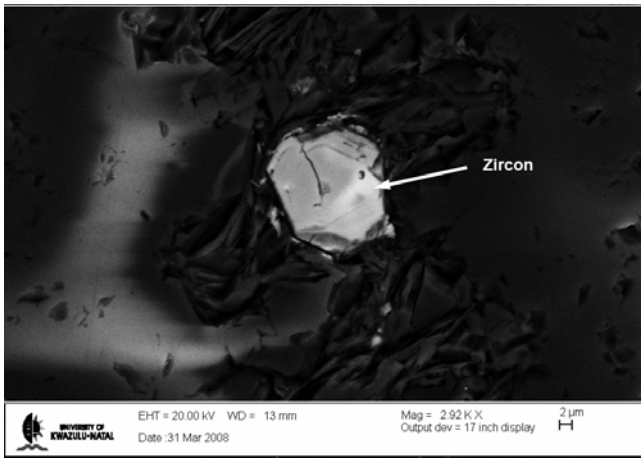
Zircon
EHT = 20.00 kV WD = 13 mm
Date :31 Mar 2008
Mag = 2.92 K X
Output dev = 17 inch display
2 µm

(B)

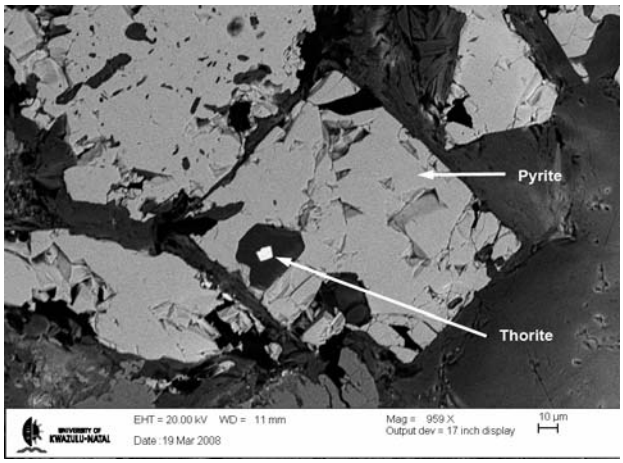
Pyrite
Thorite
EHT = 20.00 kV WD = 11 mm
Date :19 Mar 2008
Mag = 959 X
Output dev = 17 inch display
10 µm

(F)

Figure 4.34: Backscattered and secondary electron images of other ore and heavy minerals found within the Mandeva Formation conglomerates.

A: Secondary electron image of detrital chromite grain (CG 1)

B: Detrital zircon grain (CG 4).

C: Galena inclusions within rounded pyrite grain (CG 4).

D: Sphalerite and intergrowths of authigenic arsenopyrite and gersdorffite replacing gangue and pyrite between rounded pyrite grains (CG 4).

E: Authigenic sphalerite overgrowing and replacing apatite; galena crystal is evident at the bottom of the image (CG 4).

F: Euhedral authigenic pyrite crystal partially replaced by gangue. Thorite crystal evident in gangue within pyrite (CG 2).

4.5 ORE MINERALOGY DISCUSSION

4.5.1 ROUNDED PYRITE

The rounded pyrite grains evident in the Mandeva conglomerates resemble pyrites from the Witwatersrand basin as described by Ramdohr (1958), Saager (1970) and Utter (1980). Saager (1970) identified "compact rounded pyrite" in the Witwatersrand basin and indicated that this pyrite would have been deposited in an exceptionally unweathered state due to the lack of alteration evident in the pyrite.

Saager (1970) attributed much of the rounded pyrite in the Witwatersrand Supergroup to pyritization of hematite and magnetite sand grains within the Basal Reef by identifying rare replacement relics of black sand in some pyrite grains. A number of authors (Barnicoat et al., 1997; Phillips & Law, 1994; Phillips & Law, 2000) have argued for a hydrothermal origin for the rounded pyrite within the Witwatersrand basin. Barnicoat et al. (1997) envisaged the replacement of iron-rich minerals by pyrite during diagenesis. They indicated that fluid flow along major thrusts, bedding planes and foresets during compressive deformation would allow for mineralization in these areas (Barnicoat et al., 1997). Within the Mandeva Formation however, only minor compression is evident with no major thrusting. Localized shearing along the Nsuze-Mozaan unconformity and minor bedding-parallel shearing along lithological contrasts could have provided channelways for mineralized fluid flow; however the lack of strong deformation and alteration could account for the lower gold grades identified in the Pongola Supergroup.

Viljoen (1967) and Frimmel (2005) however, concluded that the amount of "black sands" in the Main Reef in the Witwatersrand basin was negligible as no replacement relics could be found No primary

or partially replaced hematite or magnetite grains have been observed in the Mandeva Formation conglomerates and it can therefore be said that there was little input of magnetite and hematite "black sands" during deposition and that the rounded pyrite grains are predominantly of primary origin.

Carling and Breakspear (2006) emphasized that in the proximal facies of a fluvial environment, sediment is dominated by coarse-grained sand and gravel which is transported predominantly as bedload. Detrital heavy minerals within the bed load are often retained in the proximal facies as they are easily entrained and deposited in pore spaces between larger clasts (pebbles and cobbles) of lighter material (Carling & Breakspear, 2006). In zones of flow convergence in a braided stream environment heavy minerals tend to be deposited with the coarse fraction in the deeper parts of channels. Winnowing of these deposits removes the finer particles, leaving a concentration of small heavy mineral grains surrounded by large light pebble and cobble clasts as a lag deposit (Carling & Breakspear, 2006; Smith & Beukes, 1983). The rounded pyrite grains are concentrated in the matrix of all conglomerate layers in the Mandeva Formation and would therefore have been entrained during deposition in a fluvial environment.

The relative abundance of rounded pyrite associated with heavy minerals of detrital origin (chromite and zircon) within the mineralized conglomerates is an indication of a possible detrital origin. The rounded to subrounded and abraded nature of the Mandeva Formation pyrite is indicative of transport from primary ore deposits in a separate source terrane. Rounding of the pyrites in the Pongola basin is less pronounced than in the Witwatersrand basin (Saager et al., 1986). This could indicate a more proximal provenance for the pyrite grains in the Denny Dalton conglomerates.

4.5.2 EUHEDRAL PYRITE

Post-sedimentary hydrothermal and/or metamorphic processes within the White Umfolozi Inlier were responsible for the formation of euhedral pyrite in the Denny Dalton conglomerates. The cubic form and lack of etched or abraded surfaces of the crystals is evidence for in situ crystallization. The close association of euhedral crystals with quartz veins cross-cutting the conglomerates is indication of a possible hydrothermal origin for the pyrite, possibly representing crystallization from sulphur-rich fluids migrating along the unconformity between the Mozaan and Nsuze Groups.

Saager (1970) postulated that compact idiomorphic pyrite crystals in the Witwatersrand Supergroup were formed by mobilization and recrystallization during metamorphism of the Witwatersrand Supergroup sedimentary rocks. He also identified hydrothermal pyrite associated with intrusions of dykes during Ventersdorp times (Saager, 1970). Idiomorphic pyrite also occurs as porous crystals within the Mandeva Formation. Internal replacement by quartz is evident within singular crystals and

crystal aggregates. This replacement indicates a much later silicification of the Mandeva Formation sedimentary rocks (Figure 4.12).

4.5.3 POROUS AND RADIAL PYRITE

Porous concretionary pyrite is a major pyrite constituent in CG 1 at Denny Dalton. These well-rounded, pebble-sized pyrite grains have also been documented by Saager (1970) in the Basal Reef in the Witwatersrand Supergroup. The well-rounded nature of the pyrite is indicative of transport before deposition. The fragile and friable nature of the porous grains is however, evidence against any major transportation. Hallbauer (1986) defined the porous pyrite as being syn-sedimentary in origin and concluded that the rounded porous grains would have formed close to the depositional environment.

Saager (1970) identified a number of inclusions of gold and base metal sulphides within pore spaces in concretionary pyrite grains. He postulated that the concretionary pyrite formed prior to the remobilization of the gold and acted as a trap in which the gold and sulphides could recrystallize (Saager 1970). The lack of gold and base metal sulphide inclusions within concretionary pyrite from the Denny Dalton conglomerates indicates that no gold remobilization has occurred and that the gold evident is most likely of primary origin.

The radial pyrite evident at Denny Dalton has also been documented in the Witwatersrand Supergroup reefs (Hallbauer, 1986). This pyrite is defined by radial growth from a central point and is classified as syn-sedimentary in origin (Hallbauer, 1986). The radial pyrites of the Witwatersrand Supergroup often contain inclusions of iron-rich chlorite and chloritoid (Hallbauer, 1986). The friable nature of the radial pyrites from Denny Dalton did not allow for SEM or thin section analysis of the grains as they were consistently destroyed during slide preparation and it can only be assumed that inclusions could have been present in the grains. In hand specimen, radial pyrite grains from Denny Dalton often show abraded grain edges suggesting transport similar to that of the compact rounded pyrite grains. Due to their radial nature it is probable that these pyrite grains were once marcasite, but have subsequently been replaced by pyrite.

4.5.4 RUTILE AND LEUCOXENE

Allogenic rutile is a minor constituent in the Denny Dalton conglomerates and occurs as subrounded massive rutile grains with minor inclusions of pyrite. Detrital rutile grains are also evident in the Witwatersrand Supergroup and Dominion Group reefs but are also only a minor heavy mineral component (Feather and Koen, 1975).

Leucoxene, a micro-crystalline rutile, forms by the alteration of ilmenite ($FeTiO_3$) to rutile (TiO_2) (Coetzee, 1965). Leucoxene is a major heavy mineral constituent in the Denny Dalton conglomerates and is evident in equivalent Mozaan Group conglomerates in the main Pongola basin (Saager & Stupp, 1983). Coetzee (1965) working in the Witwatersrand concluded that although the primary grains had undergone alteration the original grain shapes could often still be determined. He indicated that the primary grains had similar grain-sizes to other heavy minerals such as chromite and zircon and would therefore have been a mineral with a similar specific gravity (Coetzee, 1965). As leucoxene forms from the alteration of ilmenite and the specific gravity of ilmenite is close to that of chromite and zircon it was concluded that the primary mineral would have been ilmenite (Coetzee, 1965). No unaltered ilmenite grains are evident in the Denny Dalton conglomerates however, indicating complete replacement of ilmenite to leucoxene, probably during diagenesis.

4.5.5 MONAZITE

Monazite is an abundant heavy mineral in the lower conglomerates at Denny Dalton. The high ThO_2 values (160 g/t) recorded at Denny Dalton Mine (Saager et al., 1986) are probably due to high concentrations of monazite within the lower conglomerates. Monazite is the most abundant heavy mineral within the Dominion Reefs, but is rare in the Witwatersrand Supergroup (Feather and Koen, 1975). Monazite is generally indicative of a granitic or pegmatitic provenance (Battey & Pring, 1997) and the monazite evident in the Denny Dalton conglomerates could have originated from the granites and gneisses that form the basement to the White Umfolozi Inlier.

4.5.6 GOLD

Hallbauer (1986) indicated that the majority of gold won from the Witwatersrand Supergroup reefs occurs in five forms.

i. Detrital gold in the matrix

ii. Biochemically redistributed gold (associated with carbon)

iii. Gold recrystallized and redistributed by metamorphic processes in the reef

iv. Primary gold as inclusions in detrital allogenic sulphides

v. Gold in secondary quartz veins

Up to 90% of the gold won from many Witwatersrand Supergroup reefs occurs as detrital gold particles in the matrix, with up to 40% occurring as recrystallized gold under certain conditions (Hallbauer, 1986). Less than 2% of the gold won however, comes from primary gold inclusions in detrital pyrite grains (Feather & Koen, 1975). Primary gold inclusions within both detrital pyrite and arsenopyrite have been identified within the Basal Reef in the Witwatersrand Supergroup (Hallbauer, 1986).

No free gold within the matrix is evident in the conglomerates at Denny Dalton; gold is rather hosted in massive rounded pyrite grains and in anhedral aggregates of scorodite ($FeAsO_4 . 2H_2O$). The gold inclusions identified at Denny Dalton are similar to primary gold inclusions identified by Hallbauer (1986) and Ramdohr (1958) in massive detrital pyrite grains in the Witwatersrand. When compared to the Witwatersrand Supergroup reefs, the lack of free gold in the matrix suggests that no recrystallization of gold occurred at Denny Dalton.

At Denny Dalton, gold inclusions within massive pyrite show primary origins as the crystal edges mimic the original cubic and pyritiohedron crystal shapes of hydrothermal pyrite aggregates. The high optical reflectivity of the gold suggests a high Ag content and indicates a primary rather than recrystallized origin for the gold, unlike the duller gold found in the matrix of the Witwatersrand Supergroup ores (Feather & Koen, 1975). The gold and its detrital pyrite host could therefore have been derived from primary ore deposits such as vein-type lode deposits within greenstone settings.

Collectively the Witwatersrand gold fields have been mined at an average grade of 9 g/t (McCarthy, 2006) and have won ~46 000 t of gold. The Denny Dalton conglomerates have an average grade of 4

g/t (Table 4.6). As the gold is refractory and no free gold is evident the gold tenor is substantially less than that seen in the Witwatersrand gold fields.

Table 4.6: Average gold tenor identified in the CG 1 at Denny Dalton

Gold Tenor for CG 1 (the MCR) at Denny Dalton			
Author	Year	No. of samples	Average Au. (g/t)
Denny Dalton Mining Company *	1895	continuous mining	4.1
Denny Dalton Tribute Syndicate *	1905 - 1906	continuous mining	3.2
Colonel Peakman *	1908	continuous mining	3.4
Hatch, F.H.	1910	82	4.7
Delpierre, M.E.R.	1969	15 (borehole)	trace
Delpierre, M.E.R.	1969	2 (selected surface)	7.41
Campbell, D.	1982	242	1.4
Saager et al.	1986	?	4

* Continuous mining grades documented in Hatch (1910).

4.5.7 URANIUM MINERALS

Uranium mineralization has been identified by numerous authors (Campbell, 1982; Delpierre, 1969; Saager & Stupp, 1983; Saager et al., 1986; von Backstrom, 1967; von Rahden & Hiemstra, 1967) within three of the Mandeva Formation conglomerates. Most reports conclude that the tenor is extremely low but for small patches of higher grade.

Table 4.7: Average Uranium Tenor identified in the Denny Dalton conglomerates.

Uranium Tenor for CG 1 (the MCR) at Denny Dalton			
Author	Year	No. of samples	Average U_3O_8 grade (g/t) unless stated
von Backstrom, J.W.	1967	11	0.016 % U_3O_8
von Rahden, H.V.R. and Hiemstra, S.A.	1967	4	0.0128 % U_3O_8
Delpierre, M.E.R.	1969	30	45.36
Campbell, D.	1982	128	310
Saager et al.	1986	?	< 1 200

Saager and Stupp (1983) conclude that the leucoxene represents part of a continuous mineral series from rutile to brannerite. Leucoxene is essential for brannerite formation as the framework is infilled

with interstitial U and Ca (Amme et al., 2005). A number of authors (Saager & Stupp, 1983; Saager et al., 1986; von Rahden & Hiemstra, 1967) attribute uranium values within the lower reefs to brannerite formation. A problem arises however, as the U_3O_8 values identified within the CG 1 and CG 2 conglomerates require a large percentage of brannerite within the matrix. As mentioned previously, SEM analysis of leucoxene grains showed no appreciable amounts of brannerite within the Mandeva Formation conglomerates and that it occurred only as minor accessory crystals along the edges of leucoxene grains. Saager and Stupp (1983) warn that the actual occurrence of metamict brannerite within the Pongola Supergroup conglomerates must be regarded with reservation and that diagenesis and metamorphism did not lead to the formation of authigenic brannerite but rather uraniferous leucoxene. The uranium grades evident in CG 1 cannot be attributed to the occurrence of brannerite or uraniferous leucoxene and a more suitable source needs to be found.

The high concentrations of disseminated uraninite within black chert pebbles from CG 1 can account for the ore grades evident at Denny Dalton. The average U_3O_8 grade for CG 1, as seen in Table 4.7, is similar to the 310 g/t identified by Campbell (1982). Geochemical analysis of chert pebbles from the same conglomerate identified uranium values in the order of 398 ppm uranium (Appendix II). This also accounts for the erratic nature of the uranium grades identified at Denny Dalton. As the uranium is directly associated with black chert pebbles the grades would be greatest in zones rich in chert. However, chert clasts are dominant only within cobble-sized conglomerate zones and are thus, due to their size, associated with the deepest parts of the palaeo-channels. Where the conglomerate grades laterally into a large-pebble, vein quartz dominated conglomerate the U_3O_8 grades would be negligible.

Uranium within the chert pebbles appears as aggregates along fractures and as disseminated crystals. The uranium is often associated with euhedral pyrite and forms coatings around the pyrite crystal (Figure 4.28). This occurrence along fractures and within pore spaces, as well as its association with hydrothermal cubic pyrite, indicates a secondary origin for the uranium. The overall geochemistry of the chert pebbles at Denny Dalton is very similar to cherts analysed by Hofmann and Wilson (2007) from the Nondweni Greenstone Belt. A major difference however, is the anomalous uranium values within the Denny Dalton pebbles (Table 4.8). This anomalously high uranium grade, compared with the low values within the Nondweni cherts, is indicative of a possible secondary source for the uranium in the Denny Dalton conglomerates. The lower uranium values identified in the analysed samples of CG 1 and CG 4 in comparison to the black chert pebbles is due to dilution from barren vein quartz clasts, both as pebbles, and grains in the matrix.

Table 4.8: Uranium values obtained from X-Ray Florescence (XRF) Geochemistry of samples from Denny Dalton and from the Nondweni Greenstone Belt. Nondweni data after (Hofmann & Wilson, 2007)

Element		CG 1	CG 4		Denny Dalton Black Chert Pebbles	Nondweni Black Chert
U		17.2 ppm	8.8 ppm		360 - 400 ppm	0.1 - 0.4 ppm

The ore grade uranium identified in CG 4 by Campbell (1982) occurs as secondary uraninite and coffinite. Hallbauer (1986) showed that low-temperature, hydrothermally derived uraninite has a very low thorium content compared to detrital uraninite derived from granites or pegmatites. The uraninite evident in CG 4 has no associated thorium values and therefore a secondary hydrothermal origin is favoured. This uraninite is authigenic in origin as no detrital grains have been observed.

Secondary uranium mineralization similar to that of CG 4 is also evident within the Witwatersrand Supergroup reefs and is associated with carbonaceous matter (carbon). The "carbon" is either derived from fossil remains of in situ algal mats (England et al., 2002), or from hydrocarbons migrating through the rock after deposition (England et al., 2002). The lack of carbon within CG 4 however, negates the formation of secondary uraninite due to carbonaceous matter.
Hemingway (1982) indicated that coffinite can be produced from "the reduction of UO_2^{2+} to UO_2 + (U^{5+}), which decreases the solubility of the dissolved U and leads to adsorption UO_2^{+} onto a silicate or sulfide grain boundary surface." This process is identified in the Witwatersrand Supergroup reefs where uraninite nodules undergo chemical breakdown and the remobilized uranium is reprecipitated on the surface of grains as coffinite (Smits, 1992).

Therefore, the most plausible argument for a source of uranium is that primary uraninite grains were remobilized from within the lower conglomerates (CG 1 and CG 2). The uranium enriched fluids migrated along bedding parallel shears and zones of increased porosity. Within Conglomerate 4 the localized abundance of pyrite grains produced a reducing environment within which the uranium was recrystallized as secondary uraninite and coffinite encrustations around locally reducing pyrite grains.

CHAPTER 5

GEOCHEMISTRY

5.1 INTRODUCTION

Wronkiewicz and Condie (1989) analysed pelite and quartz arenite samples from both the Mozaan and Nsuze Groups in the White Umfolozi Inlier. They concluded that 3.2 to 3.0 Ga hood granites were the source of major detrital input into the Pongola basin with only minor amounts of komatiite and tonalite input (Wronkiewicz and Condie, 1989). They determined that quartz arenite compositions and detrital modes in the Pongola Supergroup are very similar to Phanerozoic passive-margin sandstones.

Alexander et al. (2008) analysed a number of samples from the Vlakhoek Member shales and banded iron formation. They suggested that the banded iron formation formed as near-shore chemically-derived sediments with REE patterns typical for marine waters during the Proterozoic (Alexander et al., 2008). They propose that positive Eu anomalies in banded iron formation samples indicate a high temperature hydrothermal source for REE's in the seawater that precipitated the BIF (Alexander et al., 2008). Alexander et al. (2008) are in agreement with the findings of Wronkiewicz and Condie (1989), and suggest that the Valkhoek Member shale and BIF was derived from a primarily homogeneous cratonic source older than 3.2 Ga.

5.2 WHOLE-ROCK GEOCHEMISTRY

Whole rock geochemistry was carried out on all four conglomerates within the Mandeva Formation (Figure 5.1). Two samples of both quartz arenite and grit and six samples of shale were also analysed from samples taken from diamond drill cores TSB 06-23 and TSB 07-26 (Figure 5.1 and 5.2). Five samples of black shale (TSB 07/26-169.4 to TSB 07/26-175) were taken from below the Banded Iron Formation, one sample (TSB 07/26-168) taken from shale interbedded within the BIF, two samples (TSB 07/26-163.9 and TSB 07/26-165.2) were taken from the green shale that overlies the BIF (Figure 5.2).

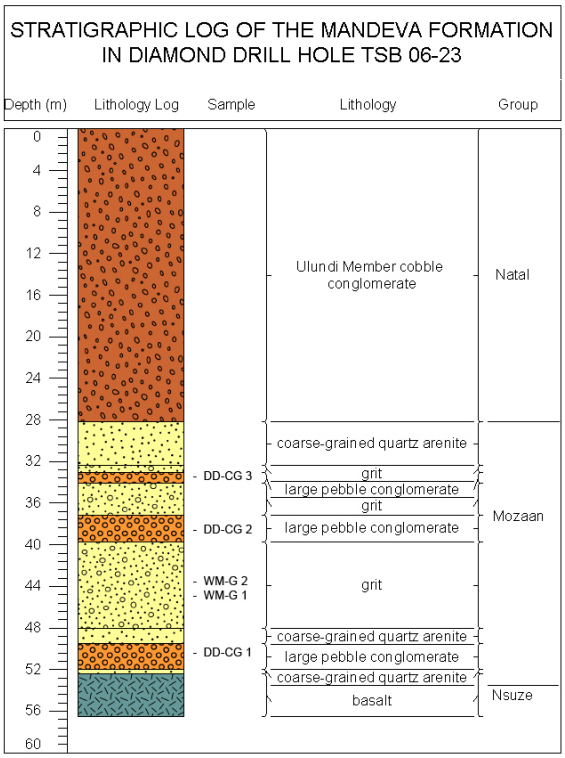

Figure 5.1: Stratigraphic log of diamond drill core TSB 06-23 with sample localities.

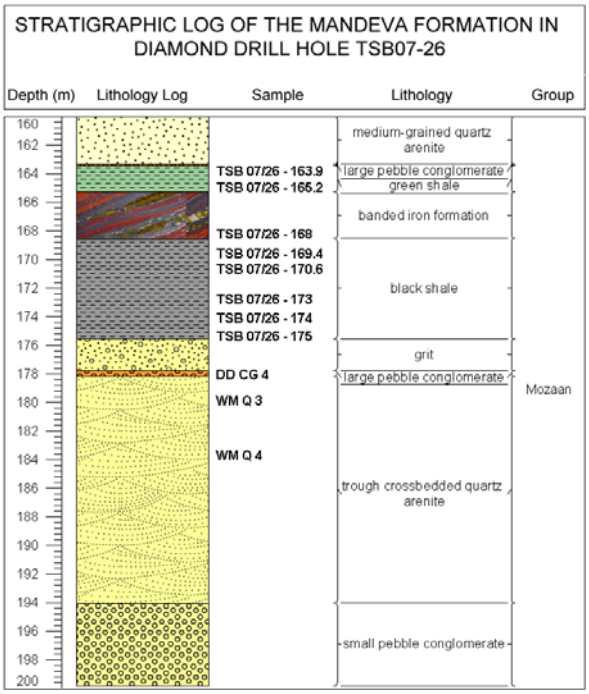

Figure 5.2: Stratigraphic log of diamond drill hole TSB 07-26 with sample localities.

5.2.1 MAJOR ELEMENTS

5.2.1.1 CONGLOMERATE, QUARTZ ARENITE AND GRIT

SiO_2 contents in the conglomerates are consistently high and range between 94.37-97.6% wt.% (average 95.9 wt.%). The low Al_2O_3 and TiO_2 contents compared to PAAS (Post Archaean average Australian Shale, Taylor and McLennan, (1985)) suggests low clay content for the conglomerates. The low values for all other major elements are indicative of the high SiO_2 content of the conglomerates (Figure 5.3).

5.2.1.2 SHALES

The Vlakhoek Member shales show highly variable concentrations of major elements (Al_2O_3, K_2O and Fe_2O_3) through the unit. The black shales at the base of the member (TSB07/26-175 - TSB07/26-169.4) have high Al_2O_3 and K_2O values with low Fe_2O_3. The green shales above the banded iron formation (TSB07/26-168 - TSB07/26-163.9) have low Al_2O_3 and high Fe_2O_3 (Figure 5.4).

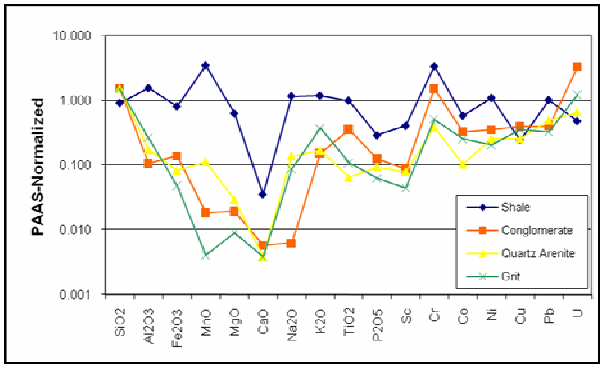

Figure 5.3: Major and selected trace elements for average shale, conglomerate, quartz arenite and grit normalized to PAAS.

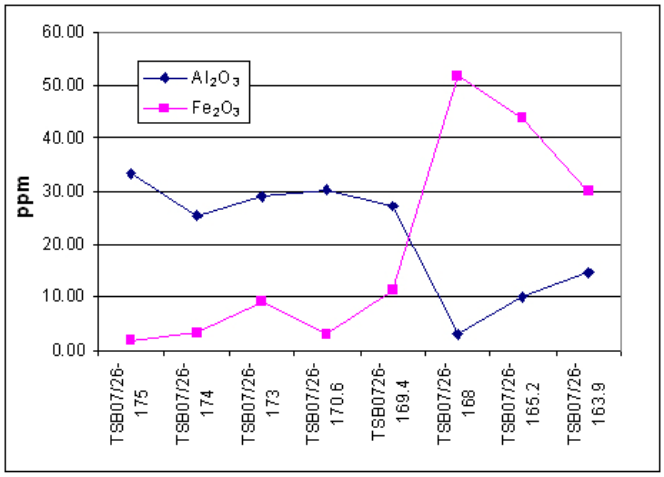

Figure 5.4: Al_2O_3 vs. Fe_2O_3 for Vlakhoek Member shales showing transition from detrital input (high Al_2O_3) to chemical precipitation (high Fe_2O_3).

5.2.2 TRANSITION GROUP ELEMENTS (Sc, V, Cr, Co, Ni)

5.2.2.1 CONGLOMERATE, QUARTZ ARENITE AND GRIT

The Mandeva Formation conglomerates are depleted in Sc, Co, Ni compared to PAAS (Figure 5.3). Cr is enriched in all conglomerates except CG 3 and also shows enrichment when average conglomerate is normalized to PAAS (Figure 5.3). Cr is however depleted in average grit and quartz arenite samples when normalized to PAAS (Figure 5.3).

5.2.3 LARGE-ION LITHOPHILE ELEMENTS (LILE; Rb, Sr, Ba)

5.2.3.1 CONGLOMERATE, QUARTZ ARENITE AND GRIT

All samples have low LILE values (Rb 2.55-37.14 ppm, Sr 3.23-30.59 ppm, Ba, 10.99-98.17 ppm) relative to PAAS. LILE in the samples are also lower compared to LILE of average shale in the Vlakhoek Member.

5.2.3.2 SHALES

Rb and Sr values are higher in the samples below the iron formation (TSB07/26-175 to TSB07/26-169.4), compared to the uppermost shale samples. These higher LILE values are in accordance with higher values of Al_2O_3 in the lower shale unit. When plotted against K_2O, Rb has a strong positive correlation. Sr has no correlation when plotted against CaO. Ba values vary drastically in the shale samples ranging from 0.37-211.78 ppm.

5.2.4 HIGH FIELD STRENGTH ELEMENTS (HFSE; Y, Zr, Nb, Ta, Hf, Th) and U

5.2.4.1 CONGLOMERATE, QUARTZ ARENITE AND GRIT

Zr values in conglomerates CG 1 and CG 2 are very similar to PAAS, whereas CG 3 and CG 4 as well as the quartz arenite and grit samples are depleted. The enriched U values in CG 4 are also associated with high Zr values. When normalized to PAAS, U is enriched in average Mandeva conglomerate whereas average grit and average quartz arenite show values very close to that of PAAS. Y, Nb, and Hf are all depleted relative to PAAS in average samples (Figure 5.5). Ta is depleted relative to PAAS in average grit, quartz arenite and shale but not in average conglomerate.

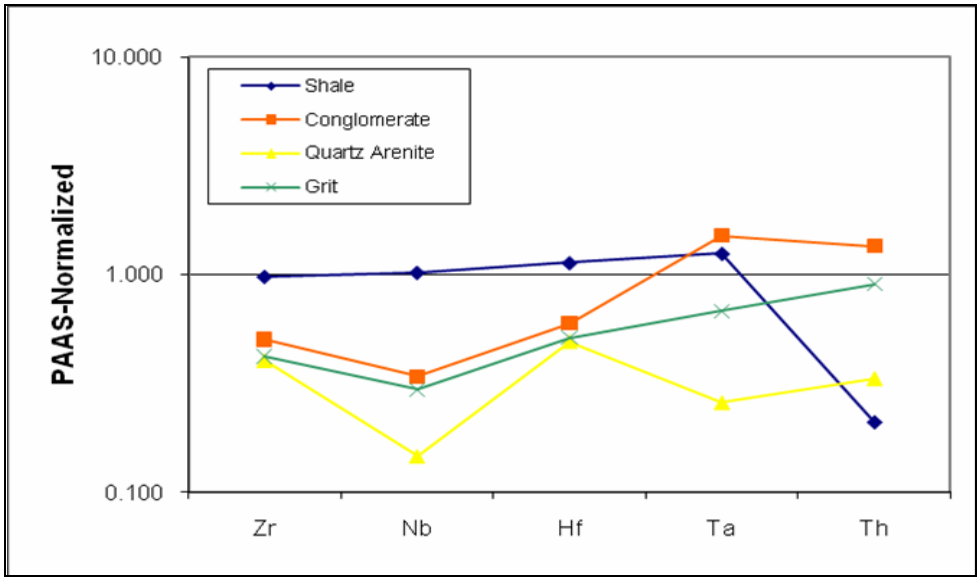

Figure 5.5: PAAS-normalized distribution of Zr, Nb, Hf, Ta and Th for average conglomerate, quartz arenite, grit and shale in the Mandeva Formation.

5.2.4.2 SHALES

HFSE values for Zr, Nb, Hf and Ta in average shale are very close to PAAS (Figure 5.5) whereas Th is depleted relative to PAAS. Hf values in the black shales are relatively high and range from 4.11 to 7.25 ppm compared to the low Hf values for the BIF and green shales (0.57-2.72 ppm). Ta also shows higher values (1.46-1.70 ppm) within the black shales compared to (0.03-0.63 ppm) in the BIF and green shales. Zr values for the black shales are high (148.00-267.37 ppm) compared to low values for the BIF and green shales (23.48-104.43 ppm), however, Zr values for the black shales decrease stratigraphically upwards towards the contact with the BIF and green shales. Both Th and U show no distinct variation between the black and green shales. Y values within the black shales are low (1.51-5.26 ppm) except for sample TSB07/26-169.4 which has values of 8.70 ppm. The BIF and green shales show values similar to that of TSB07/26-169.4 and range from 6.32 to 12.05 ppm.

5.2.5 RARE EARTH ELEMENTS (REE)

5.2.5.1 CONGLOMERATE, QUARTZ ARENITE AND GRIT

The Mandeva Formation conglomerates, grits and quartz arenites show similar REE patterns (Figure 5.6a). CG 2 shows high total REE concentrations and a very pronounced negative Eu anomaly (Eu/Eu* 0.092; Figure 5.6a). All the samples show flat HREE patterns. Average REE patterns for the conglomerates, quartz arenite and grits are similar to PAAS except for the pronounced low Eu anomalies in conglomerate and grit samples (Figure 5.6c).

5.2.5.2 SHALES

Chondrite-normalized REE patterns show low total REE concentrations for all Vlakhoek Member shales (Figure 5.6b). The LREE patterns are very similar except for lower concentrations in samples (TSB07/26)-174, -170.6 and -168. All shale samples show negative Eu anomalies with Eu/Eu* ratios between 0.72-0.99. Average total REE patterns for the Vlakhoek shales are depleted compared to PAAS but show a similar REE pattern (Figure 5.6c).

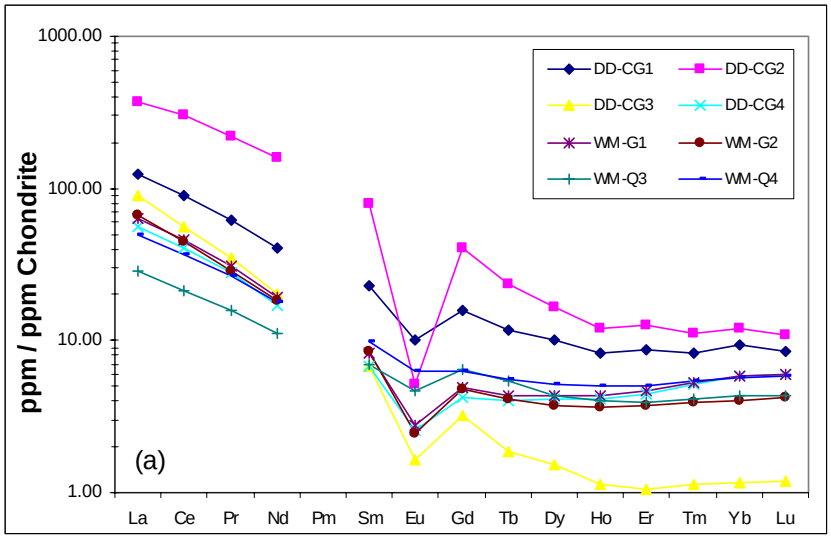

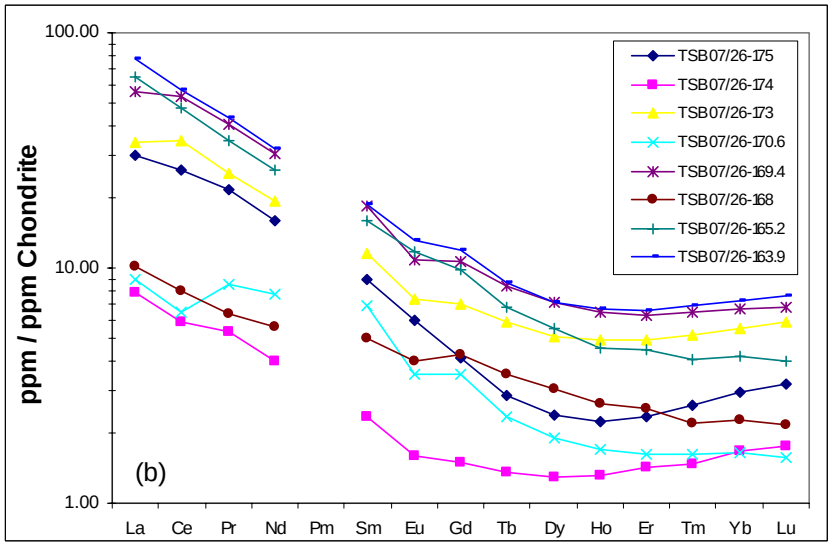

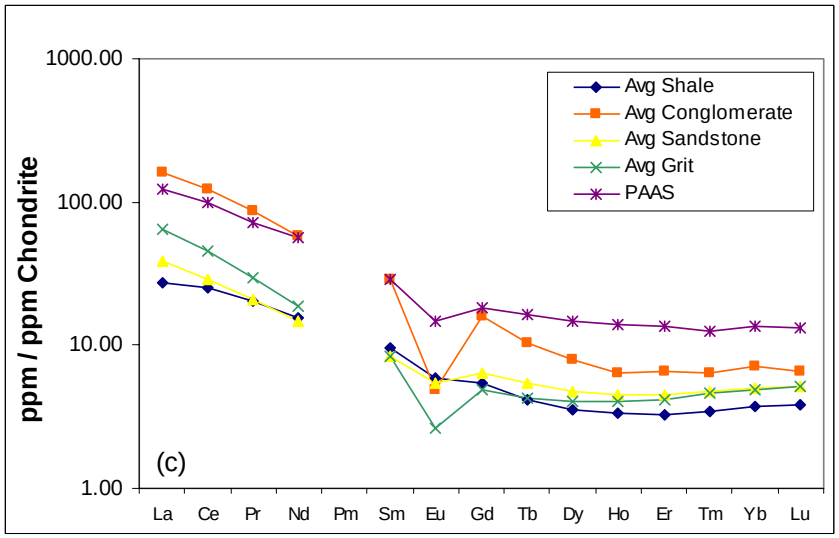

Figure 5.6: Chondrite-normalized REE patterns for (a) conglomerates (DD-CG1, DD-CG2, DD-CG3, DD-CG4), quartz arenites (WM-Q3, WM-Q4) and grits (WM-G1, WM-G2) of the Mandeva Formation, (b) Vlakhoek Member Shales and (c) average values for conglomerate, grit, quartz arenite, shale and PAAS.

5.3 GEOCHEMISTRY DISCUSSION

5.3.1 MANDEVA FORMATION CONGLOMERATE, QUARTZ ARENITE AND GRIT

Wronkiewicz and Condie (1989) reported that Pongola quartz arenites are depleted in TiO_2, Sr, Th, V, Nb, Ta, Zr and Hf in comparison to Phanerozoic sandstones. The depleted HFSE elements (Th, Nb, Ta, Zr, Hf) identified by Wronkiewicz and Condie (1989) indicate that Pongola quartz arenites have lower concentrations of heavy minerals such as zircon when compared to Phanerozoic sandstones. Cr is enriched in all conglomerates except CG 3, probably indicating a high concentration of detrital chromite in conglomerates of larger clast size, whereas a depletion of Cr in the quartz arenites and grits of the Mandeva Formation is due to a lower proportion of heavy minerals in the matrix. Cr has been identified in thin section in all conglomerates in the Denny Dalton Member, however has higher concentrations in CG 1, CG 2 and CG 4 (refer to Chapter 4). The enriched U values within CG 1 and CG 2 could be associated with Zr due to U enrichment in zircon (Harley & Kelly, 2007), but could also be due to a higher concentration of uraniferous chert pebbles within these conglomerates (refer to Chapter 4). The increased U contents in CG 4 is possibly due to secondary UO_2 coatings around detrital pyrite grains (refer to Chapter 4).

All the samples from the Mandeva Formation show similar or parallel REE trends. Wronkiewicz and Condie (1989) indicate that the parallel trends for Pongola quartzites and pelites suggest that the REE's are contained primarily within clay minerals. The depleted HREE values of average Mandeva conglomerate as well as depleted Al_2O_3 and Na_2O values when normalized to PAAS, suggests that the clay constituent in the conglomerates is low, which correlates with the high SiO_2 values. The high total LREE values for CG 2 as well as the pronounced negative Eu anomaly suggests a high concentration of LREE bearing heavy minerals, possibly monazite. Monazite, a LREE-bearing phosphate (Lapidus & Coates, 1990), is a common heavy mineral constituent in conglomerates, and SEM analysis indicated high concentrations of monazite in the CG 2 conglomerate (refer to Chapter 4). The higher values for PAAS normalized Ta in average conglomerates vs average sandstone and grit (Figure 5.5) could result from concentration of detrital heavy minerals such as monazite concentrated in the coarser fractions during sorting due to its higher density (McLennan, 1989). The flat HREE patterns for the average Mandeva Formation conglomerates, quartz arenites and grits and pronounced negative Eu anomaly indicate a possible granitic to granodioritic source terrain for the Mandeva Fomation (Figure 5.6c) (McLennan, 1989).

McLennan (1989) suggests that the production of Eu-depleted, K-rich granitic rocks during crustal stabilization and craton development changed the REE signature of the Archaean continental crust to one which is similar to that of PAAS. The conglomerate, quartz arenite and grits show REE

signatures very close to that of PAAS with pronounced negative Eu anomalies indicating an evolved stable cratonic provenance for the Mandeva Formation.

5.3.2 VLAKHOEK MEMBER SHALES

Wronkiewicz and Condie (1989) propose that, due to high CIA values, Mozaan pelites within the White Umfolozi Inlier are derived from a tectonically or volcanically active unweathered source. However the Vlakhoek Member shales formed by two differing depositional processes. The black shales at the base of the member (TSB07/26-175 - TSB07/26-169.4) have high Al_2O_3 and K_2O values with low Fe_2O_3, indicative of a high clay content derived from detrital material. The enrichment of Zr and Hf in black shales compared to green shale indicates relatively high amounts of zircon which may be used as an indicator for the amount of detrital clastic input during deposition. The decrease in Zr content stratigraphically upward in the black shales indicates progressive starvation of detrital material, and a shift towards more chemically precipitated material near the contact with the banded iron formation. Rb and K_2O substitute for each other and therefore show a strong positive correlation. The enrichment of Rb and K in Mozaan pelites when compared to quartz arenites suggests that these elements are strongly fractionated into the clay minerals (Wronkiewicz & Condie, 1989). Due to the extremely low concentrations of CaO in the shales, Sr has no correlation with CaO.

The green shales above the banded iron formation (TSB07/26-168 - TSB07/26-163.9) show high Fe_2O_3 (43.67 and 30.08 wt.%) and low Al_2O_3 values (9.96 and 14.61 wt.%), suggesting a decrease in detrital component and an increase in the amount of chemical precipitate, similar to that of the underlying banded iron formation. The low Zr and Hf contents in the green shales is in accordance with the findings of Alexander et al. (2008) and suggests that these rocks are largely chemical in origin and contain only a minor detrital component. The high total REE values for chondrite-normalized green shales relative to black shales (Figure 5.6b) could indicate REE exchange by scavenging particulates within marine waters prior to chemical precipitation of the green shales (Alexander et al. 2008). Alexander et al. (2008) propose a high-T hydrothermal source for the weak negative Eu anomalies for chondrite-normalized shales in the Vlakhoek Member. However, the overall REE patterns for the Vlakhoek shales (especially the black shales) are indicative of a detrital input derived from a cratonic source.

5.4 SULPHUR ISOTOPE ANALYSIS

Multiple sulphur isotope analysis was undertaken by A Hofmann at the Geophysical Laboratory in Washington DC in 2008 on 9 pyrite grains from Conglomerate 1 (CG 1) within the Denny Dalton mine area. Pyrite grains selected were all compact rounded pyrites of detrital origin (Figure 5.7) except for one radial pyrite. No porous pyrites were examined as their heterogeneous nature was not conducive to laser ablation techniques. $\Delta^{33}S$ values for compact rounded pyrites plot between 0.104 ‰ and 0.202 ‰. $\delta^{34}S_{CDT}$ values for the same samples also show a constrained distribution between 0.402 ‰ and 2.858 ‰. The radial pyrite examined shows similar $\Delta^{33}S$ values (0.17 ‰) to those of the compact rounded pyrite, however the $\delta^{34}S_{CDT}$ values for this sample are extremely negative and plot at -9.6 ‰ (Figure 5.8).

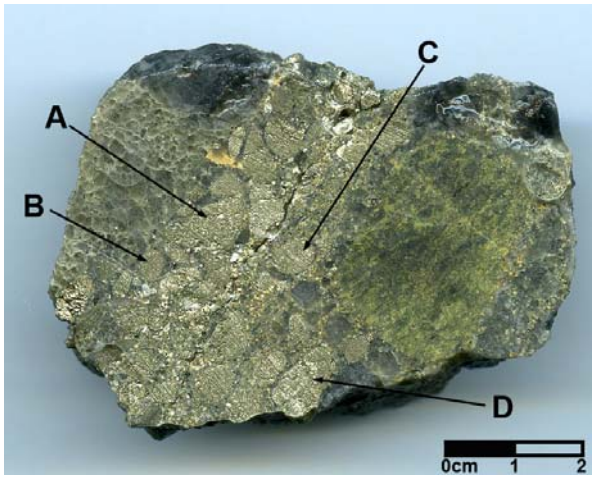

Figure 5.7: Pyrite pebble conglomerate (CG 1) showing different pyrite grains analysed.

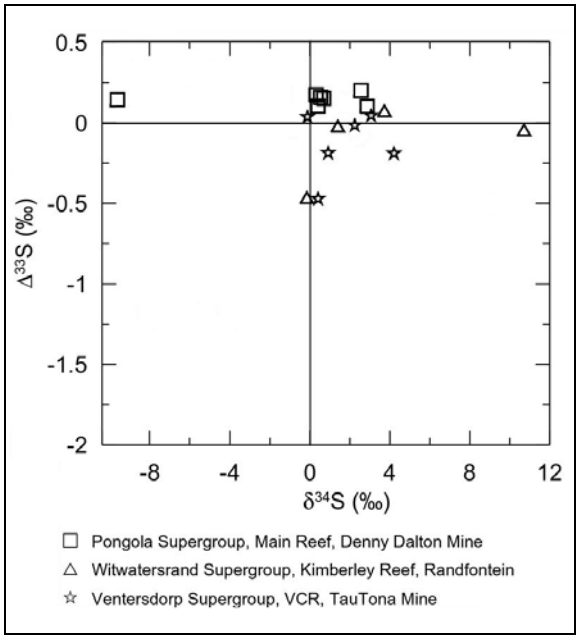

Figure 5.8: Plot of $\delta^{34}S$ vs. $\Delta^{33}S$ for Denny Dalton pyrite compared to Witwatersrand and Ventersdorp pyrite. (modified after Hofmann et al., 2008).

5.5 SULPHUR ISOTOPE DISCUSSION

Sulphur isotope analysis is often used to define the source (magmatic, meteoric, sea water or basinal fluid) of sulphur in pyrite (England et al., 2002b). Mantle derived sulphur has $\delta^{34}S$ values of 0 ± 3 ‰ (Chaussidon & Lorand, 1990; Rollinson, 1993) compared to sulphur of sedimentary origin, which has a large range of -50 to +20 ‰ in modern environments (Rollinson, 1993), although this range is generally much smaller for Archaean sulphur-bearing rocks. The wider range of $\delta^{34}S$ values displayed by sedimentary pyrite is generally due to mass-dependent fractionation during formation. Pyrite formed in igneous melts show $\delta^{34}S$ values of between 1 - 3 ‰ as fractionation is minimal (Ohmoto & Rye, 1979; Rollinson, 1993). Ohmoto and Rye (1979) showed that pyrite of hydrothermal origin has $\delta^{34}S$ values between 0.40 ± 0.08 ‰ (Rollinson, 1993). England et al. (2002b) also indicated that hydrothermal pyrite in Archaean lode gold deposits show $\delta^{34}S$ values close to zero.

$\Delta^{33}S$ isotopes carry unique signatures of Archaean sulphur and are useful in defining processes of sulphur formation (Farquhar & Wing, 2003). Deep ultraviolet radiation is the source of mass independent fractionation of sulphur isotopes and is the cause of $\Delta^{33}S$ anomalies in Archaean sulphur (Farquhar & Wing, 2003). Primitive mantle signatures for juvenile $\Delta^{33}S$ are close to 0 ‰, whereas in Archaean rocks, sedimentary sulphur derived from the atmosphere is preserved with a positive $\Delta^{33}S$ signature (Farquhar & Wing, 2003). Negative signatures in Archaean sulphur occur in oceanic sulphate due to hydrothermal or bacterial reduction (Farquhar & Wing, 2003).

England et al. (2002b) identified a broad range of $\delta^{34}S$ values (-4.7‰ to +14.2 ‰) for multiple pyrite species from the Steyn Reef in the Witwatersrand Supergroup. Rounded compact pyrite showed $\delta^{34}S$ values of -0.5‰ to -5.2‰, whereas the rounded porous pyrites had a much wider distribution with values ranging between -4.7‰ and +6.7‰ with a single grain with a value of +14.2 ‰ (England et al., 2002b). The wide range in $\delta^{34}S$ values for compact and especially, porous rounded pyrite in the Witwatersrand Supergroup is similar to those observed by Hofmann et al. (2008) in the Kimberly and Ventersdorp Contact Reef in the Witwatersrand Supergroup (-0.2‰ to 10.7 ‰) (Figure 5.8). Hofmann et al. (2008) indicate that these pyrites are therefore derived from a sedimentary origin.

Porous radial pyrite from CG 1 at Denny Dalton gives a $\delta^{34}S$ value of -9.6 ‰. This negative value is similar to values for porous pyrite identified by England et al. (2002b) within the Witwatersrand Supergroup and suggests a sedimentary origin for the radial pyrite. As mentioned in Chapter 4, the radial pyrite grains were most probably originally marcasite which was subsequently replaced by pyrite. Marcasite occurs as diagenetic concretions in sedimentary rocks (Battey & Pring, 1997). Falconer et al. (2006) identified diagenetic framboidal marcasite with $\delta^{34}S$ values between -12.1 and -45.4 ‰. They concluded that these marcasite grains were authigenic in origin and grew in pore

spaces in Tertiary non-marine sediments (Falconer et al., 2006). Diagenetic marcasite however occurs predominantly as nodules in marine shale (Schieber, 2007). The high negative $\delta^{34}S$ values for radial pyrite at Denny Dalton suggest that these grains were once authigenic marcasite which has subsequently been replaced by pyrite.

The rounded compact pyrite from CG 1 at Denny Dalton show $\delta^{34}S$ values between 0.4 ‰ and 2.9 ‰ with $\Delta^{33}S$ values between 0.104 ‰ and 0.202 ‰ (Figure 5.8). These $\delta^{34}S$ values close to 0 ‰ are comparable to authigenic pyrites in hydrothermal vein deposits within most Archaean granitoid-greenstone terrains (Hofmann et al., 2008; Ohmoto & Rye, 1979). The $\Delta^{33}S$ values close to 0 ‰ may equally indicate a mantle source for the sulphur present in the pyrite, as many Archaean sedimentary sulphides show mass-independent fractionation (Hofmann et al., 2008) Therefore a hydrothermal / mantle origin is most likely for the compact rounded detrital pyrites found at Denny Dalton.

CHAPTER 6

BASIN CORRELATION OF THE MANDEVA FORMATION

6.1 INTRODUCTION

The basal Mandeva Formation was deposited on a laterally extensive braided alluvial plain which was subsequently subjected to a cycle of marine transgression and regression. The Mandeva Formation is the most laterally extensive sequence in the Pongola Supergroup and can be traced into the main parts of the Pongola basin as well as into smaller outliers to the west within the Nondweni Greenstone Belt. Within the main part of the Pongola basin the lithostratigraphic equivalent of the Mandeva Formation is the Sinqeni Formation (Figure 6.1).

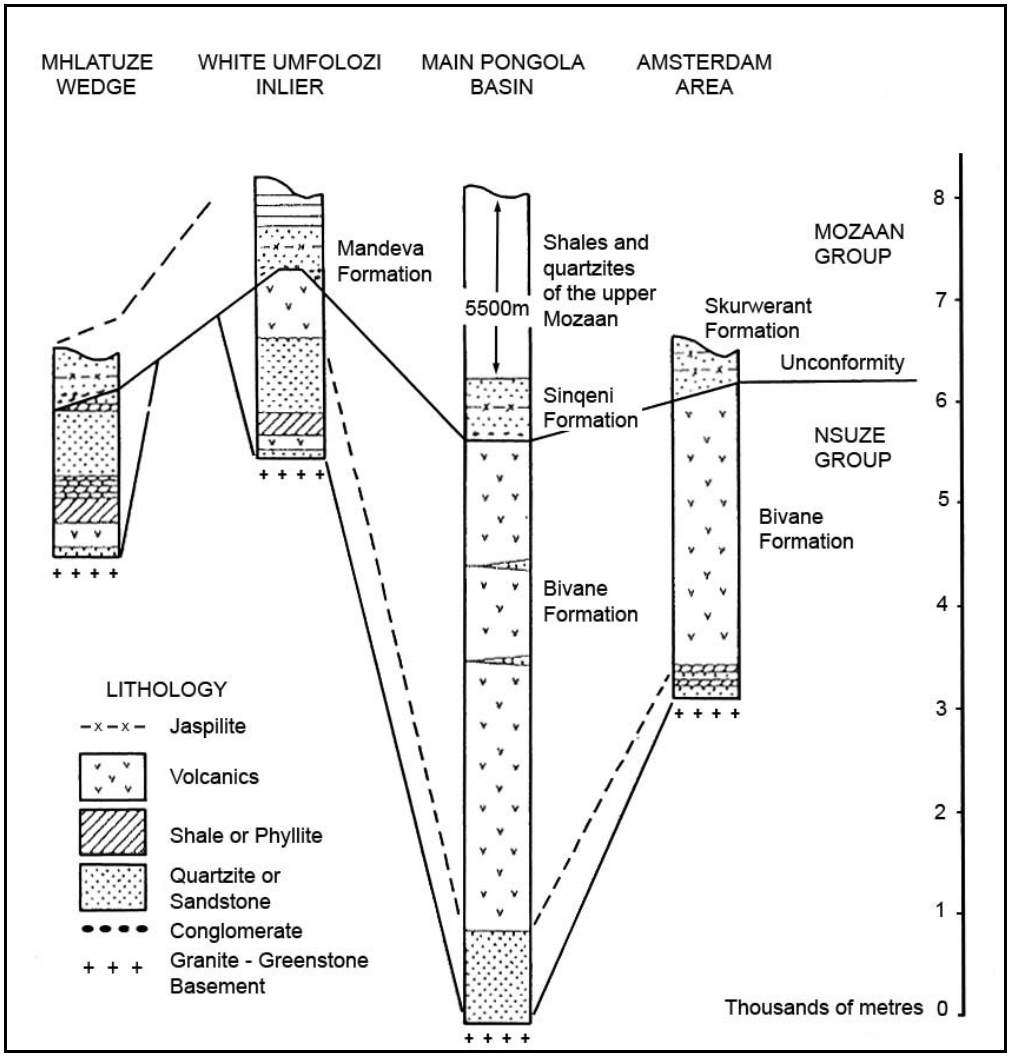

Figure 6.1: Stratigraphic logs showing correlation between the different sectors of the Pongola Basin and the correlation between the Mandeva Formation and the Sinqeni Formation. (modified after Matthews, 1990).

6.2 THE SINQENI FORMATION

Due to the sheet-like nature and lateral extent of the Mandeva Formation, sequence stratigraphic analysis can be applied to aid regional correlation of units. The Sinqeni Formation is the lateral equivalent of the Mandeva within the main Pongola Basin. The type area for the Sinqeni Formation is within the Pongola River valley west of Klipwal Gold Mine, where the sequence attains a maximum thickness of ~650 m (Gold, 1993) and gets its name from the nearby Sinqeni hill. The sequence is dominated by two major quartzite units, the lower Dipka and upper Kwaaiman Members, separated by the Izermijn Member, a thin unit of banded iron formation.

The lower Dipka Member crops out extensively on the farm Gunsteling where it caps a prominent hill in the area (Figure 6.2). At its base the Dipka Member crops out as interbedded coarse-grained sandstone and clast-supported, poorly-sorted, polymictic quartz-pebble conglomerate (Figure 6.3). Clasts are predominantly vein quartz, sandstone and minor chert; long axes of the clasts range from 5 to 50 mm with a mode of 30 mm. Clasts have random orientations with no imbrication. Both normally-graded and massive beds are evident, with internally massive gritty quartz arenite beds intercalated with the conglomerate lenses (Figure 6.3). Normally-graded conglomerates fine-up from medium-pebble conglomerate to gritty quartz arenite. Sutured grain-grain contacts predominate with minor amounts of sericitic matrix (Figure 6.4). The sericite matrix probably formed due to alteration of clay minerals within pore spaces between the larger quartz grains. Palaeocurrent orientations show a unimodal southerly palaeoflow within the trough cross-bedded sandstone units.

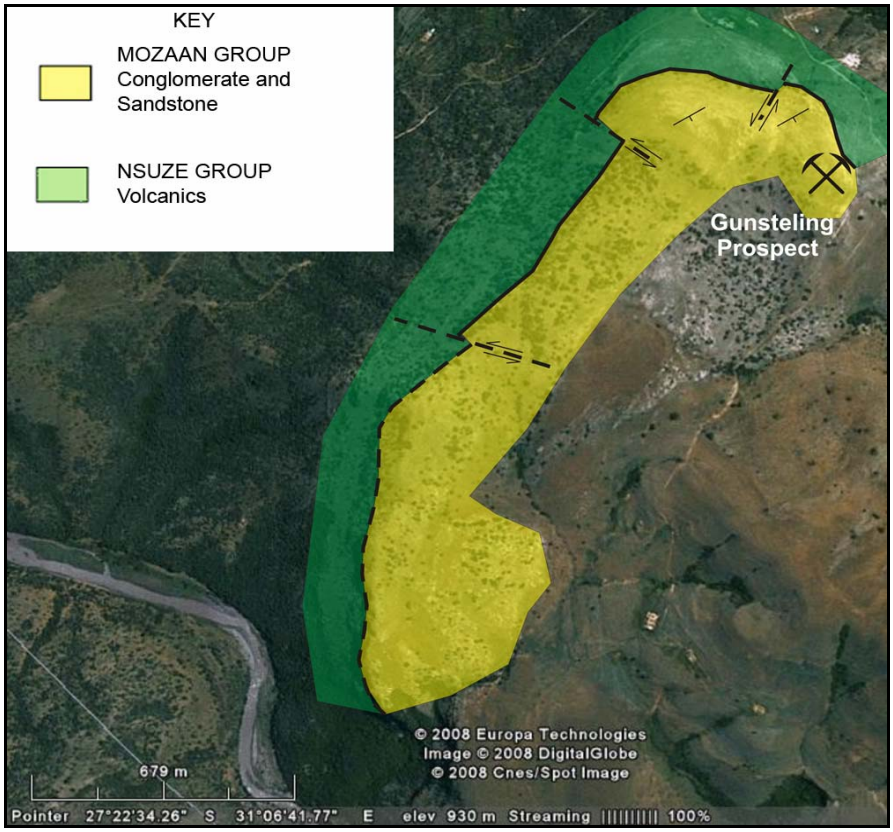

Figure 6.2: Google Earth image showing a schematic geological map of the Nsuze-Mozaan unconformity on the farm Gunsteling.

Figure 6.3: Interbedded quartz-pebble conglomerate and coarse-grained sandstone of the Dipka Member on the farm Gunsteling. The sharp rock edge shown on the right of the figure marks the entrance to a 6 m prospect adit driven into the conglomerate.

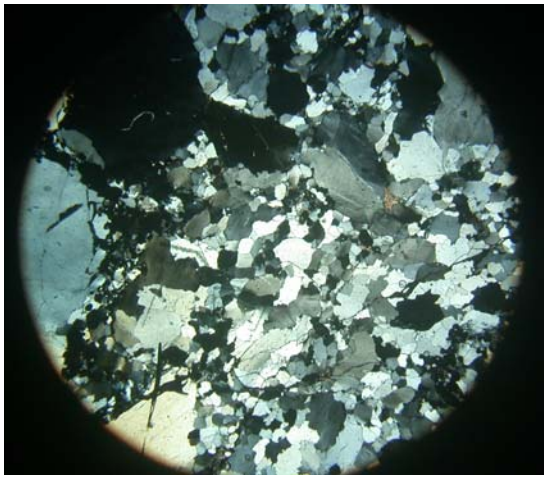

Figure 6.4: Cross-polarised photomicrograph of Gunsteling conglomerate showing high quartz content within the matrix. No chert evident, large clasts are quartz. Field of view: 8 mm

On the farm Altona (Figure 6.5), the conglomerates of the Dipka Member form 5 prominent but laterally discontinuous ~20 to 50 cm thick lenses at the base of the Sinqeni Formation. The conglomerates crop out in a ~30 m thick succession on the southern side of the main road to the west of the Bethu Anticline (Figure 6.6) and extend for a distance of ~200 m along strike. The conglomerates are generally poorly-sorted, matrix-supported and fine-up to, or are sharply overlain by gritty quartz arenite (Figure 6.7). Clast size varies between 10 and 50 mm with a mode of 25 mm. Clasts are predominantly subrounded black and banded chert with minor sandstone. Imbrication is rare, but locally developed in some lenses. The matrix is predominantly immature, poorly-sorted, coarse-grained quartz, feldspar and sericite and weathered pyrite (Figure 6.8). Minor planar cross-bedding is evident within the conglomerates with clasts concentrated on the basal parts of the foresets.

The Dipka Member conglomerates on the farm Altona are overlain by ~200 m thick planar cross-bedded quartz arenites. Gold (1993) indicated that the lower portions of the unit have undergone a high degree of quartz recrystallization with original grain shapes being locally destroyed. The quartz arenites become coarser-grained towards the top of the unit with well developed planar cross-bedding evident on farm Altona (Figure 6.7)

The quartz arenites are overlain with a sharp contact by ~30 m thick unit of ferruginous shale and banded iron formation of the Izermijn Member. The iron formation is dominated by interlayered jaspilitic chert and magnetite bands (Figure 6.9) which host localized sulphides. This iron formation forms the lateral equivalent of the Vlakhoek Member in the White Umfolozi Inlier and can be traced throughout the Pongola basin.

The banded iron formation is overlain with a sharp contact by ~170 m thick, medium to coarse-grained quartz-wacke of the Kwaaiman Member (Gold, 1993). Gold (1993) identified symmetrical ripple marks and planar and trough crossbedding within the Member which display a prominent, unimodal, southerly palaeocurrent orientation. Ferruginous and non-ferruginous mudstones and siltstones of the Ntombe Formation overlie the quartz-wackes of the Kwaaiman Member with a sharp contact (Gold 1993).

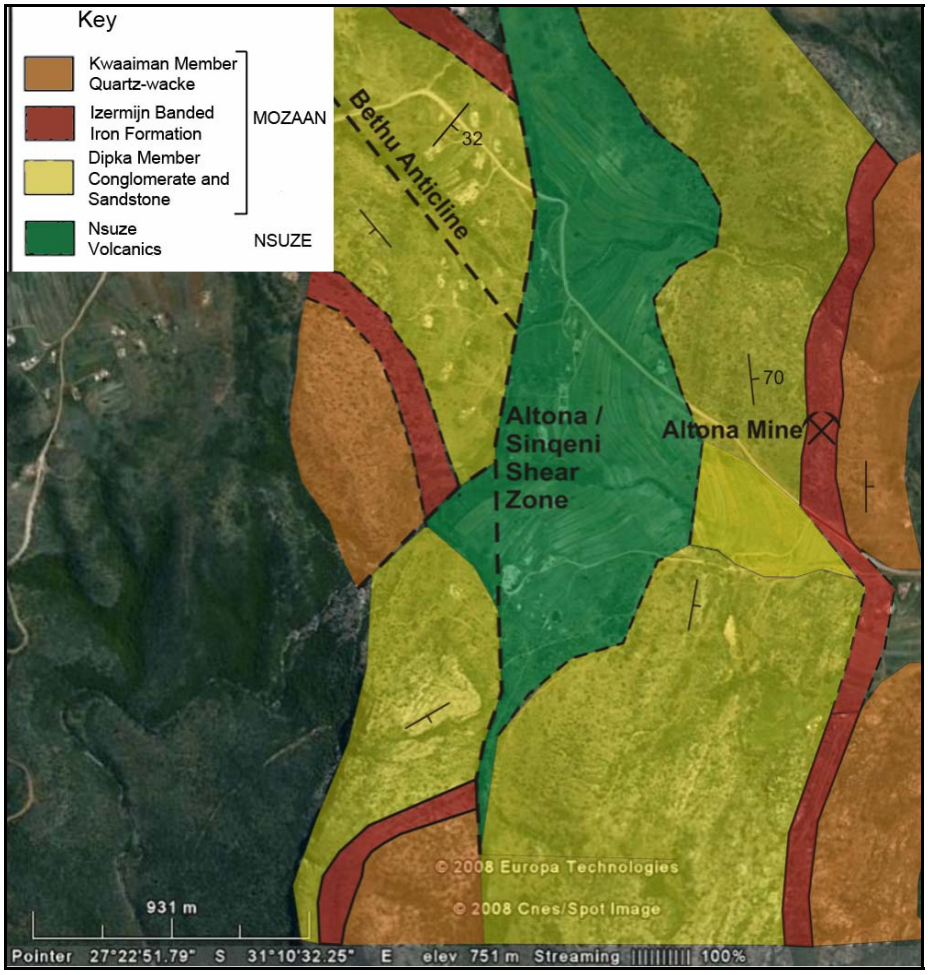

Figure 6.5: Geological map of the Nsuze-Mozaan unconformity on the farm Altona, Bethu anticline and Altona/Sinqeni shear orientations after Gold (1993).

Figure 6.6: Planar cross-bedded conglomerate on farm Altona. Pebbles focussed on foresets dipping from right to left. Lense is ~10 m above Nsuze Mozaan unconformity.

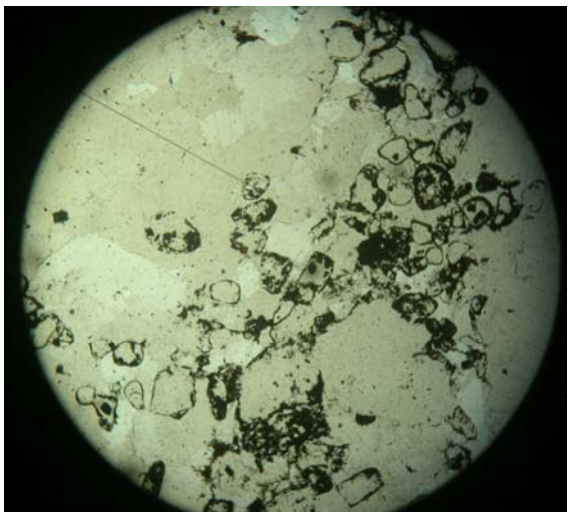

Figure 6.8: Plane-polarised photomicrograph of Gunsteling conglomerate showing weathered rounded pyrite grains within quartz matrix. Field of view: 2 mm.

Figure 6.7: Planar cross-bedding within coarse-grained quartz arenites ~10 m below the Izermijn banded iron formation on farm Altona. Foresets dip to the south.

Figure 6.9: Banded chert within the Izermijn banded iron formation at Altona mine, Farm Altona. Hammer handle for scale.

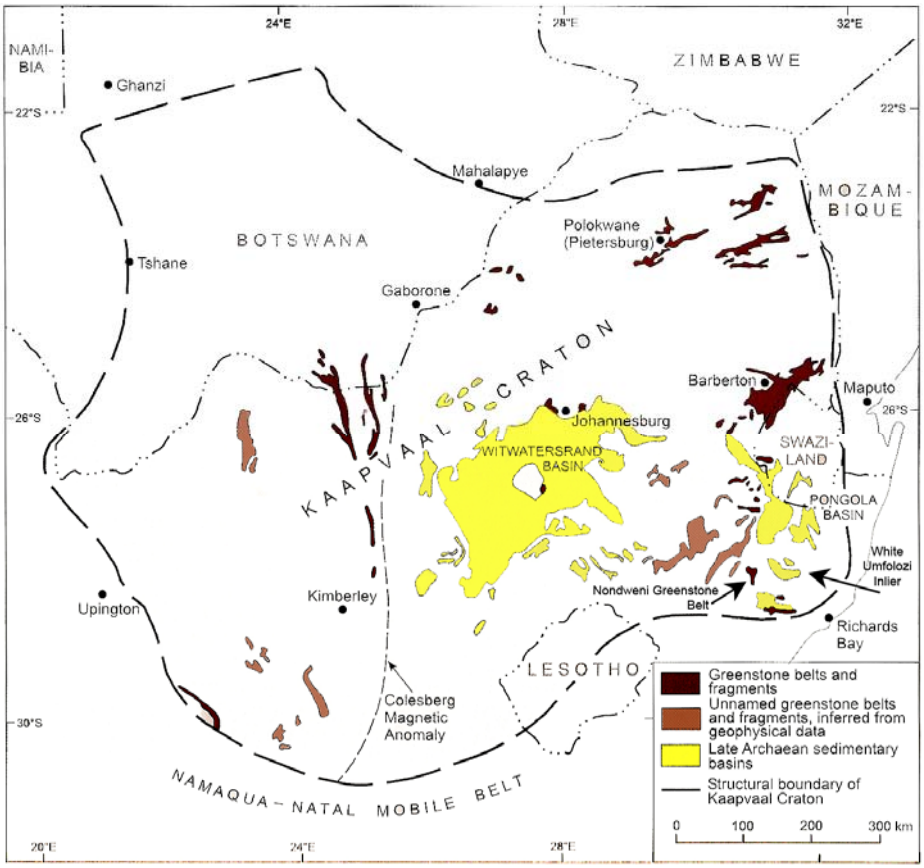

Figure 6.10: Distribution of greenstone remnants and Archaean sedimentary basins on the Kaapvaal Craton. (modified after Brandl et al., 2006).

6.3 MOZAAN LITHOLOGIES IN THE NONDWENI AREA

The 3.4 Ga Nondweni Greenstone Belt crops out over ~100 km^2 in northern KwaZulu-Natal as a number of small inliers within younger sedimentary rocks (Riganti & Wilson, 1995). Greenstone lithologies are dominated by mafic and ultramafic with minor sedimentary rocks (Riganti & Wilson, 1995; Versfeld, 1988). The belt is intruded in the east by a batholithic granite, which may be part of the same suite of granites that form the basement to the Pongola Supergroup in the White Umfolozi Inlier. This belt forms only a small remnant of what was possibly a much larger greenstone terrain as has been inferred by geophysical data (Figure 6.10; Brandl et al., 2006).

Pongola Supergroup lithologies crop out in small isolated occurrences that rest unconformably on rocks of the Nondweni Greenstone Belt. Versfeld (1988) correlated these units with Nsuze Group rocks mapped by du Toit (1931) in the Nkandla area to the south. The basal unconformity between the Pongola Supergroup and Nondweni Group rocks can be seen at Mystery Hill and Patsoana Mission Station (Figure 6.11).

At Mystery Hill the basal Pongola units crop out as a ~10 m thick, upward fining, poorly-sorted cobble conglomerate. Clasts are predominantly chert and vein quartz with minor amounts of volcanic clasts. The conglomerate is overlain by ~60 m thick cross-bedded quartz arenites which form the uppermost unit of the Pongola in this area (Figure 6.15). The arenites are capped by Karoo age sandstones. This sequence of rocks can be correlated with the Denny Dalton conglomerate of the Mandeva Formation within the White Umfolozi Inlier ~30 km east.

At Patsoana Mission (Figure 6.12), the lowermost Pongola rocks crop out as altered andesites which are capped by a ~5 m thick sheared talc schist. This talc schist can be correlated with the sheared unconformity between the Nsuze and Mozaan Groups as identified in the White Umfolozi Inlier to the east. Overlying the talc schist, the lowermost unit of the Mozaan Group is a ~5 m thick, upward fining, poorly-sorted, polymictic, cobble conglomerate (Figure 6.14 and 6.15). Sub-angular volcanic fragments as well as black and green chert pebbles are the dominant clast types, with vein quartz pebbles being rare. The conglomerate is predominantly clast-supported but matrix-supported in some areas. The matrix is composed of chloritised, fine-grained mafic-volcanic material, possibly derived from the Nondweni succession (Figure 6.16 and 6.17). Versfeld (1988) indicated that the clasts within the Patsoana conglomerate were also derived from rocks of the Nondweni succession. The conglomerates are overlain by ~30 m of grits and cross-bedded quartz arenites.

Minor traces of gold are localised within the Patsoana conglomerate which has been prospected on a small scale in the past. A number of pits and shallow adits driven into the basal parts of the

conglomerate are all that remain of the mining operations (Figure 6.18). Hatch (1910) reported grades which do not reach economic level, and channel sampling by Versfeld (1988) indicated grades of 0.55 g/t Au over 0.5 m. Sulphides occur as stringers within the conglomerate matrix. As the clasts within the conglomerate are derived from the Nondweni succession it is plausible to presume that the gold was derived from the same succession (Versfeld, 1988).

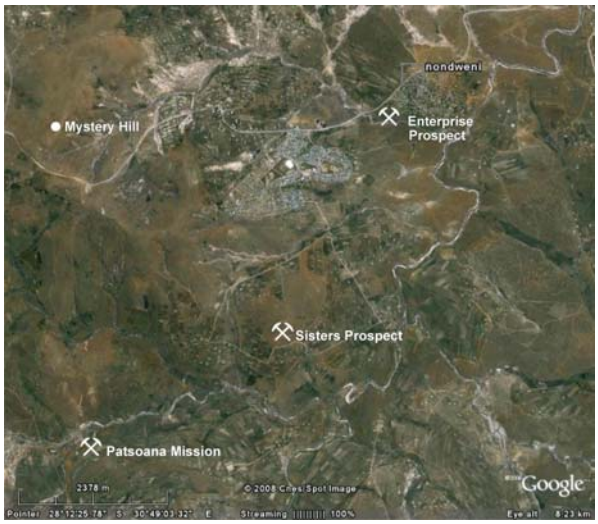

Figure 6.11: Google earth image of the Nondweni area in Northern KwaZulu-Natal showing localities of Pongola outcrops at Mystery Hill and Patsoana Mission as well as gold prospects within the Nondweni Greenstone Belt (Enterprise and Sisters Prospects)

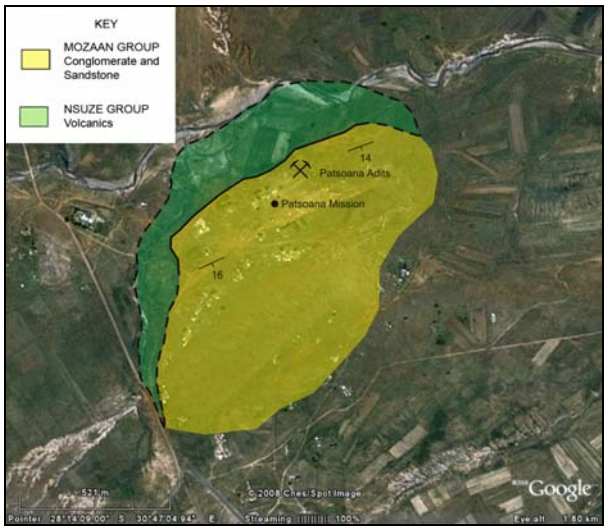

Figure 6.12: Google Earth image of the Pongola outcrop at Patsoana Mission near Nondweni. Non coloured areas are areas of no outcrop or Nondweni greenstone lithologies

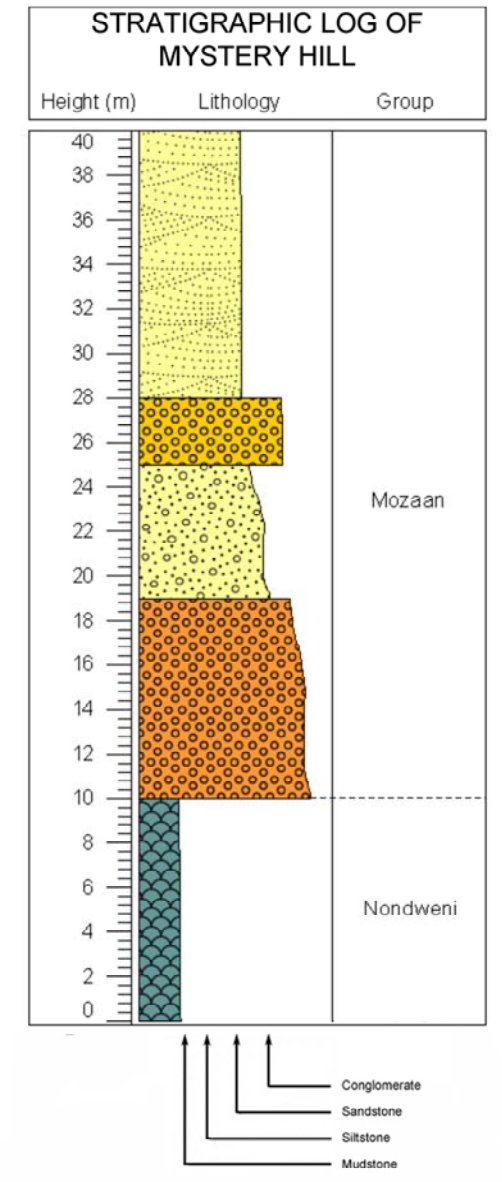

Figure 6.13: Stratigraphic log of Mystery Hill. Note how the basal conglomerates and overlying trough cross-bedded quartz arenites are lithostratigraphically similar to those of Patsoana Mission and of Denny Dalton. Refer to lithology key log on page 5.

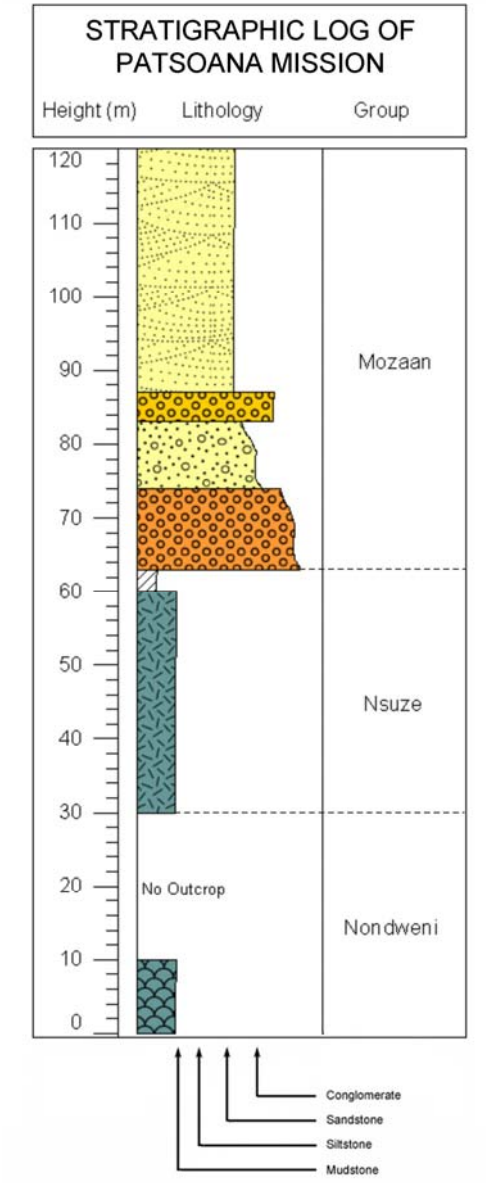

Figure 6.14: Stratigraphic log of Patsoana Mission. Note how the basal conglomerates and trough cross-bedded quartz arenites of the Mozaan Group overlie talc schist and altered andesites of the Nsuze Group. Refer to lithology key log on page 5.

Figure 6.15: Poorly sorted polymictic conglomerate at Patsoana Mission. Note the large range of pebble roundness.

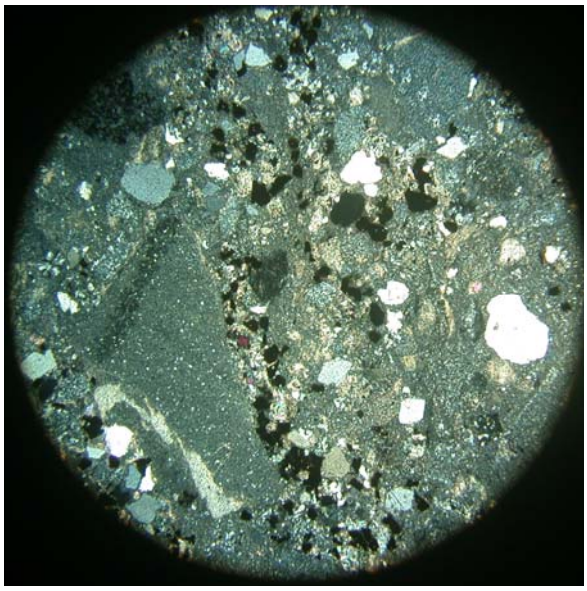

Figure 6.16: Cross-polarised photomicrograph of Patsoana conglomerate. Note the high percentage of volcanic fragments within the matrix (dark grey material); clasts are subangular with some quartz and pyrite. Field of view: 2 mm

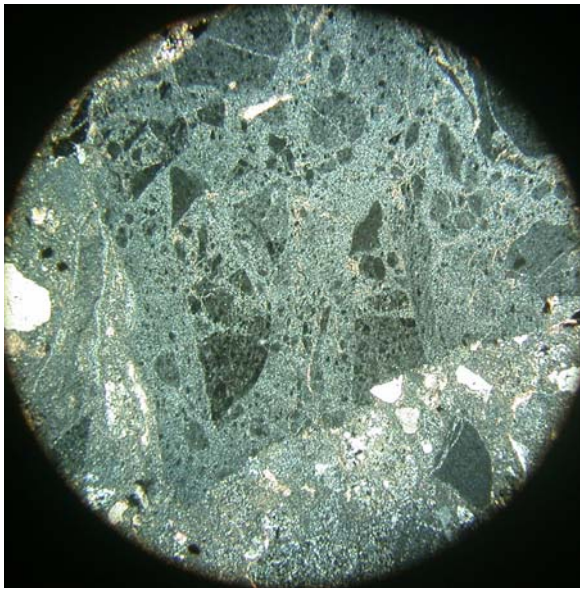

Figure 6.17: Photomicrograph of angular volcanic clast within the Patsoana conglomerate. Clast is comprised of altered mafic volcanic breccia derived from the Nondweni Greenstone lithologies. Field of view: 2 mm

Figure 6.18: Prospect adit into basal conglomerate at Patsoana Mission. Conglomerates in the foreground are overlain by trough cross-bedded quartz arenite.

6.4 DISCUSSION

6.4.1 THE SINQENI FORMATION

A number of authors (Beukes & Cairncross, 1991; Gold, 1993) draw exact correlations between the Sinqeni and Mandeva Formations as it retains its three-fold subdivision throughout the entire Pongola depository (Figure 6.19). Although the units are lithostratigraphically similar, they exhibit substantial mineralogical differences and a common provenance for the formation throughout the basin seems unlikely.

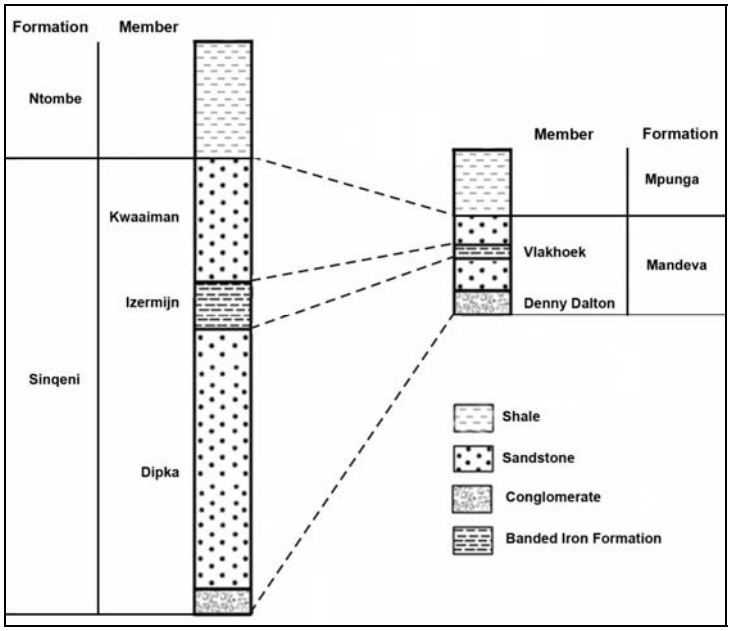

Figure 6.19: Schematic lithology logs of the Sinqeni and Mandeva Formations showing lithostratigraphical correlation between the units.

The Dipka Member conglomerates on the farm Gunsteling in the main Pongola basin exhibit a markly different mineralogical composition as compared to the Denny Dalton conglomerate. The clast-supported large chert pebble conglomerates which dominate the adit area at Denny Dalton are not evident in the Dipka Member conglomerates. The conglomerates do not host much chert and are dominated by medium to large vein quartz pebbles (Figure 6.3). The vein quartz clasts would have originated from quartz veins within a predominantly granitic source area to the north, with minimal input from greenstone belts accounting for the lack of chert clasts in the conglomerates. Within the White Umfolozi Inlier however, the high concentrations of chert pebbles and cobbles within the Denny Dalton area point to a more likely granitoid-greenstone origin for the conglomerates.

Palaeocurrent orientations for the Sinqeni Formation in the main Pongola basin display a predominantly unimodal southerly trend (Beukes & Cairncross, 1991; Gold, 1993); within the White

Umfolozi Inlier however palaeocurrent orientations indicate a provenance to the west of the inlier. This is in accordance with Dix (1984) who also postulated a southerly to south-westerly provenance for the lower units of the Mandeva Formation. Von Brunn and Hobday (1976) and Von Brunn and Mason (1977) identified WNW-ESE trending elongate depressions in the Klipkloof quartz arenites of the Mandeva Formation. Although no data was compiled for the underlying fluvial Denny Dalton Member, Von Brunn and Mason (1977) postulate that the scours in the quartz arenites represent tidal scours in a shallow marine shoreface setting. The unimodal easterly palaeocurrent orientations for the Denny Dalton Member infer a granitoid-greenstone provenance to the west of the inlier.

In a broad sense, the units of the lower Mozaan are lithostratigraphically correlative throughout the Pongola depository. Thickness varies drastically, however the units maintain their three-fold subdivision of basal conglomerate and quartz arenite, banded iron formation, and upper quartz arenites. The conglomerates differing mineralogy and palaeocurrent orientations are however indicative of differing source terrains for the Dipka and Mandeva Formations.

6.4.2 MOZAAN LITHOLOGIES IN THE NONDWENI AREA

Mozaan lithologies within the Nondweni area have in the past tentatively been associated with Nsuze Group strata. Versfeld (1988) identified debris flows within the Pongola lithologies to the southwest of the Nondweni Greenstone Belt which are lithologically similar to flows identified in the Nkandla area by Groenewald (1984). Versfeld indicated however, that debris flows of identical appearance are also exposed in lithologies of the upper Mozaan Group in the main Pongola basin (Versfeld, 1988; Watchorn, 1978) and the lithological correlations should be treated with caution. The sheared unconformity (Figure 6.14) identified at Patsoana Mission, however, is likely correlative with the Nsuze-Mozaan unconformity evident in the White Umfolozi Inlier. The Mozaan conglomerates at Patsoana Mission have a markly different mineralogy to those seen in the White Umfolozi Inlier. The Patsoana conglomerates consist primarily of silicified volcanic material derived directly from the Nondweni Greenstone Belt (Figure 6.16). The sub-angular shape and high volcanic content is indicative of a very proximal source for the Patsoana conglomerates (Figure 6.17). Although the Nondweni Greenstone Belt hosts a number of chert-rich lithologies, based on mineralogical and geochemical data it appears unlikely that the conglomerates of the Mandeva Formation were derived from this succession. The differing rare-earth-element patterns between Nondweni cherts and chert pebbles from Denny Dalton indicates that the pebbles identified at Denny Dalton were derived from a similar greenstone belt which is either covered by younger lithologies or has been removed by erosion.

6.4.3 GOLD OCCURRENCES WITHIN THE NONDWENI GREENSTONE BELT

Gold has been mined on a small scale from a number of prospects within the Nondweni Greenstone Belt. All occurrences form part of the Witkop Formation and occur within altered and sheared andesites and komatiitic basalts (Versfeld 1988). No records of any major gold production are available, but it appears that the amount of gold production was minimal. Most occurrences are lode gold-style deposits associated with subvertical quartz veins, however the Sisters Prospect (Figure 6.11) occurs as auriferous quartz and carbonate veins in calc-silicate and talc schist stratigraphically beneath a 5 m thick chert horizon. Maximum gold grade recorded by Versfeld from grab sampling was 2.69 g/t (Versfeld, 1988). Of the lode gold occurrences, only the Enterprise Prospect (Figure 6.11) yielded payable gold with grades on average of 20.8 g/t (Versfeld 1988) however ore collected from the mine dumps has a poor sulphide content. It can therefore be concluded that the detrital gold evident in the Denny Dalton conglomerates is not derived from the Nondweni succession, but must have come from similar greenstones which were enriched in gold-bearing sulphides.

CHAPTER 7

DISCUSSION AND CONCLUSIONS

The Denny Dalton Member comprises a stacked succession of three upward-fining conglomerate beds. Scour channels and sharp lateral facies variation over 10's of metres indicate the conglomerates were deposited as basal lag deposits in a proximal braided alluvial plain environment. The large pebble to cobble clast size (up to 10 cm in diameter) and unimodal east-north-easterly palaeocurrent orientation suggest a proximal depositional site with the provenance to the west of the White Umfolozi Inlier.

Kodama (1994) showed that clast lithology plays an important part in clast distribution within modern river channels. This author determined that chert clast concentrations within the Watarase River in Japan increase 20-50 km from source whilst soft rock lithologies were dominant upstream. Plumley (1948) indicated that in river terrace deposits, the proportion of hard rock (chert, quartz and quartzite) increases away from the provenance and constitutes ~90% of the deposits at a distance of ~50 km. This suggests that within the Nondweni area the conglomerates identified at Patsoana Mission may reflect the more proximal facies of the Denny Dalton Member river system as clast composition is dominated by "soft" sub-angular volcanic material with some chert. In the Denny Dalton area the river system can be regarded as less proximal as the dominant (~95%) clast types are "hard" chert and quartz clasts which show significant rounding due to transport. It is therefore plausible to suggest that the provenance for the auriferous conglomerates at Denny Dalton was ~50 - 100 km west of the mine. The almost complete lack of "soft lithology" clasts, such as basalt within the Denny Dalton Member conglomerates, despite the fact that they overlie Nsuze basalts along an angular unconformity, suggests that these clasts may have undergone intense chemical weathering postulated for the Archaean (Wronkiewicz and Condie, 1987).

The conglomerates are overlain by a ~30 m thick sequence of shallow marine, trough cross-bedded quartz arenites that were likely deposited as shoreface sands. The consistent trough cross-bedding in this unit reflects deposition by shoreface dunes which formed due to offshore currents (Eriksson et al., 1998). The mineralogical and textural maturity of the quartz arenites as well as cross-cutting scour channels which contain trough cross-bedding is evidence for intense reworking by shallow marine processes. The lateral extent and consistent thickness of the unit, as well as hummocky cross-stratification and herringbone cross-bedding, is indicative of deposition in a storm-dominated shoreface environment. The lack of a transitional facies (foreshore-beach or delta plain) between the Denny Dalton Member conglomerates and the Klipkloof quartz arenites is possibly due to erosion

during marine transgression, however beach and foreshore facies are seldom preserved in Archaean clastic shelf sequences (Eriksson et al., 1998).

A polymictic conglomerate and grit overlie the trough cross-bedded quartz arenites with a sharp erosive contact and probably formed during marine transgression. As sea level begins to rise rapidly and the shoreface retreats inland, all the facies above the transgressive ravinement surface (foreshore-beach or barrier-lagoon) are reworked, truncated or destroyed; and a winnowed lag of coarse-grained clasts is deposited along the erosion surface (Rodriguez et al., 2001). The CG 4 conglomerate likely represents a lag deposit along the transgressive ravinement surface and marks the onset of a major marine transgression into the Pongola basin.

The conglomerates and grits of CG 4 are overlain by black shale, banded iron formation and green shale of the Vlakhoek Member. Intercalations of fine-grained ripple-marked sandstone in shale within the lowermost 3 m of the Vlakhoek Member signify storm events above the storm wave base. Continued marine transgression towards deeper marine, sub-wave base environments resulted in the deposition of the upper part of the black shale. Sediments were deposited in quiet-water environments below the storm wave base. Geochemical analysis of the black shales correlates with the work of Wronkiewicz and Condie (1989) and the large negative Eu anomalies suggest that a high proportion of granites were present in the source area. These authors also interpreted the high Fe contents of the shales as evidence for high proportions of komatiite and basalt in the source area which suggests a granite-greenstone provenance for the black shales of the Vlakhoek Member. Geochemical analysis of the banded iron formation and overlying green shales suggests that these units formed on a sediment-starved shelf with a high percentage of chemical precipitation as iron oxides. Due to its lateral continuity throughout the Pongola Basin, the banded iron formation is defined as Superior-type and thus represents the oldest documented iron formation of this type in the world (Alexander et al., 2008). The upper quartz arenites overlie the Vlakhoek Member with a sharp erosive contact and were deposited in an intertidal to upper shoreface environment signifying marked marine regression and an erosional hiatus as neither the high stand systems tract, nor the falling stage systems tract are preserved.

Beukes and Cairncross (1991) proposed that the Sinqeni Formation (the equivalent to the Mandeva Formation) in the main Pongola basin is lithostratigraphically correlative to the Orange Grove Formation of the West Rand Group of the Witwatersrand Supergroup, as both are composed of predominantly shallow marine lithologies and comprise two quartz arenite units separated by shale. Eriksson et al. (1998) agreed with this correlation and suggested that both the West Rand and Mozaan Groups are coeval and were deposited in a large epeiric embayment on the Kaapvaal Craton. This correlation may however be problematic as the units can only be correlated lithostratigraphically and

the Orange Grove Formation rests nonconformably on granite-greenstone basement, whereas the Sinqeni and Mandeva Formations unconformably overlie Nsuze Group volcanics. Detailed geochronological work would be necessary to test this hypothesis.

The lowermost conglomerate (CG 1) of the Denny Dalton Member is a polymict, matrix-supported, and rare clast-supported conglomerate which host erratic gold and uranium mineralization. Of the twelve adits driven into the CG 1 at Denny Dalton mine only six adits were extensively worked. Hatch (1910) indicated that adits 1S, 2S, 3S, 5S and 6S and 2N host the highest grade ore and correlate to 2 separate ENE trending palaeochannels in which the ore is concentrated (Figure 4.3). Campbell (1982) indicated that of 128 boreholes drilled in the mine area, only 11 payable intersections of CG 1 were found. These results show the erratic nature of the reef along strike as grades can vary between 0.1 g/t and 7 g/t over 5 m (Campbell, 1982).

Where mineralized, the CG 1 hosts abundant rounded detrital pyrite which occurs in three varieties, compact, porous and radial. Compact rounded pyrite is the most abundant phase in the Denny Dalton Member conglomerates and hosts primary inclusions of gold, galena, arsenopyrite and minor pyrrhotite. Pyrites are concentrated as grains in the matrix between large pebble and cobble clasts. Within the reef zone pyrite makes up 95% of ore minerals present, no "black sands" in the form of Fe-Ti-oxides are evident and concentrations of zircon and monazite are minor. Abraded edges on compact rounded pyrite indicate transport and erosion of the pyrite before deposition. Multiple sulphur isotope analysis (^{34}S, ^{33}S, ^{32}S) of compact rounded pyrite indicates relatively unfractionated $\delta^{34}S$ (0.2 to 2.9 ‰) and $\Delta^{33}S$ (0.10 to 0.21 ‰) values that are inconsistent with a sedimentary source of the sulphur and comparable to pyrites from igneous sources or hydrothermal vein deposits in Archaean granitoid-greenstone terrains (Hofmann et al., 2008).

Radial and porous pyrites are associated with the smaller compact pyrite within the main reef zone of CG 1. The well-rounded nature of the pyrite is indicative of transport before deposition. Radial pyrite grains have a texture that resembles that of diagenetic marcasite. Multiple sulphur isotope analysis of these pyrites indicate a sedimentary source, possibly diagenetic marcasite derived from the erosion of nodules in marine shale (Schieber, 2007). It has been shown by Bannister (1932) and Van Horn and Van Horn (1933) that diagenetic marcasite can be inverted to pyrite. The radial pyrites of Denny Dalton were therefore possibly once marcasite, but have subsequently been replaced by pyrite. Falconer et al. (2006) indicated that pyrite can be transported for tens of kilometres whereas marcasite can only be transported short distances and still remain stable. This indicates that the radial pyrite and compact pyrite have different sources with the radial pyrite being eroded from older marine lithologies within a few kilometres from Denny Dalton.

No free gold is evident in the conglomerates at Denny Dalton; gold is rather hosted as primary inclusions in massive rounded pyrite grains and in anhedral aggregates of scorodite. The gold inclusions are very similar to primary gold inclusions identified by Hallbauer (1986) and Ramdohr (1958) in massive detrital pyrite grains in the Witwatersrand. The high optical reflectivity of the gold suggests a high Ag content and indicates a primary rather than recrystallized origin for the gold. The gold and its detrital pyrite host could therefore have been derived from primary ore deposits such as vein-type lode deposits within greenstone settings. The CG 1 reef is therefore of low grade as this deposit hosts only minor amounts of primary gold and there has been no enrichment by the introduction of secondary gold.

The CG 1 reef at Denny Dalton is however similar to a number of reefs within the Central Rand Group (Ada May, Vaal, C, Denny's and Ventersdorp Contact Reefs; McCarthy, 2006) as it overlies an angular unconformity with underlying strata. Erosion of the underlying strata could allow for increased gold concentrations along unconformities such as these, and may account for the higher gold grades identified at Denny Dalton when compared to the Sinqeni Formation in the main Pongola basin. The reefs of the Denny Dalton Member however show closer similarities to reefs within the West Rand Group, such as the Promise Reef (Meyer et al., 1990) and the No. 5 Reef in the Rietkuil Formation (Watchorn and O'Brien, 1991). Although the reefs do not match lithostratigraphically they are mineralogy similar with high concentrations of quartz and chert pebbles, and with monazite and brannerite evident as heavy and ore minerals in the matrix.

Uranium at Denny Dalton is present as both secondary inclusions of uraninite within carbonaceous black chert pebbles and as minor phases of uraniferous leuxocene and brannerite. As some of the uranium is directly associated with black chert pebbles, unpublished assay results identified highest grades within clast-supported chert cobble conglomerate with negligible U_3O_8 grades in large-pebble vein quartz-dominated conglomerates. This creates the erratic grade identified within the Denny Dalton Mine area. Uranium identified within the upper conglomerate (CG 4) occurs as secondary uraninite and coffinite encrustations around rounded detrital pyrite grains. Within CG 4 the localized abundance of pyrite grains produced a reducing environment within which the uranium was recrystallized as encrustations around locally reducing pyrite grains. This possibly occurred relatively recently with the uranium having been remobilized by meteoric waters.

No detrital uraninite grains are evident within either CG 1 or CG 4, suggesting a secondary origin for the uranium mineralization. The presence of uraninite of secondary origin suggests that remobilization of primary uraninite grains could have occurred in CG 1 after deposition, and mineralisation occurred within the chert pebbles in CG 1, and around detrital pyrite in CG 4.

Therefore a modified placer model can be suggested for the uranium mineralization if the reefs, whereas the gold at Denny Dalton is primary and occurs as a true placer deposit.

The main findings of this thesis can be summarized as follows:

- Four conglomerate horizons are evident in the Mandeva Formation. The three lowermost horizons (CG 1, CG 2 and CG 3) make up the Denny Dalton Member. CG 4 crops out higher up in the stratigraphy above a ~30m thick unit of quartz arenite, the Klipkloof quartz arenite.
- The conglomerates of the Denny Dalton Member were deposited in a fluvial braid-plain environment.
- The Klipkloof quartz arenites were deposited in a shallow marine, shoreface environment.
- The CG 4 conglomerate is indicative of a winnowed lag deposit along the transgressive ravinement surface.
- The banded iron formation and overlying green shales show chemical precipitation of Fe-oxides in shallow water on a sediment-starved shelf in an epeiric sea.
- Auriferous and uraniferous reefs at Denny Dalton occur in the deepest parts of fluvial palaeochannels.
- Three generations of pyrite are evident at Denny Dalton.
    - Compact rounded pyrite of detrital origin
    - Porous and radial pyrite of detrital origin
    - Euhedral pyrite of authigenic origin
- Multiple sulphur isotope analysis indicates a hydrothermal/igneous origin is most likely for the compact rounded detrital pyrites found at Denny Dalton, while radial pyrites were derived from sedimentary sources.
- Gold at Denny Dalton occurs as primary gold inclusions in compact rounded detrital pyrite within CG 1.
- Uranium mineralization is secondary and occurs as disseminated uraninite in pore spaces within carbonaceous black chert pebbles in CG 1; and as uraninite and coffinite coatings around detrital pyrite grains in CG 4.

ACKNOWLEDGEMENTS

The author would like to acknowledge Dr. Axel Hofmann of the University of KwaZulu-Natal for his assistance as project supervisor. The NRF is to be acknowledged for its bursary supplied to the author for the project, as is the GSSA and the A.G. Bain Fund for awarding the author a research grant for this project.

Mr. Mukesh Seyambu from the University of KwaZulu-Natal must be thanked for cutting and preparing all the thin sections and polished blocks used in this report. Mr. Andrew de Klerk, of Prime Resources (formerly of CCIC) and John Hancox of Caracle Creek International Consulting (CCIC) must be acknowledged for giving me the opportunity to work on their drilling project in my field area and allowing me to use the drill cores for my project.

Other people who deserve credit for their help are as follows:

- Prof. John Dunlevey of the University of KwaZulu-Natal for organising the XRD analysis for my samples.
- Dr. Andrew Green of the University of KwaZulu-Natal for his proof-read and continued input.

And finally to my mom and dad, and girlfriend Jo, thank you for always being there for me, and putting up with me during the period of this project. If it weren't for you guys this could never have been possible.

REFERENCES

Alexander, B. W., Bau, M., Andersson, P. & Dulski, P., 2008. Continentially-derived solutes in shallow Archean seawater: Rare earth element and Nd isotope evidence in iron formation from the 2.9 Ga Pongola Supergroup, South Africa. *Geochimica et Cosmochimica Acta*, **72**, 378-394.

Amme, M., Wiss, T., Thiele, H., Boulet, P. & Lang, H., 2005. Uranium secondary phase formation during anoxic hydrothermal leaching processes of UO_2 nuclear fuel. *Journal of Nuclear Materials*, **341**, 209-223.

Anhaeusser, C. R., 2006. Ultramafic and Mafic Intrusions of the Kaapvaal Craton. In: *The Geology of South Africa* (eds Johnson, M. R., Anhaeusser, C. R. & Thomas, R. J.). Geological Society of South Africa / Council for Geoscience. pp 9-56.

Armstrong, R. A., 1989. 1988 Annual technical report of the Geological Survey of South Africa, pp. 27, Department of Mineral and Energy Affairs. pp 27.

Bannister, F.A., 1932. The distinction of pyrite from marcasite in nodular growths. *Mineralogical Magazine*, **23**, 179-187.

Barnicoat, A. C., Henderson, I. H. C., Knipe, R. J., Yardley, B. W. D., Napier, R. W., Fox, N. P. C., Kenyon, A. K., Muntingh, D. J., Strydom, D., Winkler, K. S., Lawrence, S. R. & Cornford, C., 1997. Hydrothermal gold mineralization in the Witwatersrand basin. *Nature*, **386**, 820-824.

Battey, M. H. & Pring, A., 1997. *Mineralogy for Students*. Longman Asia Ltd. pp 363.

Beukes, N. J. & Cairncross, B., 1991. A Lithostratigraphic-sedimentological reference profile for the Late Archaean Mozaan Group, Pongola Sequence: application to sequence stratigraphy and correlation with the Witwatersrand Supergroup. *South African Journal of Geology*, **94**(1), 44-69.

Brandl, G., Cloete, M. & Anhaeusser, C. R., 2006. Archaean Greenstone Belts. In: *The Geology of South Africa* (eds Johnson, M. R., Anhaeusser, C. R. & Thomas, R. J.). Geological Society of South Africa / Council for Geoscience. pp 9-56.

Burger, A. J. & Coertze, F. J., 1973. Radiometric age measurements on rocks from Southern Africa to the end of 1971. *Bulletin of the Geological Survey of South Africa* (58), 1-46.

Burke, K., Kidd, W. S. F. & Kusky, T. M., 1985. The Pongola structure on southeastern Africa: The worlds oldest preserved rift? *Journal of Geodynamics*, **2**, 35-49.

Campbell, D., 1982. Notes on Southern Sphere's borehole results in the Denny Dalton area. Unpublished Internal Report - Gold Fields of South Africa Limited. pp 19.

Carling, P. A. & Breakspear, R. M. D., 2006. Placer formation in gravel-bedded rivers: A review. *Ore Geology Reviews*, **28**, 377-401.

Chaussidon, M. & Lorand, J. P., 1990. Sulphur isotope composition of orogenic spinel lherzolite massifs from Ariege (N.E. Pyrenees, France): An ion microprobe study. *Geochimica et Cosmochimica Acta*, **54**, 2835-2846.

Coe, A. L., Bosence, D. W., Church, K. D., Flint, S. S., Howell, J. A. & Wilson, R. C. L., 2003. *The Sedimentary Record of Sea-Level Change*. Press Syndicate of the University of Cambridge, Cambridge. pp 288.

Coetzee, F., 1965. Distribution and grain size of gold, uraninite, pyrite, and certain other heavy minerals in gold bearing reefs of the Witwatersrand basin. *Transactions of the Geological Society of South Africa*, **68**, 61-89.

Davies, R. D., Allsopp, H. L., Erlank, A. J. and Manton, W. I., (1970). Sr-isotopic studies on various layered mafic intrusions in southern Africa. *In: Symposium on the Bushveld Igneous Complex and other Layered Intrusions.* (eds. Visser, D. J. L. and Von Gruenewaldt, G.) Special publication of the Geological Society of South Africa., **1**, pp 576-593.

de Klerk, A., 2006. Results of a first phase drilling programme completed at Denny Dalton by Caracle Creek International Consulting Inc on behalf of Acclaim Exploration NL. Unpublished report of Acclaim Exploration NL. pp 96.

Delpierre, M. E. R., 1969. Report on uranium and gold in the Denny Dalton area. Unpublished internal report - Department of Mines. pp 25.

Dix, O. R., 1984. Early Proterozoic Braided Stream, Shelf and Tidal Deposition in the Pongola Sequence, Zululand. *Transactions of the Geological Society of South Africa*, **87**, 1-10.

Dixon, J. G. P., 2003. Archaean geology of the Buffalo River gorge, KwaZulu-Natal, Ph.D. Thesis, *University of Natal, Durban.* pp 283.

Duncan, A. R. & Marsh, J. S., 2006. The Karoo Igneous Province. In: *The Geology of South Africa* (eds Johnson, M. R., Anhaeusser, C. R. & Thomas, R. J.). Geological Society of South Africa / Council for Geoscience. pp 501-520.

Du Toit, A. L., 1931. The geology of the country surrounding Nkandhla, Natal (ed Department of Mines and Industry Union South Africa, E. S. N.), pp. 1-111.

Du Toit, A. L., 1939. *Geology of South Africa*. Oliver & Boyd, London.

England, G. L., Rasmussen, B., Krapez, B. & Groves, D. I., 2002a. Archaean oil migration in the Witwatersrand Basin of South Africa. *Journal of the Geological Society*, **159**(1), 189-201.

England, G. L., Rasmussen, B., Krapez, B. & Groves, D. I., 2002b. Palaeoenvironmental significance of rounded pyrite in siliciclastic sequences of the Late Archaean Witwatersrand Basin: oxygen-deficient atmosphere or hydrothermal alteration? *Sedimentology*, **49**, 1133-1156.

Eriksson, P.G., Condie, K.C., Tirsgaard, H., Mueller, W.U., Altermann, W., Miall, A.D., Aspler, L.B., Catuneanu, O. & Chiarenzelli, J.R., 1998. Precambrian clastic sedimentation systems. *Sedimentary Geology*, **120**, 5-53.

Falconer, D. W., Craw, D., Youngson, J. H. & Faure, K., 2006. Gold and sulphide minerals in Tertiary quartz pebble conglomerate gold placers, Southland, New Zealand. *Ore Geology Reviews*, **28**, 525-545.

Farquhar, J. & Wing, B. A., 2003. Multiple sulphur isotopes and the evolution of the atmosphere. *Earth and Planetary Science Letters*, **213**, 1-13.

Feather, C. E. & Koen, G. M., 1975. The Mineralogy of the Witwatersrand reefs. *Minerals Science & Engineering*, **7**(3), 189-223.

Folk, R.L., 1974. *Petrology of Sedimentary Rocks.* Hemphill Publishing Company, Austin. pp 182.

Frimmel, H. E., 2005. Archaean atmospheric evolution: evidence from the Witwatersrand gold fields, South Africa. *Earth-Science Reviews*, **70**, 1-46.

Frimmel, H. E. & Minter, W. E. L., 2002. An overview of geological processes that controlled the distribution of gold in the Witwatersrand deposits. In: *Giant Ore Deposits: Characteristics, Genesis and Exploration* (eds Cooke, D. R. & Pongratz, J.), CODES Special Publication. Centre for Ore Deposit Research, Hobart, Australia. pp 221-241.

Gold, D. J. C., 1993. The Geological Evolution of a part of the Pongola Basin, Southeastern Kaapvaal Craton. Ph.D. Thesis*, University of Natal, Pietermaritzburg.* pp 168.

Gold, D. J. C., 2006. The Pongola Supergroup. In: *The Geology of South Africa* (eds Johnson, M. R., Anhaeusser, C. R. & Thomas, R. J.). Geological Society of South Africa / Council for Geoscience. pp 135-148.

Gold, D. J. C. & Von Veh, M. W., 1995. Tectonic evolution of the Late Archaean Pongola-Mozaan basin, South Africa. *Journal of African Earth Sciences*, **21**(2), 203-212.

Griffin, K. R., 2002. Magmatic and tectonic development of the Pongola Supergroup and post-Pongola granitoids, Kaapvaal Craton, South Africa. M.Sc. Thesis, *University of Michigan.* pp 58.

Griffith, M., 2005. The Ph-dependence of scorodite dissolution kinetics. In: *2005 Salt Lake City Annual Meeting* (ed America, G. S. o.), pp. 377, Geological Society of America, Salt Lake City. pp 377.

Groenewald, P. B., 1984. The lithostratigraphy and petrogenesis of the Nsuze Group northwest of Nkandla, Natal*,* M.Sc. Thesis, *University of Natal, Pietermaritzburg.* pp 323.

Gutzmer, J., Nhleko, N., Beukes, N. J., Pickard, A. and Barley, M. E., 1999. Geochemistry and ion microprobe (SHRIMP) age of a quartz porphyry sill in the Mozaan Group of the Pongola Supergroup: implications for the Pongola and Witwatersrand Supergroups. *South African Journal of Geology.,* **102** (2), pp 139-146.

Hallbauer, D. K., 1986. The mineralogy and geochemistry of Witwatersrand pyrite, gold, uranium, and carbonaceous matter. In: *Mineral Deposits of Southern Africa* (eds Anhaeusser, C. R. & Maske, S.), pp. 731-752, Geological Society of South Africa, Johannesburg.

Hammerbeck, E. C. I., 1982. The Geology of the Usushwana Complex and associated formations - southeastern Transvaal. *Memoir, Geological Survey South Africa*, **80**, pp 1-11.

Harley, S. L. & Kelly, N. M., 2007. Zircon tiny but timely. *Elements*, **3**, 13-18.

Hatch, F. H., 1910. *Report on the mines and mineral resources of Natal (other than coal)*. R. Clay and Sons Ltd., London. pp 155.

Hegner, E., Kröner, A. & Hunt, P., 1994. A precise U-Pb zircon age for the Archaean Pongola Supergroup volcanics in Swaziland. *Journal of African Earth Sciences*, **18**(4), 339-341.

Hemingway, B. S., 1982. Thermodynamic properties of selected uranium compounds and aqueous species at 298.15K snf 1 bar and at higher temperatures. Preliminary models for the origin of coffinite deposits. U.S. Geological Survey Open-File Report. pp 60.

Heubeck, C. & Lowe, D. R., 1994. Depositional and tectonic setting of the Archaean Moodies Group, Barberton greenstone belt, South Africa. *Precambrian Research*, **68**, 257-290.

Heubeck, C., Wendt, J. I., Toulkeridis, T., Kröner, A. & Lowe, D. R., 1993. Timing of deformation of the early Archaean Barberton Greenstone belt, South Africa: constraints from zircon dating of the Sailsbury Kop pluton. *Transactions of the Geological Society of South Africa*, **96**, 1-8.

Hofmann, A., Bekker, A., Rumble, D. & Master, S., 2008. Multiple sulphur isotope analysis of detrital pyrite as a tool for provenance analysis in Archaean sedimentary rocks. In: *EGU General Assembly 2008, Geophysical Research Abstracts*, EGU, Vienna. pp 2.

Hofmann, A., Dirks, P.H.G.M. & Jelsma, H.A., 2004. Clastic sedimentation in a late Archaean accretionary terrain, Midlands greenstone belt, Zimbabwe. *Precambrian Research*, **129**, 47-69.

Hofmann, A. & Wilson, A. H., 2007. Silicified Basalts, Bedded Cherts and Other Sea Floor Alteration Phenomena of the 3.4 Ga Nondweni Greenstone Belt, South Africa. . In: *Earth's Oldest Rocks* (eds van Kranendonk, M. J., Smithies, R. H. & Bennett, V. C.). *Developments in Precambrian Geology*, Elsevier, Amsterdam, The Netherlands. pp 571-606.

Johnson, M. R., van Vuuren, C. J., Visser, J. N. J., Cole, D. I., Wickens, H. d. V., Christie, A. D. M., Roberts, D. L. & Brandl, G., 2006. Sedimentary Rocks of the Karoo Supergroup. In: *The Geology of South Africa* (eds Johnson, M. R., Anhaeusser, C. R. & Thomas, R. J.). Geological Society of South Africa / Council for Geoscience. pp 461-500

Joubert, P. & Johnson, M. R., 1998. *Abridged Lexicon of South Africa Stratigraphy*. South African Committee for Stratigraphy, Council for Geoscience. pp 160.

Kamo, S. L. & Davis, D. W., 1994. Reassessment of Archean crustal development in the Barberton Mountain Land, South Africa, based on U-Pb dating. *Tectonics*, **13**(1), 167-192.

Kodama, Y., 1994. Downstream changes in the lithology and grain size of fluvial gravels, the Watarase River, Japan: evidence of the role of abrasion in downstream fining. *Journal of Sedimentary Research*, **A64**(1), 68-75.

Kohler, E. A. & Anhaeusser, C. R., 2002. Geology and geodynamic setting of Archaean silicic metavolcanics of the Bein Venue Formation, Fig Tree Group, northeast Barberton greenstone belt, South Africa. *Precambrian Research*, **116**, 199-235.

Kröner, A., Retief, E. A., Compston, W., Jacob, R. E. & Burger, A. J., 1991. Single-grain and conventional zircon dating of remobilized basement gneisses in the central Damara belt of Namibia. *South African Journal of Geology*, **94**(5/6), 379-387.

Kröner, A. & Tegtmeyer, A., 1994. Gneiss-Greenstone relationships in the early Archaean Ancient Gneiss Complex of southwestern Swaziland, Southern Africa, and implications for early crustal evolution. *Precambrian Research*, **67** (1/2), 109-139.

Lapidus, D. F. & Coates, D. R., 1990. *Collins Dictionary of Geology*. Collins. pp 565.

Liu, K. W. & Cooper, M. R., 1998. Tidalites in the Natal Group. *South African Journal of Geology*, **101**(4), 307-312.

Maphalala, R. M. and Kröner, A., 1993. Pb-Pb single zircon ages for the younger Archaean granitoids of Swaziland, southern Africa. *Extended Abstract 16th Colloquium on African Geology,* Mbabane, Swaziland. pp 201-206.

Marshall, C. G. A., 2006. The Natal Group. In: *The Geology of South Africa* (eds Johnson, M. R., Anhaeusser, C. R. & Thomas, R. J.). Geological Society of South Africa / Council for Geoscience. pp 433-460.

Martens, F., 2005. Geological report on the uranium and gold potential of the Denny Dalton project. Unpublished report for Savanna Diamonds (Proprietary) Limited. pp 18.

Mason, T.R. & Von Brunn, V., 1977. 3-Gyr-old stromatolites from South Africa. *Nature*, **266**, 47-49.

Matthews, P. E., 1967. The Pre-Karroo Formations of the White Umfolozi Inlier, Northern Natal. *Transactions of the Geological Society of South Africa*, **70**, 39 - 63.

Matthews, P. E., 1985. Archaean post-Pongola granites in the southeastern Kaapvaal Craton. *South African Journal of Science*, **81**, 479-484.

Matthews, P. E., 1990. A Plate Tectonic Model for the Late Archaean Pongola Supergroup in Southeastern Africa. In: Crustal evolution and orogeny (ed Sychanthavong, S.P.H.), Oxford Publishers., New Delhi. pp 41-73.

Matthews, P. E., Charlesworth, E. G., Eglington, A. A. & Harmer, R. E., 1989. A minimum 3.29 Ga age for the Nondweni greenstone complex in the south-eastern Kaapvaal Craton. *South African Journal of Geology*, **92**, 272-278.

McCarthy, T. S., 2006. The Witwatersrand Supergroup. In: *The Geology of South Africa* (eds Johnson, M. R., Anhaeusser, C. R. & Thomas, R. J.). Geological Society of South Africa / Council for Geoscience. pp 155-186.

McLennan, S. M., 1989. Rare Earth Elements in Sedimentary Rocks: Influence of Provenance and Sedimentary Processes. *Reviews in Mineralogy and Geochemistry*, **21**(1), 169-200.

Meyer, F. M., Reimold, W. U. & Walraven, F., 1993. The evolution of the Archaean granitic crust in the southwestern Kaapvaal Craton, South Africa. In: *European Union Geosciences VII*, pp. 319, Strasbourg, France.

Meyer, F.M., Tainton, S. & Saager, R., 1990. The mineralogy and geochemistry of small-pebble conglomerates from the Promise Formation in the West Rand and Klerksdorp areas. *South African Journal of Geology,* **93**(1), 118-134.

Nhleko, N., 2003. The Pongola Supergroup in Swaziland, Ph.D. Thesis, *Rand Afrikaans University, Johannesburg.* pp 299.

Noffke, N., Beukes, N., Bower, D., Hazen, R. M. & Swift, D. J. P., 2008. An actualistic perspective into Archean worlds - (cyano-)bacterially induced sedimentary structures in the siliciclastic Nhlazatse Section, 2.9 Ga Pongola Supergroup, South Africa. *Geobiology*, **6**, 5-20.

Ohmoto, H. & Rye, R. O., 1979. Isotopes of sulphur and carbon. In: *Geochemistry of hydrothermal ore deposits* (ed Barnes, H. L.). Wiley, New York. pp 509-567.

Petzer, G., 2007. An investigation into the chemical composition of dolerite dykes in the White Mfolozi area, in KwaZulu-Natal, in South Africa. Honours Thesis (unpubl.), University of KwaZulu-Natal. pp 46.

Phillips, G. N. & Law, J. D. M., 1994. Metamorphism of the Witwatersrand gold fields: A review. *Ore Geology Reviews*, **9**, 1-31.

Phillips, G. N. & Law, J. D. M., 2000. Witwatersrand Gold Fields: Geology, Genesis, and Exploration. *SEG Reviews* **13**, 439-500.

Plumley, W.J., 1948. Black Hills terrace gravels: a study in sediment transport. *Journal of Geology*, **50**, 526-577.

Ramdohr, P., 1958. New observations on the ores of the Witwatersrand in South Africa and their genetic significance. *Transactions of the Geological Society of South Africa*, **61**, 1-50.

Reineck, H.-E. & Singh, I. B., 1975. *Depositional Sedimentary Environments*. Springer-Verlag. pp 439.

Riganti, A. & Wilson, A. H., 1995. Geochemistry of the mafic / ultramafic volcanic associations of the Nondweni greenstone belt, South Africa, and constraints on their petrogenesis. *Lithos*, **34**, 235-252.

Rodriguez, A.B., Fassell, M.L. & Anderson, J.B., 2001. Variations in shoreface progradation and ravinement along the Texas coast, Gulf of Mexico. *Sedimentology*, **48**, 837-853.

Rollinson, H., 1993. *Using geochemical data: evaluation, presentation, interpretation*. Prentice Hall. pp 352.

Saager, R., 1970. Structures in pyrite from the Basal reef in the Orange Free State Gold-field. *Transactions of the Geological Society of South Africa*, **73**, 29-46.

Saager, R. & Stupp, H. D., 1983. U-Ti phases from Precambrian quartz-pebble conglomerates of the Elliot Lake area, Canada, and the Pongola basin, South Africa. *Mineralogy and Petrology*, **32**(2-3), 83-102.

Saager, R., Stupp, H. D., Utter, T. & Matthey, H. O., 1986. Geological and mineralogical notes on placer occurrences in some conglomerates of the Pongola Sequence. In: *Mineral Deposits of Southern Africa* (eds Anhaeusser, C. R. & Maske, S.). Geological Society of South Africa. pp 473-487.

SACS, 1980. *SOUTH AFRICAN COMMITTEE FOR STRATIGRAPHY (SACS)* Lithostratigraphy of the Republic of South Africa, South West Africa/Namibia, and the Republics of Boputhatswana, Transkei and Venda: Hand Book No. 8. In: *Stratigraphy of South Africa. Part 1.* (comp. L.E. Kent). Geological Survey of the Government of South Africa. pp 76-80.

Schieber, J., 2007. Oxidation of detrital pyrite as a cause for Marcasite Formation in marine lag deposits from the Devonian of the eastern US. *Deep-Sea Research II*, **54**, 1312-1326.

Smith, N. D. & Beukes, N. J., 1983. Bar to bank flow convergence zones: a contribution to the origin of alluvial placers. *Economic Geology*, **78**, 1342-1349.

Smits, G., 1992. The kerogen-gold-uraninite association in the Witwatersrand reefs. In: *A short course reviewing recent developments in the understanding of the Witwatersrand Basin*. Department of Geology, Economic Geology Research Unit, University of Witwatersrand, University of Witwatersrand. pp 168-181.

Tankard, A. J., Jackson, M. P. A., Eriksson, K. A., Hobday, D. K., Hunter, D. R. & Minter, W. E. L., 1982. *Crustal Evolution of Southern Africa: 3.8 Billion Years of Earth History*. Springer-Verlag. pp 523.

Taylor, S. R. & McLennan, S. M., 1985. *The Continental Crust: Its Composition and Evolution*. Blackwell, Oxford. pp 311.

Utter, T., 1980. Rounding of ore particles from the Witwatersrand gold and uranium deposit (South Africa) as an indicator of their detrital origin. *Journal of Sedimentary Petrology*, **50**(1), 71-76.

Van Horn, F.R., & Van Horn, K.R., 1933. X-ray study of pyrite or marcasite concretions in the rocks of the Cleveland, Ohio, quadrangles. *American Mineralogist*, **18**, 288-294.

Versfeld, J. A., 1988. The Geology of the Nondweni Greenstone Belt, Natal. Ph.D. Thesis, *University of Natal, Pietermaritzburg, South Africa.* pp 298.

Viljoen, R. P., 1967. The composition of the Main Reef and Main Reef Leader Conglomerate Horizons in the Northeastern Part of the Witwatersrand Basin, Information Circular no. 40, Economic Geology Research Unit, University of the Witwatersrand, Johannesburg.

Visser, D. J. L., 1998. *The Geotectonic Evolution of South Africa and Offshore Areas*. Council for Geoscience. pp 318.

von Backstrom, J. W., 1967. Preliminary report on the geology of the area around Denny Dalton. Unpublished internal report - Atomic Energy Board. pp 11.

Von Brunn, V. & Hobday, D. K., 1976. Early Precambrian Tidal Sedimentation in the Pongola Supergroup of South Africa. *Journal of Sedimentary Petrology*, **46**(3), 670-679.

Von Brunn, V. & Mason, T. R., 1977. Siliciclastic-Carbonate Tidal Deposits from the 3000 M.Y. Pongola Supergroup, South Africa. *Sedimentary Geology*, **18**, 245-255.

von Rahden, H. V. R. & Hiemstra, S. A., 1967. Mineralogical examination of the radioactive minerals present in the Denny Dalton Gold Mine, Vryheid district. Geological Survey / Department of Mines. pp 6.

Walraven, F. & Pape, J., 1994. Pb-Pb Whole Rock Ages for the Pongola Supergroup and the Usushwana Complex, South Africa. *Journal of African Earth Sciences*, **18**(4), 297-308.

Watchorn, M. B., 1978. Sedimentology of the Mozaan Group in the southeastern Transvaal and northern Natal. M.Sc. Thesis, *University of Natal, Pietermaritzburg.* pp 111.

Watchorn, M.B. & Armstrong, N.V., 1980. Contemporaneous Sedimentation and Volcanism at the base of the Early Precambrian Nsuze Group, South Africa. *Transactions of the Geological Society of South Africa.* **83**, 231-238.

Watchorn, M.B. & O'Brien, M.F., 1991. The significance of marine modification in some Witwatersrand placers - an example from the Lower Witwatersrand West Rand Group. *South African Journal of Geology*, **94**(5/6), 333-339.

Weilers, B. F., 1990. A Review of the Pongola Supergroup and its setting on the Kaapvaal Craton. Economic Geology Research Unit, University of Witwatersrand, Johannesburg. pp 68.

Wendt, J. I., 1993. Early Archean crustal evolution in Swaziland, southern Africa, as revealed by the combined use of zircon geochronology, Pb-Pb and Sm-Nd systematics Ph.D. Thesis, *Mainz, Mainz.* pp 123.

Wilson, A. H. & Grant, C. E., 2006. Physical volcanology and compositions of the basaltic lavas in the Archean Nsuze Group, White Mfolozi inlier, South Africa. In: *Processes on the Early Earth* (eds Reimold, W. U. & Gibson, R. L.). Geological Society of America Special Paper. pp 225-289.

Wronkiewicz, D.J. & Condie, K.J., 1987. Geochemistry of Archaean shales from the Witwatersrand Supergroup, South Africa: source-area weathering and provenance. *Geochimica et Cosmochimica Acta*, **51**, 2401-2416.

Wronkiewicz, D. J. & Condie, K. J., 1989. Geochemistry and provenance of sediments from the Pongola Supergroup, South Africa: Evidence for a 3.0-Ga-old craton. *Geochimica et Cosmochimica Acta*, **53**, 1537-1549.

APPENDICIES

APPENDIX I

MAPPING DATA

Appendix I – Contents

Refer to Map A in back sleeve for overall map of the White Umfolozi Inlier

Refer to Map B in back sleeve for detailed map of the Denny Dalton mine area

Dune Pavement Sketches

Points 1 and 2 have no detailed map as:

Point 1 is partially covered by recent sand brought down by the White Umfolozi River.

Point 2 is on a private farm which is inaccessible.

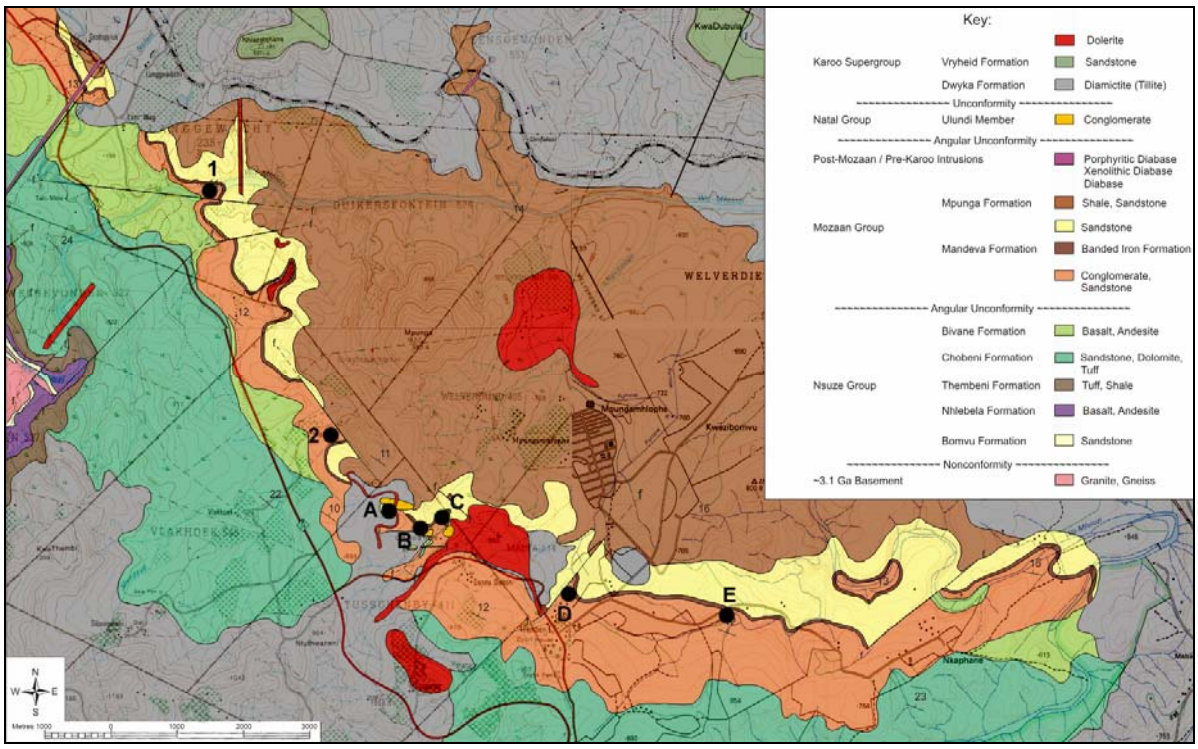

Geological Map of the White Umfolozi Inlier showing outcrop positions of Dune Pavements.

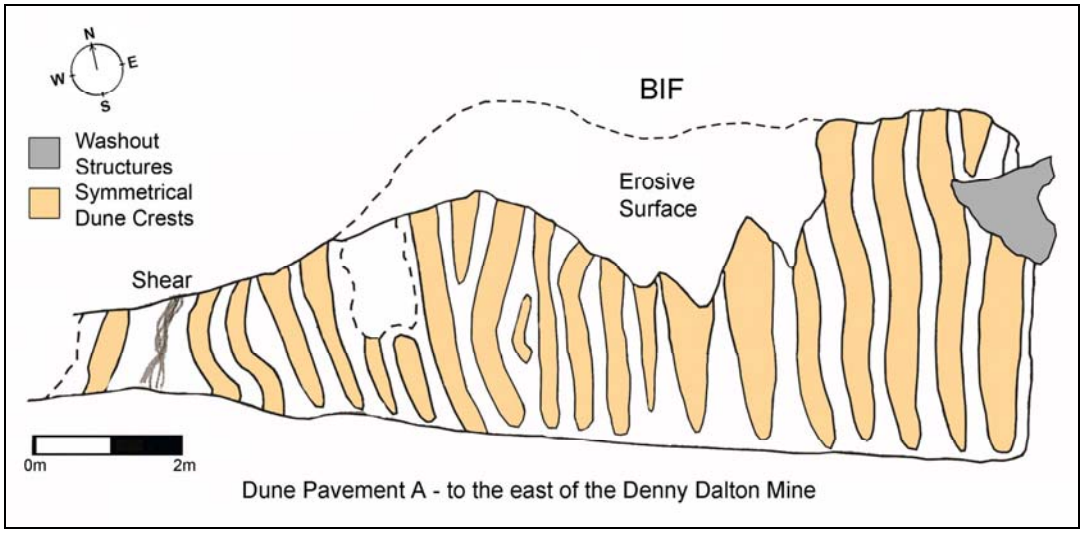

Sketch of Dune Pavement A

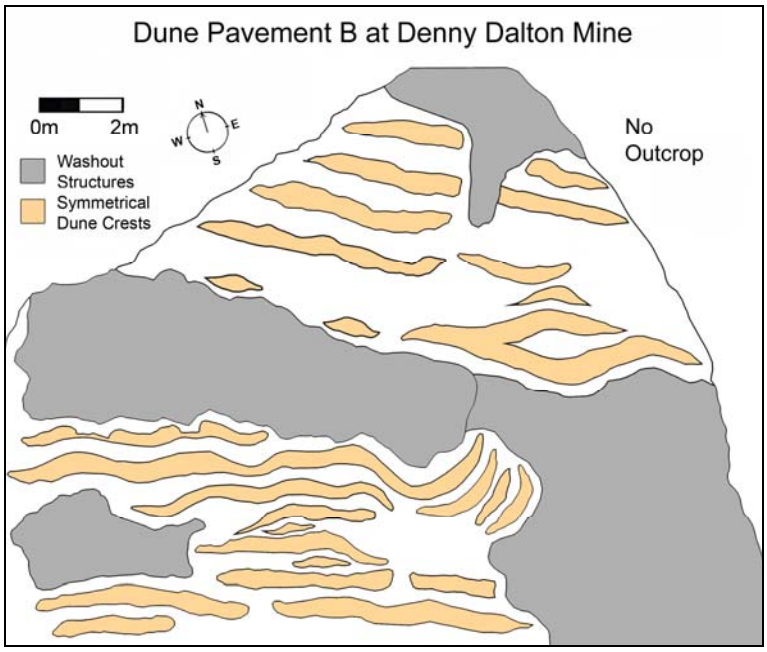

Sketch of Dune Pavement B

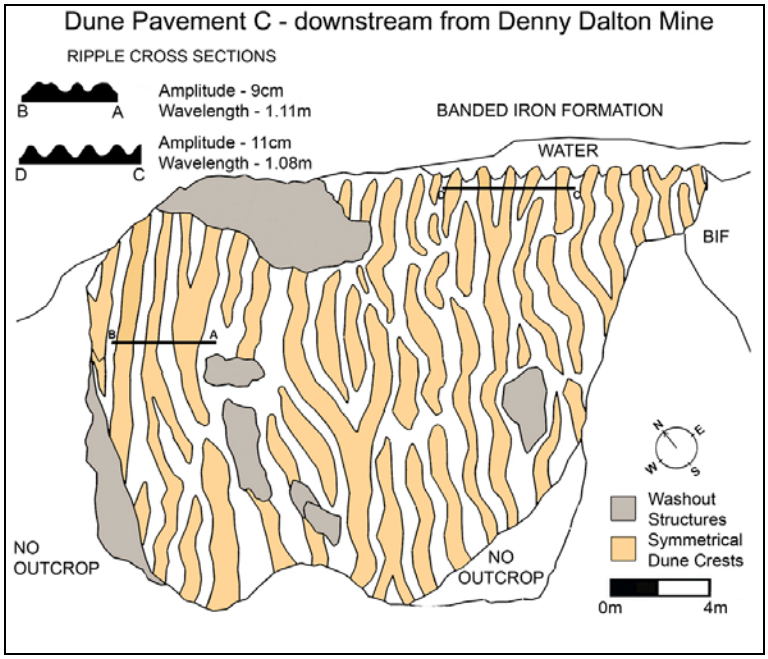

Sketch of Dune Pavement C

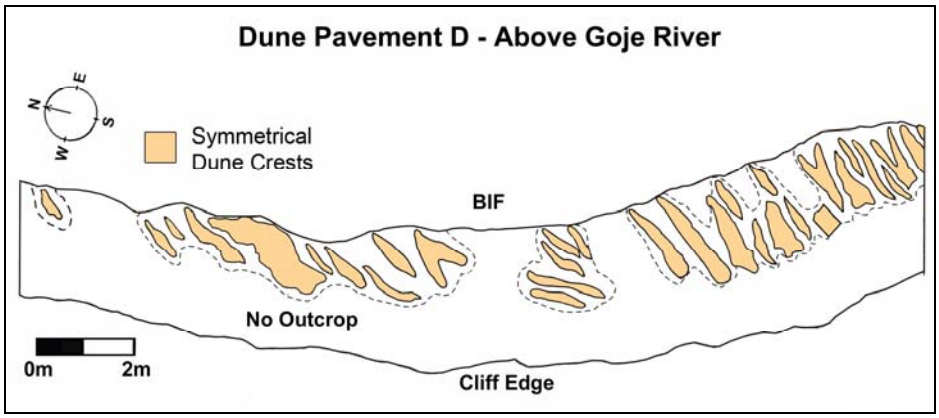

Sketch of Dune Pavement D

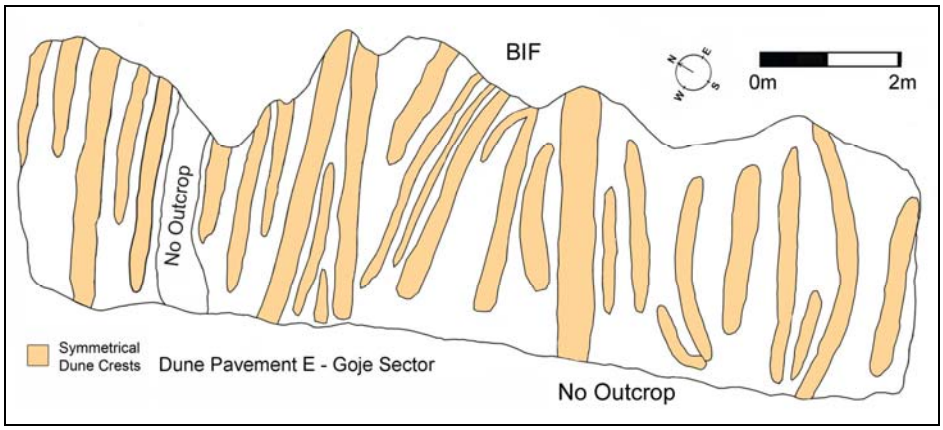

Sketch of Dune Pavement E

Bedding readings for the Mandeva Formation in the three mapping sectors within the White Umfolozi Inlier.

White Umfolozi Sector			**Denny Dalton Sector**			**Nobamba Sector**	
dip	**strike**		**dip**	**strike**		**dip**	**strike**
11	336		16	298		22	280
11	330		12	292		21	285
13	284		14	292		12	295
18	322		12	278		23	283
21	287		11	298		18	283
14	313		9	282		20	285
17	308		12	310		17	285
16	299		8	287		18	280
12	332		13	311		14	280
8	334		16	283		16	284
13	292		12	295		10	292
9	288		10	293		12	288
21	318		8	281		11	283
7	323		10	278		15	260
13	277		9	312		17	277
						11	273
						12	290
						16	4

Palaeocurrent readings taken from cross bedding (sx) for the Denny Dalton Member in the three mapping sectors within the White Umfolozi Inlier.

	White Umfolozi Sector			Denny Dalton Sector			Nobamba Sector	
	Dip	**Dip Direction**		**Dip**	**Dip Direction**		**Dip**	**Dip Direction**
sx	33	273		14	280		15	45
sx	24	54		25	72		24	320
sx	25	103		23	63		26	112
sx	30	75		28	120		28	79
sx	25	58		32	114		31	103
sx	25	108		13	254		20	113
sx	30	69		24	55		28	42
sx	22	64		29	55		24	58
sx	28	117		28	12		15	108
sx	16	56		31	25		24	74
sx	13	62		19	120		23	104
sx	21	123		28	20		27	112
sx	21	57		28	70		32	264
sx	26	54		21	74		13	57
sx	32	100		25	103		26	45
sx	23	120		31	101		23	26
sx	38	62		25	60		28	20
sx	22	54		24	64		14	119
sx	27	60		13	108		19	58
sx	23	112		22	56		22	104
sx	30	67		34	87		24	27
sx	32	45		28	67		21	67
sx	18	97		12	120		24	80
sx	29	230		24	86		22	57
sx	31	276		23	63		28	78
sx	26	57		32	85		19	111
sx	25	114		20	34		12	72
sx	23	68		12	72		23	65
sx	26	63		22	58		32	79
sx	22	104		21	69		26	76
sx	31	62		25	67		34	120
sx	28	67		25	116		25	118
sx	26	113		28	130		25	46
sx	18	61		18	49		28	106
sx	23	63		34	58		19	112
sx	18	125		22	22		31	49
sx	23	63		28	117		28	58
sx	21	54		33	25		23	74

	White Umfolozi Sector			Denny Dalton Sector			Nobamba Sector	
	Dip	**Dip Direction**		**Dip**	**Dip Direction**		**Dip**	**Dip Direction**
sx	18	120		22	82		28	25
sx	26	54		31	97		27	34
sx	23	116		27	61		18	120
sx	32	65		22	62		34	68
sx	18	57		17	113		24	109
sx	19	110		23	67		22	33
sx	24	60		31	120		30	74
sx				25	108		21	83
sx				22	87		25	62
sx				15	63		29	80
sx				32	84		17	106
sx				26	86			
sx				21	45			

Palaeocurrent readings taken from cross bedding (sx) for the Klipkloof Quartz Arenite in the three mapping sectors within the White Umfolozi Inlier.

	White Umfolozi Sector			**Denny Dalton Sector**			**Nobamba Sector**	
	Dip	**Dip Direction**		**Dip**	**Dip Direction**		**Dip**	**Dip Direction**
sx	20	40		31	82		12	311
sx	23	32		22	64		31	67
sx	12	311		20	75		26	68
sx	21	50		20	78		26	74
sx	24	60		28	18		28	108
sx	23	58		25	30		22	63
sx	22	54		15	140		25	30
sx	25	60		20	84		28	51
sx	23	57		23	110		10	64
sx	28	62		22	81		22	25
sx	31	74		23	85		28	74
sx	27	51		21	56		30	53
sx	22	52		25	50		10	264
sx	23	80		24	100		24	58
sx	25	66		26	46		23	55
sx	22	45		25	84		28	24
sx	30	70		20	80		22	20
sx	31	66		23	102		19	10
sx	23	55		20	88		28	58
sx	14	58		21	72		24	70
sx	18	62		20	76		21	55
sx	21	51		27	66		34	79
sx	21	56		23	73		16	62
sx	26	32		29	67		28	108
sx	32	98		21	69		17	48
sx	35	54		28	95		34	54
sx	22	73		20	73		22	68
sx	27	78		27	139		28	36
sx	28	52		25	89		26	53
sx	34	67		25	106		16	65
sx	18	55		22	66		19	58
sx	22	62		19	94		32	122
sx	27	75		26	72		35	80
sx	29	69		29	45		26	54
sx	21	52		35	85		28	70
sx	24	88		21	73		24	65
sx	32	62		27	66		21	27
sx	35	43		32	83		18	30
sx	22	72		25	29		29	54

	White Umfolozi Sector			**Denny Dalton Sector**			**Nobamba Sector**	
	Dip	**Dip Direction**		**Dip**	**Dip Direction**		**Dip**	**Dip Direction**
sx	25	66		28	46		27	74
sx	29	45		18	73			
sx	18	102		24	74			
sx	18	52		22	102			
sx	23	69		25	81			
				21	102			
				24	48			
				28	56			
				33	45			
				38	87			
				22	83			
				18	106			
				15	88			
				24	76			

APPENDIX II

GEOCHEMICAL DATA

Appendix II - Contents

Geochemistry Data

	TSB07/26-175	TSB07/26-174	TSB07/26-173	TSB07/26-170.6	TSB0726-169.4	TSB07/26-168
SiO_2	54.77	63.34	53.27	57.99	54.45	24.23
Al_2O_3	33.23	25.30	28.98	30.22	27.11	2.96
Fe_2O_3	1.84	3.46	9.13	3.16	11.32	51.66
MnO	0.14	0.20	0.58	0.22	0.74	11.78
MgO	0.31	0.90	2.31	0.73	2.64	8.34
CaO	0.07	0.04	0.03	0.05	0.04	0.87
Na_2O	2.56	1.26	0.96	1.75	0.40	0.04
K_2O	5.86	4.39	3.53	5.25	2.63	0.00
TiO_2	1.20	0.97	1.06	0.87	0.82	0.11
P_2O_5	0.05	0.04	0.04	0.05	0.05	0.09
Cr_2O_3	0.09	0.08	0.07	0.06	0.06	0.00
NiO	0.01	0.01	0.02	0.00	0.01	0.01
TOTAL	100.12	99.99	99.98	100.34	100.25	100.08
L.O.I.	5.37	4.87	5.81	4.99	5.60	27.70
P	161.41	153.39	165.77	171.65	182.76	151.91
Sc	7.08	2.11	10.44	0.86	11.65	1.47
V	219.79	140.21	144.85	111.17	111.21	6.96
Cr	481.22	382.05	377.09	291.13	286.21	38.37
Co	12.03	18.39	12.80	11.84	11.18	7.76
Ni	33.96	78.02	105.65	34.46	45.36	45.52
Cu	5.58	26.53	16.13	7.71	4.75	9.87
Zn	19.47	96.47	143.32	34.62	171.86	103.46
As	27.82	21.23	0.56	12.12	0.54	0.85
Rb	117.88	55.91	17.99	77.87	22.31	0.03
Sr	43.98	13.62	41.97	6.30	37.30	1.86
Y	2.88	1.51	5.26	1.98	8.70	6.32
Zr	223.81	267.37	226.80	162.69	148.00	23.48
Nb	21.07	18.77	20.62	19.58	16.99	0.50
Ba	129.94	73.21	126.45	55.55	155.19	0.37
La	9.28	2.43	10.56	2.79	17.37	3.13
Ce	20.95	4.78	28.20	5.27	43.05	6.48
Pr	2.64	0.65	3.09	1.04	4.95	0.78
Nd	9.50	2.40	11.60	4.65	18.30	3.37
Sm	1.75	0.45	2.26	1.36	3.59	0.98
Eu	0.44	0.12	0.54	0.26	0.80	0.30
Gd	1.08	0.39	1.81	0.91	2.77	1.11
Tb	0.14	0.06	0.28	0.11	0.40	0.17
Dy	0.77	0.42	1.64	0.61	2.29	0.98
Ho	0.16	0.09	0.35	0.12	0.46	0.19
Er	0.49	0.30	1.03	0.34	1.31	0.53
Tm	0.08	0.05	0.17	0.05	0.21	0.07
Yb	0.62	0.35	1.16	0.34	1.40	0.48
Lu	0.10	0.06	0.19	0.05	0.22	0.07
Hf	6.17	7.25	6.24	4.55	4.11	0.57
Ta	1.70	1.55	1.69	1.61	1.46	0.03
W	1.62	1.35	1.63	1.41	1.37	0.01
Pb	20.75	12.28	13.42	12.07	41.90	7.23
Th	2.69	1.15	4.24	0.90	6.29	1.11
U	1.94	1.51	1.81	0.62	1.49	0.49
REE tot	48.00	12.54	62.88	17.92	97.13	18.64

	TSB07/26-165.2	TSB07/26-163.9	DD-CG1	DD-CG2	DD-CG3	DD-CG4	WM-G1	WM-G2	WM-Q3	WM-Q4
SiO_2	37.49	47.87	94.37	95.65	96.11	97.60	91.22	94.48	98.57	92.06
Al_2O_3	9.96	14.61	3.20	1.99	1.73	1.08	6.12	3.89	0.86	5.65
Fe_2O_3	43.67	30.08	1.05	0.78	1.13	1.00	0.34	0.35	0.46	0.73
MnO	3.32	1.37	0.00	0.00	0.00	0.00	0.00	0.00	0.00	0.02
MgO	3.65	4.74	0.10	0.01	0.00	0.06	0.03	0.01	0.00	0.13
CaO	0.53	0.11	0.02	0.00	0.01	0.00	0.01	0.00	0.00	0.01
Na_2O	0.00	0.00	0.00	0.00	0.00	0.03	0.09	0.12	0.00	0.33
K_2O	1.03	0.54	0.93	0.58	0.51	0.21	1.66	1.08	0.16	1.09
TiO_2	0.38	0.57	0.37	0.77	0.24	0.03	0.12	0.10	0.02	0.11
P_2O_5	0.20	0.05	0.02	0.03	0.02	0.01	0.01	0.01	0.02	0.01
Cr_2O_3	0.05	0.05								
NiO	0.01	0.01								
TOTAL	100.28	100.00	100.06	99.83	99.73	100.05	99.66	100.06	100.09	100.14
L.O.I.	15.85	8.95	0.71	0.37	0.34	0.06	0.80	0.53	0.22	0.89
P	371.54	210.30	63.74	128.35	3.36	35.83	37.30	38.59	30.13	41.33
Sc	5.85	14.98	2.18	2.18	0.02	1.18	1.02	0.40	0.11	2.42
V	54.81	111.41	14.96	21.72	2.02	4.80	6.54	4.50	2.40	21.17
Cr	164.38	308.90	165.49	338.55	15.68	140.10	90.86	21.49	17.30	68.08
Co	11.19	20.58	5.08	1.80	2.48	20.79	10.79	0.82	1.73	2.97
Ni	69.76	108.95	20.54	24.70	2.58	28.76	16.85	5.50	7.24	20.82
Cu	67.48	12.46	27.03	10.66	6.40	34.18	24.69	10.84	13.14	12.44
Zn	73.28	94.81	14.91	23.49	0.00	21.34	37.27	6.31	167.77	38.20
As	0.46	1.69	17.58	21.62	10.72	37.78	19.71	1.38	6.49	1.67
Rb	29.19	17.37	27.69	17.39	2.55	7.34	24.23	26.88	5.51	37.14
Sr	19.56	6.04	4.86	6.34	3.23	10.91	9.25	6.38	6.69	30.59
Y	9.01	12.05	15.59	21.35	1.77	7.61	8.04	7.17	7.67	9.38
Zr	60.43	104.43	157.05	198.38	10.49	59.11	92.30	85.06	52.06	116.59
Nb	3.95	7.77	7.44	16.30	0.62	1.67	3.76	7.59	0.75	4.83
Ba	211.78	58.10	98.17	60.35	11.99	16.91	35.46	35.09	10.99	71.36
La	20.22	23.97	38.11	114.81	28.08	17.29	19.60	20.44	8.79	15.19
Ce	38.74	46.39	73.14	243.49	45.38	32.84	36.64	36.54	17.14	29.52
Pr	4.24	5.34	7.48	26.91	4.28	3.38	3.76	3.50	1.92	3.22
Nd	15.66	19.40	24.05	94.27	12.14	10.21	11.67	10.97	6.74	10.73
Sm	3.09	3.66	4.46	15.52	1.33	1.33	1.62	1.63	1.36	1.93
Eu	0.86	0.97	0.74	0.38	0.12	0.19	0.21	0.18	0.34	0.46
Gd	2.54	3.08	4.10	10.52	0.84	1.10	1.28	1.23	1.67	1.63
Tb	0.32	0.41	0.55	1.11	0.09	0.19	0.21	0.19	0.26	0.26
Dy	1.77	2.29	3.24	5.28	0.50	1.32	1.39	1.21	1.41	1.65
Ho	0.33	0.48	0.59	0.87	0.08	0.30	0.31	0.26	0.29	0.36
Er	0.94	1.38	1.81	2.62	0.22	0.93	0.97	0.79	0.82	1.05
Tm	0.13	0.22	0.27	0.36	0.04	0.17	0.17	0.13	0.13	0.18
Yb	0.88	1.51	1.95	2.50	0.24	1.21	1.21	0.85	0.90	1.18
Lu	0.13	0.24	0.28	0.35	0.04	0.19	0.19	0.14	0.14	0.19
Hf	1.51	2.72	3.91	6.05	0.31	1.70	2.72	2.44	1.45	3.45
Ta	0.33	0.63	1.73	5.26	0.17	0.55	0.65	1.10	0.06	0.60
W	1.02	0.80	0.80	2.20	0.02	0.14	0.21	0.34	0.10	0.35
Pb	4.89	3.91	9.20	11.12	2.52	8.83	7.35	5.63	9.99	9.58
Th	3.39	6.07	24.49	40.08	6.46	8.20	13.13	13.30	2.45	7.28
U	0.81	1.29	17.26	12.45	1.95	8.61	5.62	1.88	1.55	2.51
REE tot	89.84	109.33	160.76	518.99	93.37	70.64	79.23	78.05	41.92	67.55

Average Conglomerate, Grit, Quartz Arenite and Shale normalized to PAAS

Post Archaean average Australian Shale (PAAS) Normalized Values for Average Mandeva Samples						
	PAAS		Shale	Conglomerate	Quartz Arenite	Grit
SiO_2	62.800		0.904	1.528	1.518	1.479
Al_2O_3	18.900		1.533	0.106	0.172	0.265
Fe_2O_3	7.220		0.801	0.137	0.082	0.048
MnO	0.110		3.424	0.018	0.113	0.004
MgO	2.200		0.626	0.019	0.030	0.009
CaO	1.300		0.035	0.006	0.004	0.004
Na_2O	1.200		1.155	0.006	0.138	0.088
K_2O	3.700		1.171	0.151	0.169	0.370
TiO_2	1.000		0.983	0.353	0.064	0.108
P_2O_5	0.160		0.288	0.125	0.094	0.063
Cr_2O_3						
NiO						
TOTAL						
P						
Sc	16.000		0.402	0.087	0.079	0.044
V						
Cr	110.000		3.305	1.500	0.388	0.511
Co	23.000		0.576	0.328	0.102	0.252
Ni	55.000		1.082	0.348	0.255	0.203
Cu	50.000		0.243	0.391	0.256	0.355
Zn						
As						
Rb	160.000		0.365	0.086	0.133	0.160
Sr	200.000		0.143	0.032	0.093	0.039
Y	27.000		0.151	0.429	0.316	0.282
Zr	210.000		0.980	0.506	0.402	0.422
Nb	19.000		1.021	0.342	0.147	0.299
Ba	650.000		0.166	0.072	0.063	0.054
La	38.200		0.222	1.298	0.314	0.524
Ce	79.600		0.257	1.240	0.293	0.460
Pr	8.830		0.280	1.190	0.291	0.411
Nd	33.900		0.274	1.037	0.258	0.334
Sm	5.550		0.339	1.020	0.296	0.293
Eu	1.080		0.400	0.332	0.373	0.177
Gd	4.660		0.299	0.888	0.355	0.269
Tb	0.770		0.257	0.632	0.338	0.261
Dy	4.680		0.245	0.552	0.327	0.278
Ho	0.990		0.241	0.464	0.327	0.291
Er	2.850		0.244	0.489	0.328	0.308
Tm	0.410		0.275	0.507	0.376	0.365
Yb	2.820		0.274	0.523	0.369	0.365
Lu	0.430		0.287	0.497	0.383	0.383
Hf	5.000		1.132	0.599	0.490	0.516
Ta	1.280		1.249	1.508	0.258	0.682
W						
Pb	20.000		1.004	0.396	0.489	0.325
Th	14.600		0.209	1.357	0.333	0.905
U	3.100		0.475	3.248	0.655	1.209

Chondrite-Normalized Rare Earth Elements for all geochemical data

Chondrite Normalised Rare Earth Elements							
	Chondrite	TSB07/26-175	TSB07/26-174	TSB07/26-173	TSB07/26-170.6	TSB0726-169.4	TSB07/26-168
La	0.31	29.94	7.85	34.07	8.99	56.03	10.10
Ce	0.808	25.92	5.91	34.90	6.53	53.29	8.02
Pr	0.122	21.67	5.35	25.29	8.56	40.56	6.38
Nd	0.6	15.83	3.99	19.34	7.75	30.49	5.62
Pm							
Sm	0.195	2.27	0.60	2.78	1.34	4.10	1.51
Eu	0.0735	14.71	5.27	24.63	12.38	37.74	15.13
Gd	0.259	0.53	0.25	1.07	0.43	1.54	0.65
Tb	0.0474	16.20	8.80	34.67	12.92	48.33	20.71
Dy	0.322	0.50	0.29	1.10	0.38	1.44	0.59
Ho	0.0718	6.81	4.14	14.41	4.71	18.27	7.39
Er	0.21	0.40	0.23	0.81	0.25	1.00	0.34
Tm	0.0324	19.05	10.72	35.70	10.63	43.13	14.69
Yb	0.209	0.49	0.27	0.91	0.24	1.05	0.33
Lu	0.0322	191.56	225.21	193.73	141.17	127.57	17.81

Chondrite Normalised Rare Earth Elements											
	Chondrite	TSB07/26-165.2	TSB07/26-163.9	DD-CG1	DD-CG2	DD-CG3	DD-CG4	WM-G1	WM-G2	WM-Q3	WM-Q4
La	0.31	65.22	77.31	122.93	370.36	90.58	55.78	63.22	65.93	28.35	48.99
Ce	0.808	47.94	57.42	90.52	301.35	56.16	40.64	45.35	45.22	21.22	36.53
Pr	0.122	34.77	43.78	61.28	220.53	35.08	27.70	30.81	28.68	15.73	26.39
Nd	0.6	26.10	32.33	40.08	157.12	20.23	17.01	19.46	18.28	11.24	17.88
Pm											
Sm	0.195	4.41	4.96	3.79	1.97	0.62	0.97	1.05	0.91	1.76	2.38
Eu	0.0735	34.52	41.88	55.75	143.07	11.43	14.91	17.43	16.72	22.77	22.19
Gd	0.259	1.24	1.59	2.14	4.30	0.34	0.73	0.80	0.75	0.99	1.02
Tb	0.0474	37.42	48.29	68.45	111.39	10.49	27.85	29.31	25.61	29.77	34.74
Dy	0.322	1.02	1.48	1.82	2.70	0.25	0.93	0.97	0.82	0.90	1.11
Ho	0.0718	13.05	19.15	25.19	36.53	3.10	12.88	13.50	10.96	11.43	14.62
Er	0.21	0.63	1.07	1.28	1.70	0.17	0.80	0.82	0.61	0.63	0.84
Tm	0.0324	27.04	46.54	60.05	77.10	7.55	37.38	37.48	26.13	27.74	36.55
Yb	0.209	0.62	1.17	1.32	1.67	0.18	0.92	0.93	0.65	0.67	0.91
Lu	0.0322	46.84	84.51	121.49	187.81	9.65	52.94	84.56	75.71	45.01	107.10

Geochemical data for chert pebbles sampled at Denny Dalton Gold mine.

	PO6/11B	PO6/11C
	chert	chert
P	20.00	27.77
Sc	0.19	0.24
V	4.14	5.92
Cr	14.01	248.85
Co	17.45	7.31
Ni	53.09	23.87
Cu	16.24	25.51
Zn	108.27	0.00
As	174.91	82.60
Rb	3.98	7.21
Sr	6.22	3.14
Y	4.27	9.60
Zr	2.67	5.93
Nb	0.52	1.62
Ba	134.65	95.53
La	9.02	4.31
Ce	16.79	8.61
Pr	1.76	0.95
Nd	5.67	3.72
Sm	1.16	1.47
Eu	0.30	0.36
Gd	1.09	2.09
Tb	0.23	0.46
Dy	1.44	2.67
Ho	0.26	0.51
Er	0.66	1.23
Tm	0.10	0.16
Yb	0.57	0.87
Lu	0.06	0.10
Hf	0.07	0.16
Ta	0.21	0.44
W	1.16	1.28
Pb	43.65	25.56
Th	6.29	3.91
U	359.23	398.11

Sulphur Isotope Geochemistry data for pyrite from Conglomerate 1 at Denny Dalton gold mine

Sample #	Pyrite Type	d34Scor	d33Scor	D33Sln
PO/DD1A	Compact Rounded	0.53	0.43	0.16
PO/DD1B	Compact Rounded	0.4	0.31	0.1
PO/DD1C	Compact Rounded	2.56	1.52	0.2
PO/DD1D	Compact Rounded	2.86	1.58	0.1
PO/DD1E	Radial	-9.6	-4.78	0.17
PO/DD1F	Compact Rounded	0.69	0.51	0.15
PO/DD1G	Compact Rounded	0.31	0.33	0.17
PO/DD2-A	Compact Rounded	0.7	0.55	0.19
PO/DD2-C	Compact Rounded	0.18	0.3	0.21

APPENDIX III

TRANSMITTED LIGHT THIN SECTIONS

PHOTOMICROGRAPHS	
Magnification	**Diameter (mm)**
2x	4
10x	1
20x	0.5
40x	0.25

Thin section magnification and associated view diameter.

NB. Mineral percentages determined by visual estimates during optical microscopy.

Appendix III – Contents

Slide Number: WMQ 1.1

(Sample taken from Diamond Drill Hole TSB 07-26 at depth 178.85m)

Minerals Present:		**Percentage**
	Quartz:	95
	Chert:	2
	Opaque Minerals:	1
	Sericite:	2

Mineral Roundness: Subrounded

Sorting: Well sorted

Matrix/cement: Grain-supported

Descriptive Name: Quartz Arenite

Slide Number: WMQ 1.2

(Sample taken from Diamond Drill Hole TSB 07-26 at depth 175.65m)

Minerals Present:		**Percentage**
	Quartz:	90
	Sericite:	8
	Opaque Minerals:	2

Mineral Roundness: Subrounded to rounded

Sorting: Very well sorted

Matrix/cement: Grain-supported

Descriptive Name: Quartz Arenite

Slide Number: WMG 1.1

(Sample taken from Diamond Drill Hole TSB 06-23 at depth 45.1m)

Minerals Present:		**Percentage**
	Quartz:	82
	Chert:	5
	Sericite:	8
	Opaque Minerals:	5

Mineral Roundness: Subrounded

Sorting: Moderately sorted

Matrix/cement: Matrix-supported

Descriptive Name: Quartz Arenite

Slide Number: WMG 1.2

(Sample taken from Diamond Drill Hole TSB 06-23 at depth 44.4m)

Minerals Present:		**Percentage**
	Quartz:	84
	Chert:	2
	Sericite:	10
	Opaque Minerals:	4

Mineral Roundness: Subrounded

Sorting: Moderately sorted

Matrix/cement: Matrix supported

Descriptive Name: Quartz Arenite

Slide Number: WMG 1.3

(Sample taken from Diamond Drill Hole TSB 06-23 at depth 42.4m)

Minerals Present:		**Percentage**
	Quartz:	81
	Chert:	7
	Sericite:	5
	Muscovite:	1
	Opaque Minerals:	4
	Rock Fragments:	2

Mineral Roundness: Subangular to Subrounded

Sorting: Moderately sorted

Matrix/cement: Matrix-supported

Descriptive Name: Quartz Arenite

Slide Number: PO 5 – 14

(Sample taken 1m above the Vlakhoek Member in the Upper Quartz Arenites)

Minerals Present:	**Percentage**
Quartz:	83
Opaque Minerals:	10
Chert:	5
Muscovite:	1
Chlorite:	1

Mineral Roundness: Subrounded

Sorting: Well sorted

Matrix/cement: Grain-supported

Descriptive Name: Quartz Arenite

Slide Number: Gunsteling Conglomerate

(Sample taken from Dipka Member conglomerate on farm Gunsteling)

Scanned image of the Gunsteling conglomerate thin section

Minerals Present:		**Percentage**
	Quartz:	87
	Muscovite:	1
	Opaque Minerals:	12

Mineral Roundness: Subangular to rounded

Sorting: Well sorted

Matrix/cement: Matrix-supported

Descriptive Name: Quartz-pyrite conglomerate

Slide Number: NGB - 1

(Sample taken from ore dump at Patsoana Mission – Nondweni Area)

Scanned image of the NGB-1 conglomerate thin section

Minerals Present:		**Percentage**
	Rock Fragments:	74
	Opaque Minerals:	8
	Quartz:	5
	Chert:	13

Mineral Roundness: Subangular

Sorting: Poorly sorted

Matrix/cement: Matrix-supported / clast-supported

Descriptive Name: Conglomerate

Slide Number: NGB - 2

(Sample taken from ore dump at Patsoana Mission – Nondweni Area)

Scanned image of the NGB-2 conglomerate thin section

Minerals Present:	**Percentage**
Rock Fragments:	80
Opaque Minerals:	3
Quartz:	6
Chert:	11

Mineral Roundness: Subangular

Sorting: Poorly sorted

Matrix/cement: Matrix-supported

Descriptive Name: Conglomerate

Slide Number: NGB - 3

(Sample taken from ore dump at Patsoana Mission – Nondweni Area)

Scanned image of the NGB-3 conglomerate thin section

Minerals Present:	**Percentage**
Rock Fragments:	78
Opaque Minerals:	10
Quartz:	5
Chert:	7

Mineral Roundness: Subangular to Subrounded

Sorting: Poorly sorted

Matrix/cement: Matrix-supported / clast-supported

Descriptive Name: Conglomerate

APPENDIX IV

REFLECTED LIGHT THIN SECTIONS

Appendix IV – Contents

Slide Number: DD-1

(Sample taken from ore dump at Denny Dalton Mine)

Scanned image of the DD-1 thin section

Minerals Present:	**Percentage**
Quartz:	71
Chert:	13
Rock Fragments:	3
Opaque Minerals:	13

Major Ore Minerals Present:

Pyrite, Leucoxene

Mineral Roundness: Subrounded

Sorting: Moderately sorted

Matrix/cement: Matrix-supported

Descriptive Name: Conglomerate

Slide Number: DD-2

(Sample taken from ore dump at Denny Dalton Mine)

Scanned image of the DD-2 thin section

Minerals Present:	**Percentage**
Quartz:	68
Chert:	4
Rock Fragments:	7
Opaque Minerals:	21

Major Ore Minerals Present:

Pyrite, Leucoxene, Arsenopyrite

Mineral Roundness: Subrounded

Sorting: Moderately sorted

Matrix/cement: Matrix-supported

Descriptive Name: Conglomerate

Slide Number: DD-3

(Sample taken from ore dump at Denny Dalton Mine)

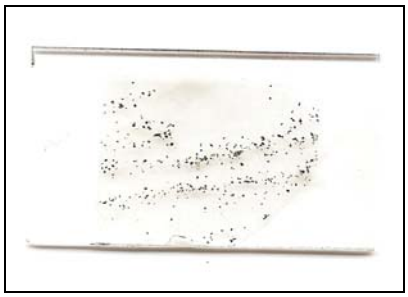

Scanned image of the DD-3 thin section

Minerals Present:		**Percentage**
	Quartz:	79
	Chert:	6
	Opaque Minerals:	15

Major Ore Minerals Present:

Pyrite, Leucoxene.

Mineral Roundness: Subrounded

Sorting: Moderately sorted

Matrix/cement: Matrix-supported

Descriptive Name: Conglomerate

Slide Number: DD-4

(Sample taken from ore dump at Denny Dalton Mine)

Scanned image of the DD-4 thin section

Minerals Present:		**Percentage**
	Quartz:	66
	Chert:	7
	Rock Fragments:	3
	Opaque Minerals:	24

Major Ore Minerals Present:

Pyrite, Leucoxene, Arsenopyrite, Monazite, Brannerite, Galena

Mineral Roundness: Subrounded

Sorting: Moderately sorted

Matrix/cement: Matrix-supported

Descriptive Name: Conglomerate

Slide Number: DD-5

(Sample taken from ore dump at Denny Dalton Mine)

Scanned image of the DD-5 thin section

Minerals Present:		**Percentage**
	Quartz:	63
	Chert:	6
	Rock Fragments:	10
	Opaque Minerals:	21

Major Ore Minerals Present:

Pyrite, Leucoxene, Arsenopyrite

Mineral Roundness: Subrounded

Sorting: Moderately sorted

Matrix/cement: Matrix-supported

Descriptive Name: Conglomerate

Slide Number: DD-6

(Sample taken from ore dump at Denny Dalton Mine)

Scanned image of the DD-6 thin section

Minerals Present:	**Percentage**
Quartz:	75
Rock Fragments:	4
Opaque Minerals:	21

Major Ore Minerals Present:

Pyrite, Leucoxene, Arsenopyrite, Brannerite, Galena

Mineral Roundness: Subrounded

Sorting: Moderately sorted

Matrix/cement: Matrix-supported

Descriptive Name: Conglomerate

Slide Number: DD-7

(Sample taken from ore dump at Denny Dalton Mine)

Scanned image of the DD-7 thin section

Minerals Present:		**Percentage**
	Quartz:	65
	Chert:	4
	Rock Fragments:	11
	Opaque Minerals:	30

Major Ore Minerals Present:

Pyrite, Leucoxene, Arsenopyrite, Brannerite, Galena

Mineral Roundness: Subrounded

Sorting: Moderately sorted

Matrix/cement: Matrix-supported

Descriptive Name: Conglomerate

Slide Number: DD CG1 HS1

(Sample taken from CG 1 reef at Adit 2S at Denny Dalton Mine)

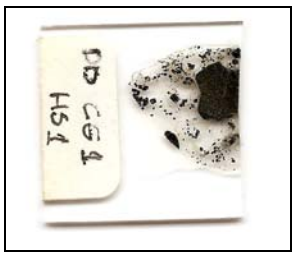

Scanned image of the DD CG1 HS1 thin section

Minerals Present:	**Percentage**
Quartz:	45
Chert:	8
Opaque Minerals:	47

Major Ore Minerals Present:

Pyrite, Leucoxene, Arsenopyrite, Gold, Brannerite, Galena

Slide Number: DD CG1 HS2

(Sample taken from CG 1 reef at Adit 2S at Denny Dalton Mine)

Scanned image of the DD CG1 HS2 thin section

Minerals Present:	**Percentage**
Quartz:	65
Chert:	5
Opaque Minerals:	30

Major Ore Minerals Present:

Pyrite, Leucoxene, Arsenopyrite, Gold, Brannerite, Galena

Slide Number: WM 1.3

(Sample taken from Diamond Drill Hole TSB 06-23 at depth 52.3m)

Scanned image of the WM 1.3 thin section

Minerals Present:		**Percentage**
	Quartz:	87
	Chert:	5
	Opaque Minerals:	8

Major Ore Minerals Present:

Pyrite, Leucoxene

Mineral Roundness: Subrounded

Sorting: Moderately sorted

Matrix/cement: Matrix-supported

Descriptive Name: Conglomerate

Slide Number: WM 1.4

(Sample taken from Diamond Drill Hole TSB 06-23 at depth 50.4m)

Scanned image of the WM 1.4 thin section

Minerals Present:		**Percentage**
	Quartz:	76
	Chert:	9
	Rock Fragments:	5
	Opaque Minerals:	10

Major Ore Minerals Present:

Pyrite, Leucoxene, Monazite

Mineral Roundness: Subrounded

Sorting: Moderately sorted

Matrix/cement: Matrix-supported

Descriptive Name: Conglomerate

Slide Number: WM 1.5

(Sample taken from Diamond Drill Hole TSB 06-23 at depth 47.7m)

Scanned image of the WM 1.5 thin section

Minerals Present:	**Percentage**
Quartz:	80
Rock Fragments:	5
Opaque Minerals:	15

Major Ore Minerals Present:

Pyrite, Leucoxene, Arsenopyrite, Brannerite, Galena

Mineral Roundness: Subrounded

Sorting: Moderately sorted

Matrix/cement: Matrix-supported

Descriptive Name: Conglomerate

Slide Number: WM CG 2.1

(Sample taken from Diamond Drill Hole TSB 06-23 at depth 39.5m)

Scanned image of the WM CG 2.1 thin section

Minerals Present:		**Percentage**
	Quartz:	77
	Opaque Minerals:	23

Major Ore Minerals Present:

Pyrite, Leucoxene, Monazite

Mineral Roundness: Subrounded

Sorting: Moderately sorted

Matrix/cement: Matrix-supported

Descriptive Name: Conglomerate

Slide Number: WM CG 2.2

(Sample taken from Diamond Drill Hole TSB 06-23 at depth 38.4m)

Scanned image of the WM CG 2.2 thin section

Minerals Present:		**Percentage**
	Quartz:	85
	Opaque Minerals:	15

Major Ore Minerals Present:

Pyrite, Leucoxene, Monazite

Mineral Roundness: Subrounded

Sorting: Moderately sorted

Matrix/cement: Matrix-supported

Descriptive Name: Conglomerate

Slide Number: WM CG 2.3

(Sample taken from Diamond Drill Hole TSB 06-23 at depth 37.65m)

Scanned image of the WM CG 2.3 thin section

Minerals Present:		**Percentage**
	Quartz:	77
	Rock Fragments:	8
	Opaque Minerals:	15

Major Ore Minerals Present:

Pyrite, Leucoxene, Monazite

Mineral Roundness: Subrounded

Sorting: Moderately sorted

Matrix/cement: Matrix-supported

Descriptive Name: Conglomerate

Slide Number: WM 3.1

(Sample taken from Diamond Drill Hole TSB 06-23 at depth 33.75m)

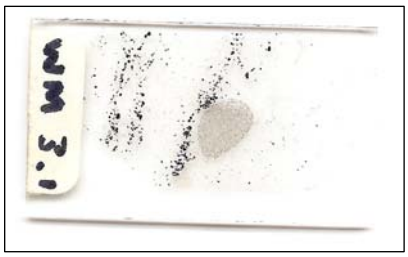

Scanned image of the WM 3.1 thin section

Minerals Present:		**Percentage**
	Quartz:	81
	Rock Fragments:	8
	Opaque Minerals:	11

Major Ore Minerals Present:

Pyrite, Leucoxene

Mineral Roundness: Subrounded

Sorting: Moderately sorted

Matrix/cement: Matrix-supported

Descriptive Name: Conglomerate

Slide Number: WM CG 3.2

(Sample taken from Diamond Drill Hole TSB 06-23 at depth 33.31m)

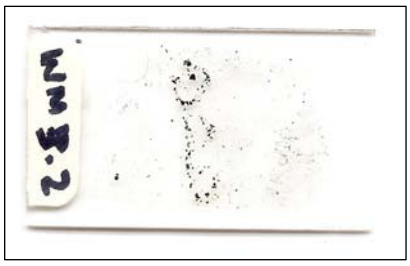

Scanned image of the WM 3.2 thin section

Minerals Present:		**Percentage**
	Quartz:	92
	Opaque Minerals:	8

Major Ore Minerals Present:

Pyrite, Leucoxene, Monazite

Mineral Roundness: Subrounded

Sorting: Moderately sorted

Matrix/cement: Matrix-supported

Descriptive Name: Conglomerate

Slide Number: WM 3.3

(Sample taken from Diamond Drill Hole TSB 06-23 at depth 33.0m)

Scanned image of the WM 3.3 thin section

Minerals Present:		**Percentage**
	Quartz:	86
	Rock Fragments:	8
	Opaque Minerals:	6

Major Ore Minerals Present:

Pyrite, Leucoxene

Mineral Roundness: Subrounded

Sorting: Moderately sorted

Matrix/cement: Matrix-supported

Descriptive Name: Conglomerate

Slide Number: WM 4.1

(Sample taken from Diamond Drill Hole TSB 07-26 at depth 178.30m)

Scanned image of the WM 4.1 thin section

Minerals Present:	**Percentage**
Quartz:	75
Rock Fragments:	3
Opaque Minerals:	22

Major Ore Minerals Present:

Pyrite, Leucoxene. Coffinite, Uraninite, Sphalerite, Arsenopyrite

Mineral Roundness: Subrounded

Sorting: Moderately sorted

Matrix/cement: Matrix-supported

Descriptive Name: Conglomerate

Slide Number: WM 4.2

(Sample taken from Diamond Drill Hole TSB 07-26 at depth 178.35m)

Scanned image of the WM 4.2 thin section

Minerals Present:		**Percentage**
	Quartz:	77
	Opaque Minerals:	23

Major Ore Minerals Present:

Pyrite, Leucoxene. Coffinite, Uraninite, Sphalerite, Arsenopyrite

Mineral Roundness: Subrounded

Sorting: Moderately sorted

Matrix/cement: Matrix-supported

Descriptive Name: Conglomerate

APPENDIX V

POLISHED BLOCKS

Appendix V – Contents

A

B

C

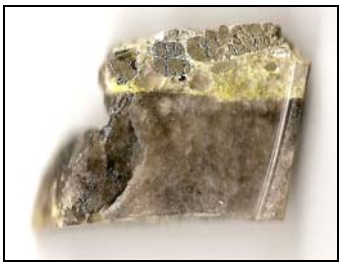

D

E

F

G

H

Polished blocks A to H were taken from grab samples of CG 1 reef at Denny Dalton mine at Adit 2 entrance.

Major Ore Minerals Present:

Pyrite, Leucoxene, Galena, Gold, Arsenopyrite, Pyrrhotite Scorodite, Brannerite


NGB F NGB G

Polished blocks NGB-F and NGB-G were made from grab samples of conglomerate from Patsoana Mission in the Nondweni area.

Major Ore Minerals Present:

Pyrite


PO6-11-B PO6-11-C

Polished blocks PO6-11-B and PO6-11-C were made from black chert pebbles within the Denny Dalton conglomerate.

Major Ore Minerals Present:

Uraninite